Passive Acoustic Monitoring for Marine Mammals in the Western Atlantic April 2015 – March 2016

Leah M. Varga, Kaitlin E. Frasier, Jennifer S. Trickey, Amanda J. Debich, John A. Hildebrand, Bruce J. Thayre, Macey Rafter, Arial M. Brewer, Sean M. Wiggins, Simone Baumann-Pickering

Marine Physical Laboratory, Scripps Institution of Oceanography
University of California San Diego, La Jolla, CA 92037

Danielle M. Cholewiak, Sofie M. Van Parijs

NOAA NMFS Northeast Fisheries Science Center, Protected Species Branch,
Woods Hole, Massachusetts 02543

Risso's dolphins, photo by Amanda J. Debich

MPL TECHNICAL MEMORANDUM # 615

April 2017

Suggested Citation

LM Varga, KE Frasier, JS Trickey, AJ Debich, JA Hildebrand, BJ Thayre, M Rafter, AM Brewer, SM Wiggins, S Baumann-Pickering, DM Cholewiak, SM Van Parijs. Passive Acoustic Monitoring for Marine Mammals in the Western Atlantic April 2015 – March 2016. Final Report. Marine Physical Laboratory Technical Memorandum 615. April 2017.

Funding provided under the Cooperative Institute for Marine Ecosystems and Climate, NOAA Award: NA10OAR4320156 from the Northeast Fisheries Science Center, under sponsorship of Sofie Van Parjis.

Table of Contents

Executive Summary

Passive acoustic monitoring was conducted in the Western Atlantic (WAT) from April 2015 to March 2016. High-frequency Acoustic Recording Packages (HARPs) were deployed at three offshore locations: Nantucket Canyon (site NC) at 980 m depth, Oceanographer Canyon (site OC) at 1100 m depth, and Heezen Canyon (site HZ) at 850 m depth.

The HARPs recorded underwater sounds between 10 Hz and 100 kHz. Data analysis consisted of analyst scans of long-term spectral averages (LTSAs) and spectrograms, and automated computer algorithm detection when possible. Two frequency bands were analyzed for marine mammal vocalizations and anthropogenic sounds: (1) Mid-frequency, between 10-5,000 Hz, and (2) High-frequency, between 1-100 kHz. No analysis was conducted for low frequency marine mammal vocalizations, such as those expected from mysticete whales.

Echolocation clicks from six known odontocete species were detected: Cuvier's beaked whale, Gervais' beaked whale, Sowerby's beaked whale, sperm whales, *Kogia* spp., and Risso's dolphins. Eight distinct click types that are not yet assigned to a species were also detected. Cuvier's, Gervais', and Sowerby's beaked whales were detected throughout the recording period at all three sites. Detections of Cuvier's and Sowerby's beaked whales were highest at site HZ. Most of the Gervais' beaked whale echolocation clicks were detected at site NC, with just one detection at site OC. Sperm whale clicks were detected at all three sites throughout the recording period. *Kogia* spp. echolocation clicks were detected in the highest numbers at site HZ. Risso's dolphin click detections peaked in May 2015 at site NC, and in July and September 2015 at site OC.

The ambient soundscape was dominated by anthropogenic sounds, primarily ship traffic and seismic exploration between 10-100 Hz at all sites. Between 100-1000 Hz the ambient soundscape was primarily a function of wind and sea state. Anthropogenic sounds including broadband ships, airguns, and echosounders were detected at all three sites, and a single explosion was detected but only at one site. Broadband ship sounds were detected the most at site OC, and the least at site HZ. There was one explosion detected throughout the recording period, at site OC. Airgun detections peaked during the summer months of 2015 and in January 2016 at sites NC and OC, and were detected in the lowest numbers at site HZ. Echosounder detections peaked at site HZ.

Project Background

In April 2015, a passive acoustic monitoring effort was initiated offshore of the northeast United States, in the Western Atlantic (WAT) with support from the National Oceanic and Atmospheric Administration (NOAA), Northeast Fisheries Science Center (NEFSC). The goal of this effort was to characterize vocalizations of marine mammal species recorded in the area and to determine their seasonal presence. This report documents the analysis of sounds recorded by High-frequency Acoustic Recording Packages (HARPs) from three sites: Nantucket Canyon (site NC) from April to September 2015, Oceanographer Canyon (site OC) from April to February 2016, and Heezen Canyon (site HZ) from June 2015 to March 2016 (Figure 1). These sites are all located on the continental slope at water depths of 845-1100 m.

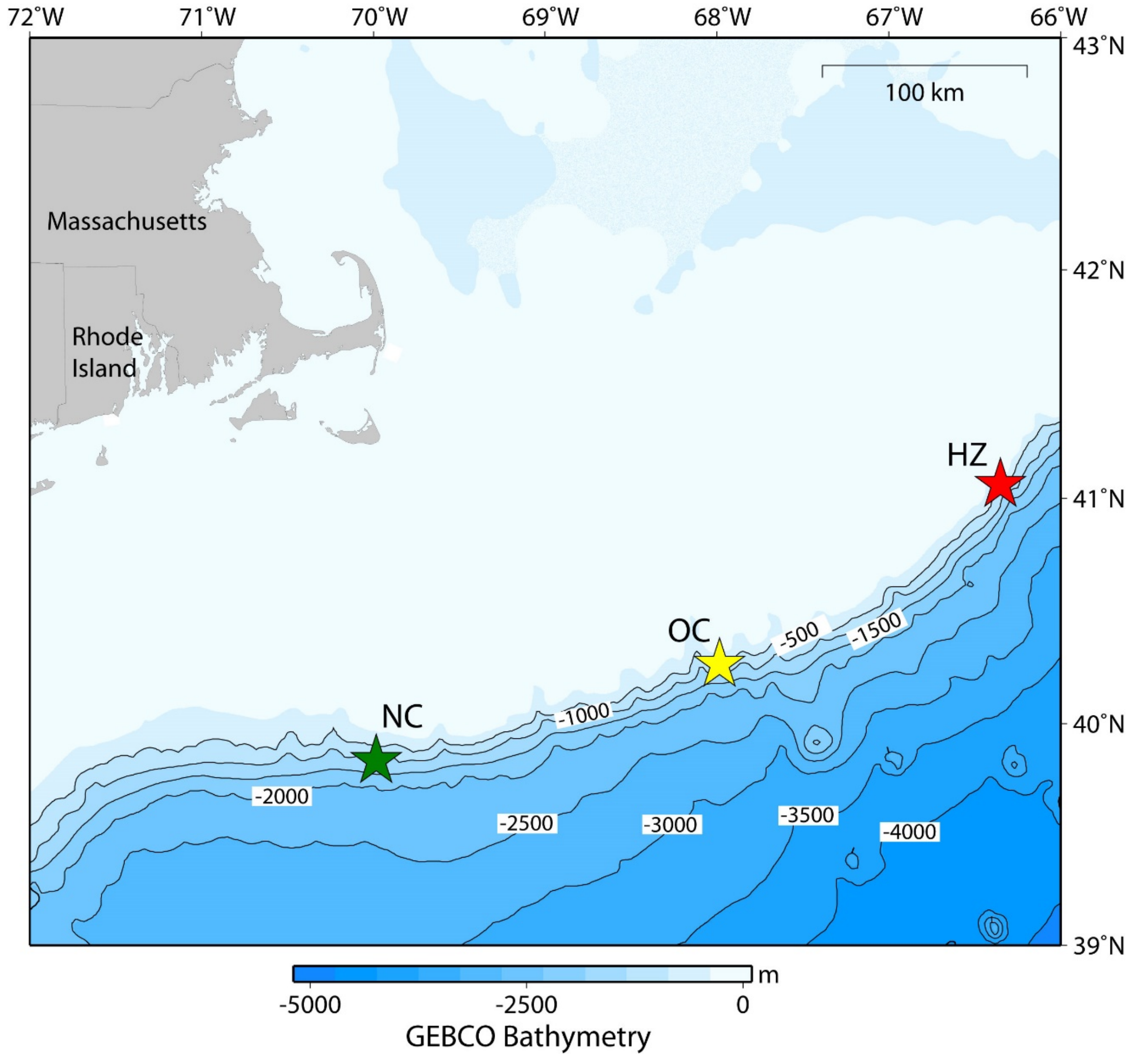

Figure 1. Location of High-frequency Acoustic Recording Packages (HARPs) at site NC (depth 977 m), site OC (depth 1100 m), and site HZ (depth 845 m). Color indicates bathymetric depth. Contours every 500 m.

Methods

High-frequency Acoustic Recording Package

HARPs are autonomous underwater acoustic recording devices that, dependent on configuration, can record sounds over a bandwidth from 10 Hz up to 160 kHz and are capable of approximately one year of continuous recording. The HARPs at sites NC, OC, and HZ were in mooring configurations with the hydrophones suspended approximately 20 m above the seafloor. Each HARP is calibrated in the laboratory to provide quantitative analysis of the received sound field. Representative data loggers and hydrophones were also calibrated at the Navy's TRANSDEC facility to verify the laboratory calibrations (Wiggins and Hildebrand, 2007).

Data Collected

Two HARPs were deployed from April 2015 to April 2016 at sites NC and OC. The instruments recorded 144.7 days from April 27, to September 18, 2015 at site NC, and 289.2 days from April 26, 2015 to February 9, 2016 at site OC. One HARP at site HZ recorded 271.3 days from June 27, 2015 to March 25, 2016 (Table 1). All three HARPs sampled continuously at 200 kHz to provide 100 kHz of effective bandwidth.

Table 1. Passive acoustic monitoring in the Western Atlantic from April 2015 – March 2016.

Deployment Name	Latitude (W)	Longitude (N)	Depth (m)	Start Date	End Date	Recording Duration	
						(days)	(hours)
NC 01	39° 49.95	69° 58.93	980	4/27/2015	9/18/2015	145	3473
OC 01	40° 15.79	67° 59.17	1100	4/26/2015	2/9/2016	289	6941
HZ 01	41° 3.72	66° 21.09	850	6/27/2015	3/25/2016	271	6511

A connection problem reduced the available data storage in the HARP at site NC, and resulted in a shortened recording. Hydrophone cable strumming from ocean tidal currents was present at site OC, creating low-frequency noise in the recording, with the greatest impact in July 2015 and January 2016 (Figure 2).

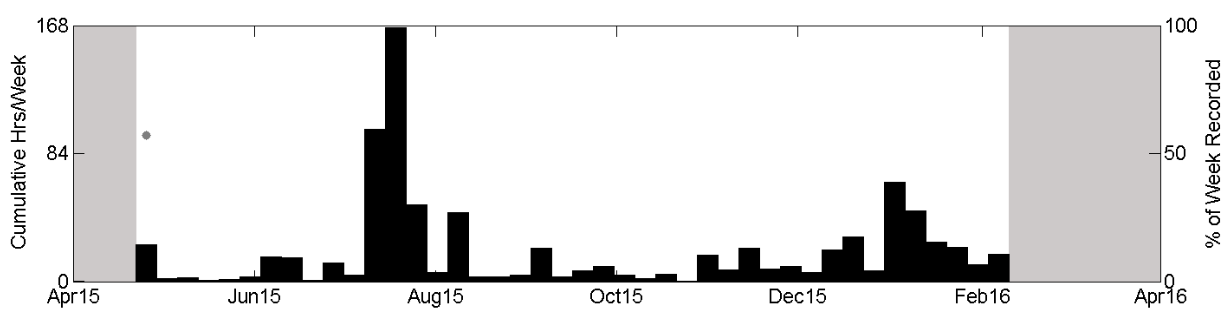

Figure 2. Cumulative weekly hours of strumming detected at site OC. The gray dot indicates a week with partial recording effort. Gray vertical shading indicates no recording effort.

Data Analysis
The data analysis process is described below in terms of the major classes of marine mammal calls and anthropogenic sounds in the WAT region, and the procedures used to detect them. For efficiency, the analysis was divided into two frequency bands: (1) Mid-frequency, 10-5,000 Hz, and (2) High-frequency, 1-100 kHz. Analysis of the low-frequency band for marine mammal calls was not within the scope of this report.

To visualize the sound recordings, sound pressure level spectra were calculated for all data using a time average of 5 seconds and two frequency bin sizes (10, 100 Hz). These Long-Term Spectral Averages (LTSAs) were visually examined by analysts as a means to detect marine mammal and anthropogenic sounds. LTSAs were analyst-scanned in source-specific frequency bands and using automatic detection algorithms (described below). During visual analysis, when a sound of interest was identified but its origin was unclear, the corresponding waveform or spectrogram was examined further to classify the sounds to source (e.g. species and anthropogenic). Signal classification was carried out by comparison to known source-specific spectral and temporal characteristics.

Each band was analyzed for the sounds of an appropriate subset of species or anthropogenic sources. Nearby shipping, explosions, and airguns were categorized as mid-frequency. Echosounders, dolphin clicks, *Kogia* spp., sperm whale clicks, and beaked whale pulses were categorized as high-frequency. For the analysis of mid-frequency recordings, the recordings were decimated by a factor of 20.

We summarize and characterize sounds detected at sites HZ, OC, and, NC. The seasonal occurrence and relative abundance for calls of different species and for anthropogenic sounds were identified in the acoustic recordings.

Low-Frequency Ambient Soundscape
To provide a means of evaluating seasonal variability, average sound pressure spectrum levels were computed per day, with partial days and days with deployment/recovery ship sounds or with known instrument self-noise problems discarded. Daily-averaged spectra were processed into monthly-averages and plotted using the same monthly color scheme for each of the deployments so that months from different sites and years can be compared.

A filter was developed and applied to the OC deployment to remove periods of strumming from the ambient soundscape monthly spectral averages. A threshold level was selected to identify strumming periods at a low frequency that exhibited highest strumming relative to background levels. Averages with levels at the selected frequency above the threshold were discarded. Any day with less than 90% of expected spectral averages was also discarded.

Odontocetes
Odontocetes (toothed whales) with sounds in the high-frequency range and possibly found in the Western Atlantic region include Atlantic white-sided dolphins (*Lagenorhynchus acutus*), short-beaked common dolphins (*Delphinus delphis*), Atlantic spotted dolphins (*Stenella frontalis*), Clymene dolphins (*S. clymene*), striped dolphins (*S. coeruleoalba*), Risso's dolphins (*Grampus griseus*), bottlenose dolphins (*Tursiops truncatus*), rough-toothed dolphins, (*Steno bredanensis*),

false killer whales (*Pseudorca crassidens*), short-finned pilot whales (*Globicephala macrorhynchus*), long-finned pilot whales (*G. melas*), killer whales (*Orcinus orca*), sperm whales (*Physeter macrocephalus*), dwarf sperm whales (*Kogia sima*), pygmy sperm whales (*K. breviceps*), Northern bottlenose dolphins (*Hyperoodon ampullatus*), Cuvier's beaked whales (*Ziphius cavirostris*), Gervais' beaked whales (*Mesoplodon europaeus*), Blainville's beaked whales (*M. densirostris*), and Sowerby's beaked whales (*M. bidens*).

Odontocete sounds can be categorized as echolocation clicks, burst pulses, or whistles. Echolocation clicks are broadband impulses with peak energy between 5 and 150 kHz, dependent upon the species. Buzz or burst pulses are rapidly repeated clicks that have a creak or buzz-like sound quality; they are generally lower in frequency than echolocation clicks. Dolphin whistles are tonal calls predominantly between 1 and 20 kHz that vary in frequency content, their degree of frequency modulation, as well as duration. These signals are easily detectable in an LTSA as well as the spectrogram (Figure 3). Echolocation clicks were analyzed as a proxy for odontocete presence because they are currently the most promising call type for species classification in the region. Further analysis might identify distinguishing whistle or burst pulse characteristics.

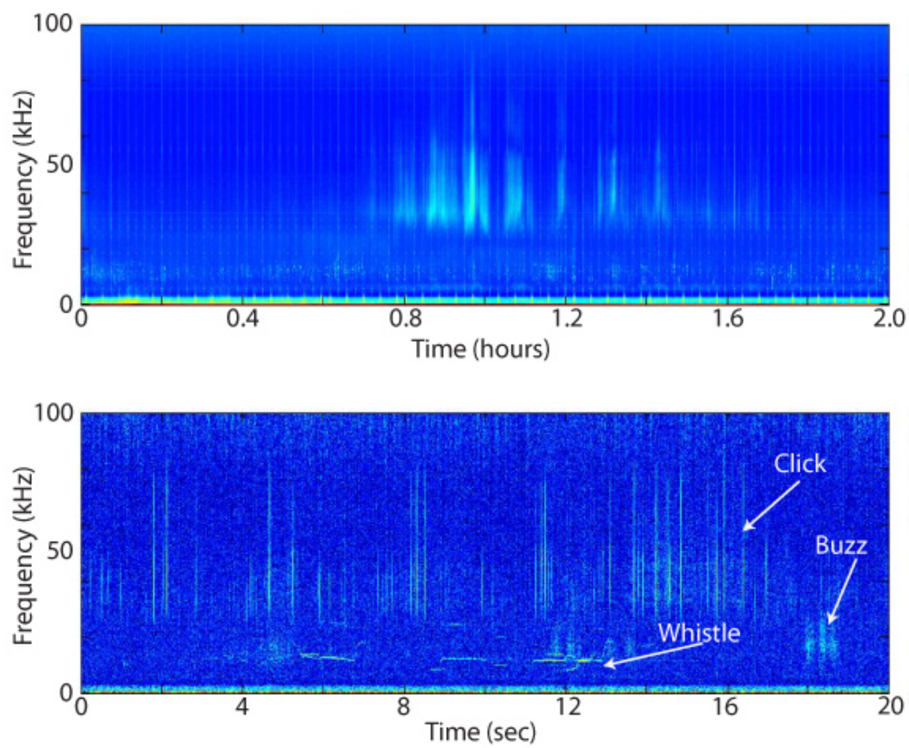

Figure 3. Generic example demonstrating odontocete signal types, in a LTSA (top) and spectrogram (bottom).

Beaked Whales

Beaked whales can be identified acoustically by their echolocation signals (Baumann-Pickering *et al.*, 2014). These signals are frequency-modulated (FM) upsweep pulses, which appear to be species specific and distinguishable by their spectral and temporal features. Identifiable signals are described for all beaked whales known to occur in the region, namely Blainville's, Cuvier's, Gervais', and Sowerby's beaked whales, and Northern bottlenose whales.

Beaked whale FM pulses were detected with an automated process. First, echolocation signals were detected with a Teager Kaiser energy detector (Soldevilla *et al.*, 2008; Roch *et al.*, 2011), then an expert system discriminated between delphinid clicks and beaked whale FM pulses. A decision about presence or absence of beaked whale signals was based on detections within a 75 second recording segment. Only segments with more than 7 detections were used in further analysis. All echolocation signals with a peak and center frequency below 32 and 25 kHz, respectively, a duration less than 355 μs, and a sweep rate of less than 23 kHz/ms were deleted. If more than 13% of all initially detected echolocation signals remained after applying these criteria, the segment was classified to have beaked whale FM pulses. A third classification step, based on computer assisted manual decisions by a trained analyst, was used to label the automatically detected segments to pulse type level and rejected false detections (Baumann-Pickering *et al.*, 2013). The rate of missed segments is approximately 5%, varying slightly across deployments.

Blainville's Beaked Whales

Blainville's beaked whale echolocation signals are polycyclic, with a characteristic frequency-modulated upsweep, peak frequency around 34 kHz and uniform inter-pulse interval (IPI) of about 280 ms (Johnson *et al.*, 2006; Baumann-Pickering *et al.*, 2013). Blainville's FM pulses are also distinguishable in the spectral domain by their sharp energy onset around 25 kHz with only a small energy peak at around 22 kHz (Figure 4).

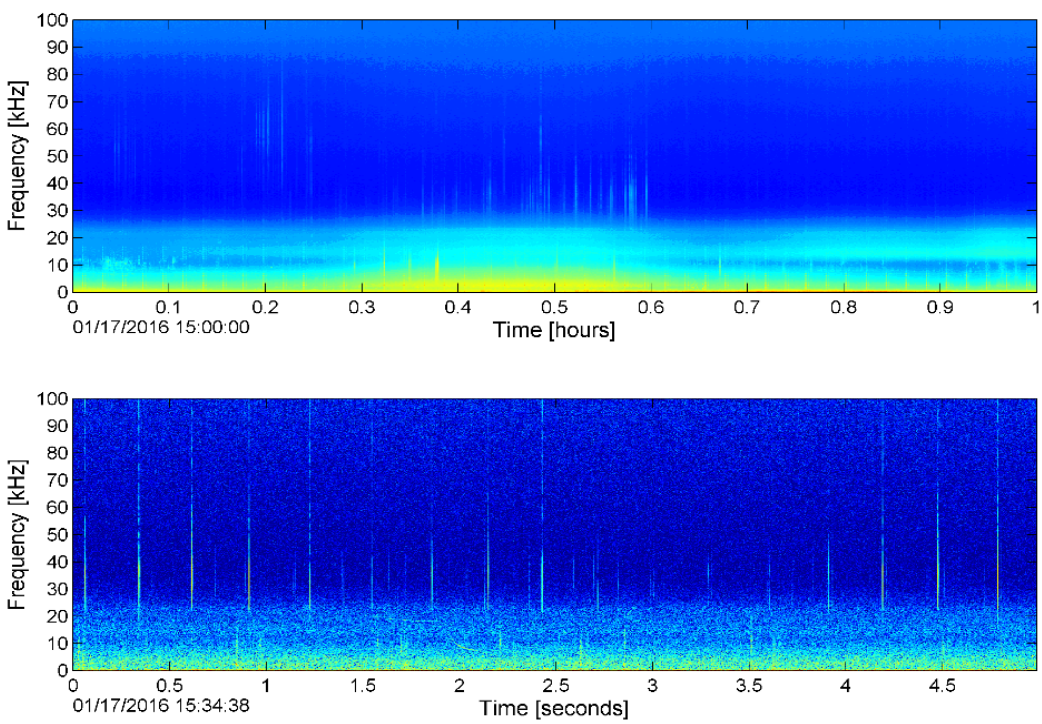

Figure 4. Blainville's beaked whale echolocation clicks in LTSA (top) and spectrogram (bottom) recorded offshore of Hatteras, North Carolina.

Cuvier's Beaked Whales

Cuvier's beaked whale echolocation signals are polycyclic, with a characteristic FM pulse upsweep, peak frequency around 40 kHz (Figure 5), and uniform inter-pulse interval of about 0.5 s (Johnson *et al.*, 2004; Zimmer *et al.*, 2005). An additional feature that helps with the identification of Cuvier's FM pulses is that they have two characteristic spectral peaks around 17 and 23 kHz.

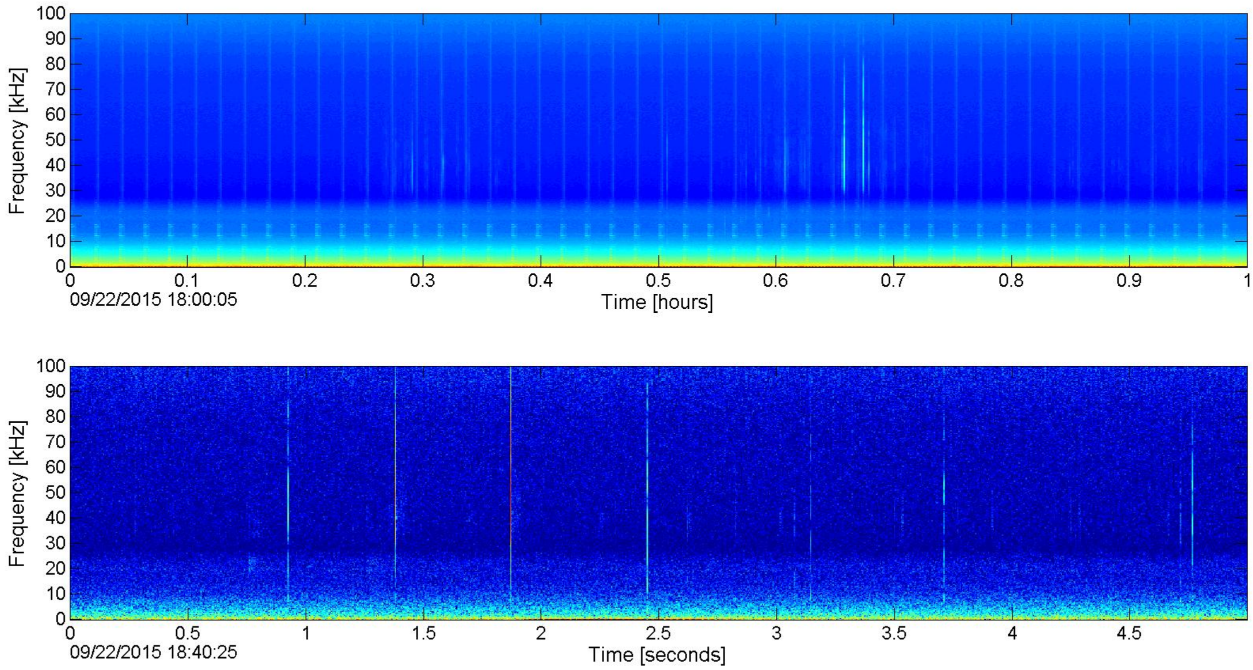

Figure 5. Cuvier's beaked whale echolocation clicks in LTSA (top) and spectrogram (bottom) recorded at site HZ.

Gervais’ Beaked Whales

Gervais’ beaked whale signals have energy concentrated in the 30-50 kHz band (Gillespie *et al.*, 2009), with a peak at 44 kHz (Baumann-Pickering *et al.*, 2013). While Gervais’ beaked whale signals are similar to those of Cuvier’s and Blainville’s beaked whales, the Gervais’ beaked whale FM pulses are at a slightly higher frequency than those of the other two species. Similarly, Gervais’ beaked whale FM pulses sweep up in frequency (Figure 6). The IPI for Gervais’ beaked whale signals is typically around 275 ms (Baumann-Pickering *et al.*, 2013).

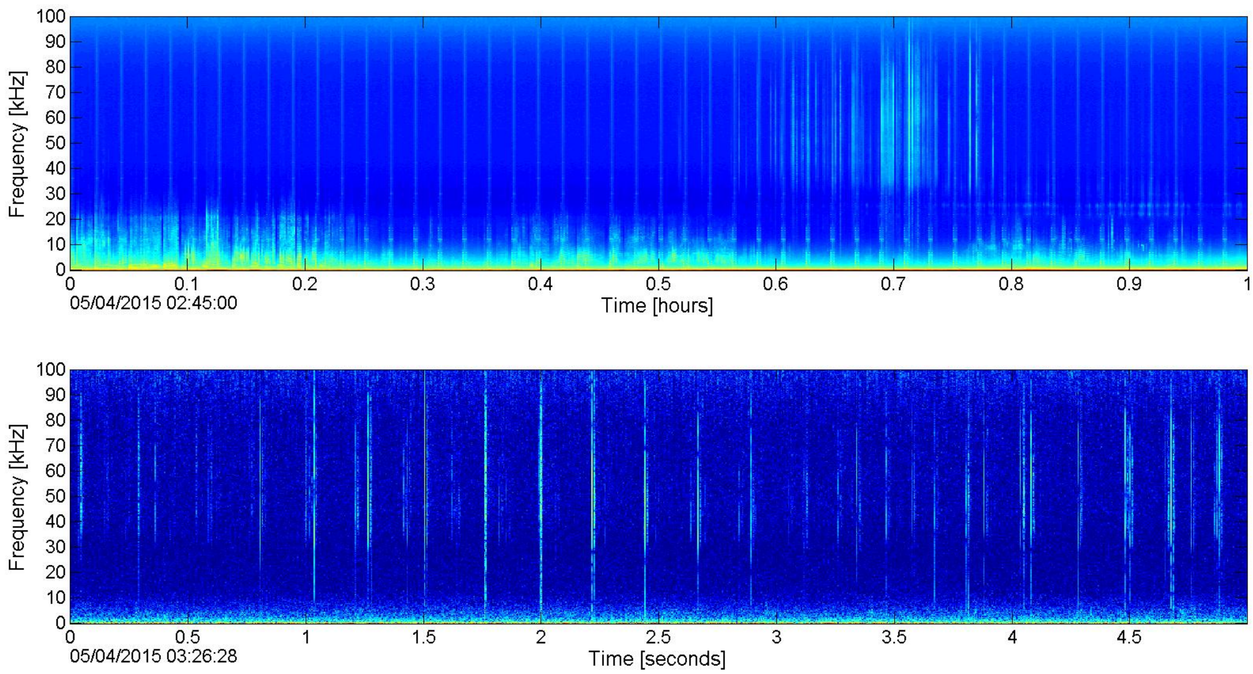

Figure 6. Gervais’ beaked whale echolocation clicks in LTSA (top) and spectrogram (bottom) recorded at site NC.

Sowerby's Beaked Whales

Sowerby's beaked whale echolocation signals have energy concentrated in the 50 – 95 kHz band, with a peak at 67 kHz (Figure 7). Sowerby's beaked whale signals have a characteristic FM upsweep, and are distinguishable from other co-occurring beaked whale signal types by their higher frequency content and a relatively short inter-pulse interval of around 150 ms (Cholewiak *et al.*, 2013).

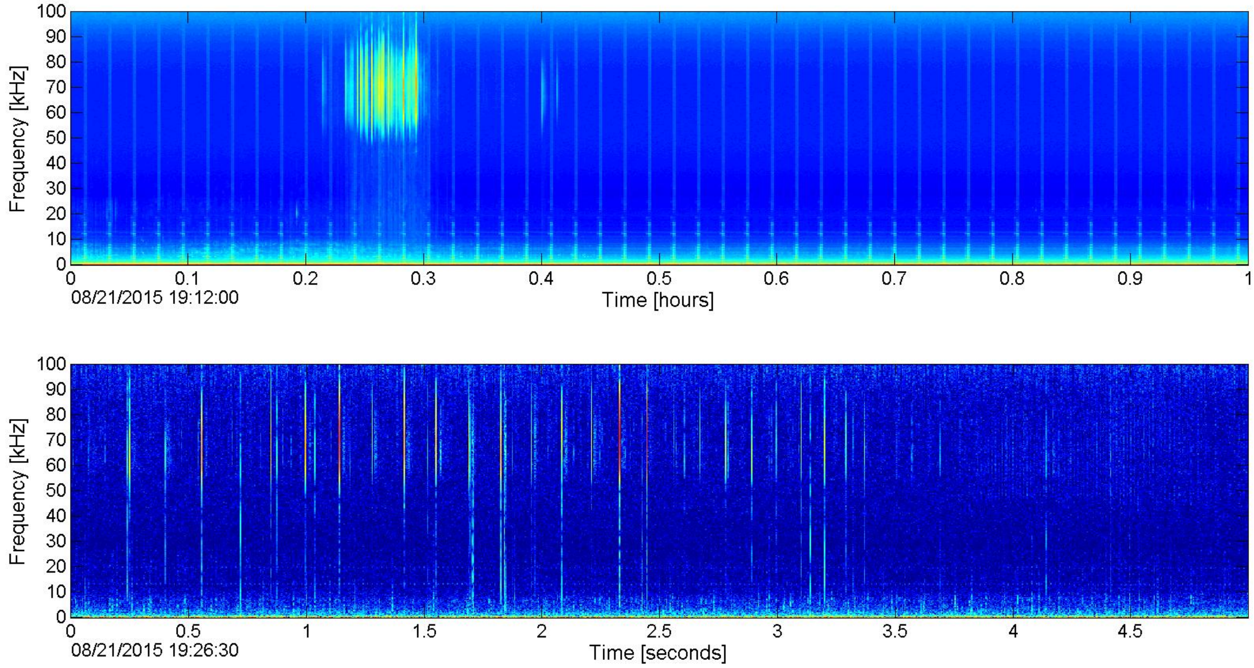

Figure 7. Sowerby's beaked whale echolocation clicks in LTSA (top) and spectrogram (bottom) recorded at site HZ.

Sperm Whales

Sperm whale clicks contain energy from 2-20 kHz, with the majority of energy between 10-15 kHz (Møhl *et al.*, 2003) (Figure 8). Regular clicks, observed during foraging dives, demonstrate an ICI from 0.25-2s (Goold and Jones, 1995; Madsen *et al.*, 2002a). Short bursts of closely spaced clicks called creaks are observed during foraging dives and are believed to indicate a predation attempt (Watwood *et al.*, 2006). Slow clicks are used only by males and are more intense than regular clicks with long inter-click intervals (Madsen *et al.*, 2002b). Codas are stereotyped sequences of clicks which are less intense and contain lower peak frequencies than regular clicks (Watkins and Schevill, 1977). Effort was not expended to denote whether sperm whale detections were codas, regular or slow clicks.

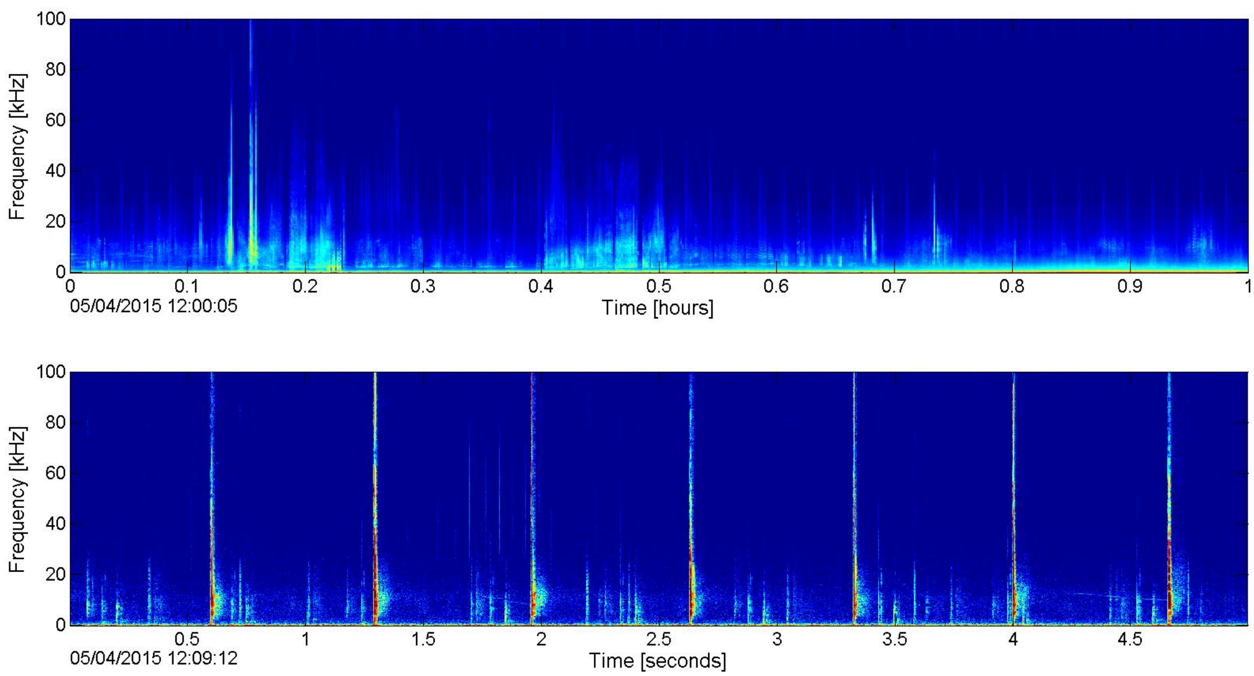

Figure 8. Sperm whale clicks in LTSA (top) and spectrogram (bottom) recorded at site OC.

Kogia spp.

Dwarf and pygmy sperm whales emit echolocation signals which have peak energy at frequencies near 130 kHz (Au, 1993). While this is above the upper frequency band recorded by the HARP during these deployments, energy from *Kogia* clicks can be recorded within the 100 kHz HARP bandwidth (Figure 9). The observed signal may result both from the low-frequency tail of the *Kogia* echolocation click spectra, and from aliasing of energy from above the Nyquist frequency of 100 kHz (Figure 10). *Kogia* echolocation clicks were analyzed using a multi-step detector. The first step was to identify clicks with energy in the 70-100 kHz band that simultaneously lacked energy in lower frequency bands. An expert system then classified these clicks based on spectral characteristics and finally an analyst verified all echolocation click bouts manually. A bimodal click peak frequency distribution (Figure 10) may represent two distinct click subtypes.

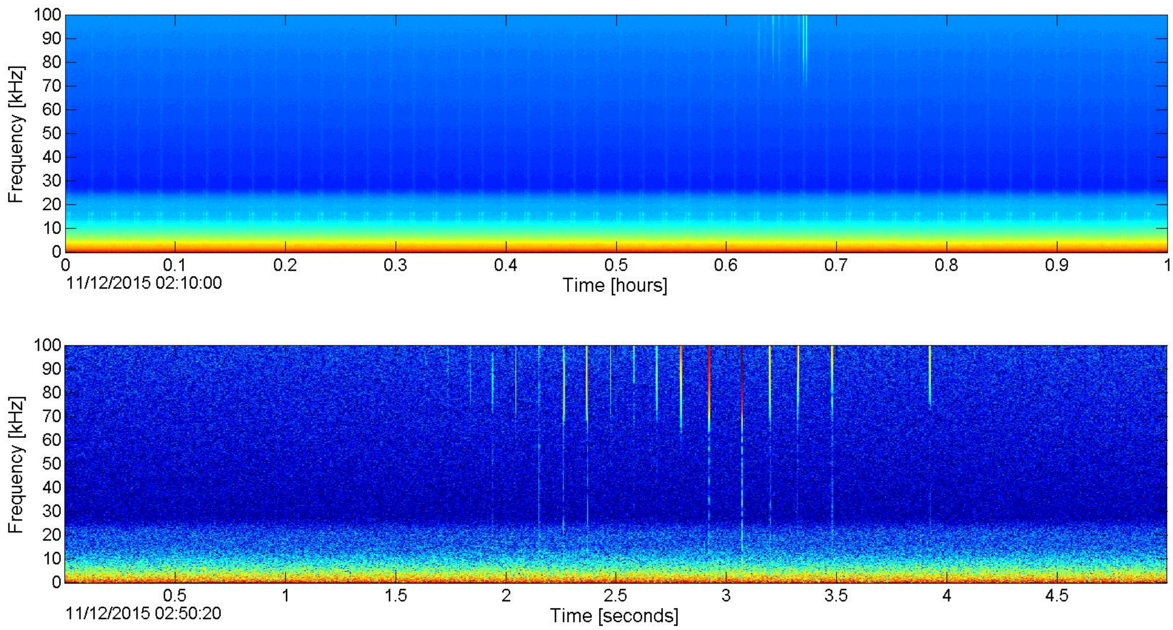

Figure 9. *Kogia* spp. clicks in LTSA (top) and spectrogram (bottom) recorded at site HZ.

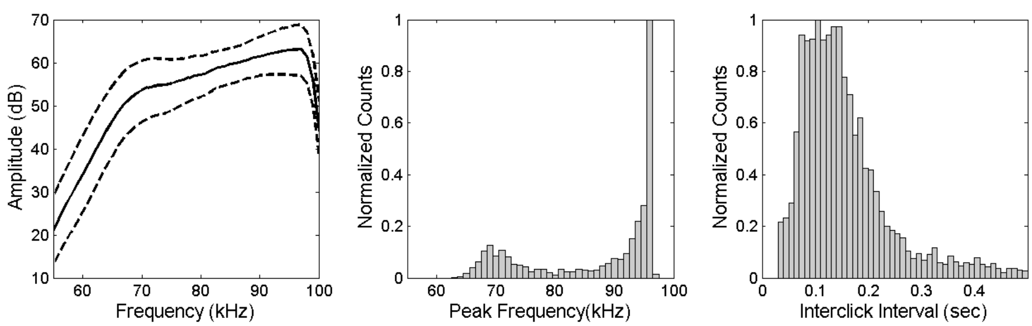

Figure 10. Left: Mean frequency spectrum of *Kogia* spp. clicks (solid line) and 25th and 75th percentiles (dashed lines); Center: Distribution of click peak frequencies with peak near the Nyquist frequency (100 kHz); Right: Distribution of inter-click-intervals.

Delphinid Click Types
Delphinid echolocation clicks were detected automatically using an energy detector with a minimum received level threshold of 120 dB_{pp} re: 1 µPa (Roch *et al.*, 2011; Frasier, 2015). False positives were identified and removed manually by an analyst, who reviewed LTSAs and mean spectra for each detected bout. A bout was defined as a period of clicking separated before and after by at least 15 minutes without clicking.

Dominant click types at these sites were identified automatically by dividing detections into successive five-minute windows and determining the dominant click type(s) in each window. An automated clustering algorithm was then used to identify recurrent types based on spectral features and inter-click interval (ICI) distributions across a subset of 10,000 windows aggregated across the three sites (Frasier et al., in prep). Recurrent types were used as templates. Templates were attributed to a specific species if known (e.g. Risso's dolphin) or assigned a number if species was unknown. Templates were compared with the click type(s) in each five-minute window for matches. Click types that matched a template were classified by the matched template. Click types that did not match a template were labeled as unknown.

At least nine delphinid click types were identified and labeled click type 1 – 8 and Risso's from across the three sites, with the highest click type diversity found at site HZ. Variable data quality at site HZ, combined with high detection rates and frequent multi-species encounters limited the ability of both manual and automated analyses to distinguish within-type from between-type variability. Some reported click types may contain multiple subtypes. Further analysis will be required to refine click types and reduce classification confusion between similar types.

Risso's Dolphins

Risso's dolphin clicks (Figure 11) have frequency peaks at approximately 22, 26, and 33 kHz. These clicks have a modal ICI of approximately 0.15 seconds (Figure 12). Past studies have shown that spectral properties of Risso's dolphin clicks have slight variations with geographic region (Soldevilla et al., in prep), although the multiple sharp frequency peaks and average ICI found at these North-Western Atlantic sites are similar to what has been found elsewhere. Two click types similar to Risso's dolphin clicks were identified at these sites, one with a distinct peak at 22 kHz, the other without. Further analysis will be required to determine whether these are distinct types.

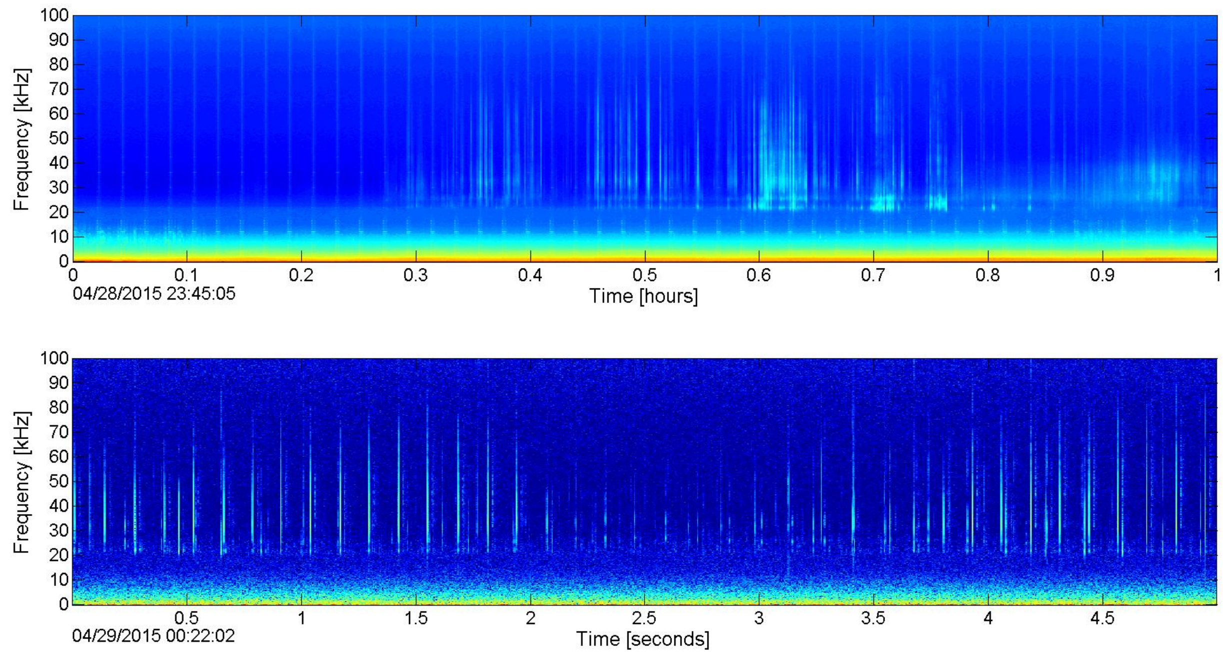

Figure 11. Risso's dolphin clicks in LTSA (top) and spectrogram (bottom) recorded at site NC.

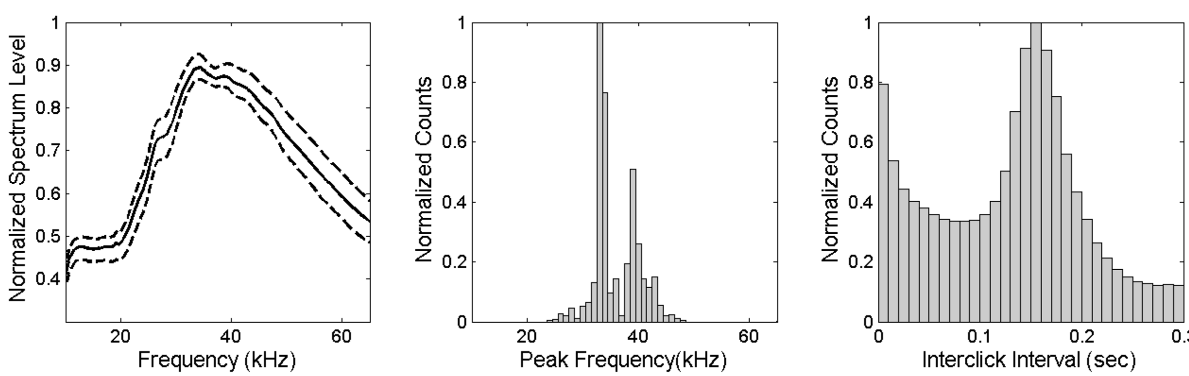

Figure 12. Left: Mean normalized received sound pressure spectrum level of Risso's dolphin click cluster (solid line) and 25th and 75th percentiles (dashed lines); Center: Distribution of click cluster peak frequencies with primary peak at 33 kHz; Right: Distribution of inter-click-intervals within cluster with modal peak at 0.15 seconds.

Click Type 1

Click type 1 clicks (Figure 13) have spectral peaks near 22, 26, and 33 kHz and a distinct trough at 28 kHz (Figure 14). These clicks have a modal ICI of approximately 0.15 seconds. Click type 1 is very similar in spectrum to Pacific white-sided dolphin clicks (Soldevilla *et al.*, 2008). The spectral peaks of this type are similar in spectrum and ICI to Risso's dolphins, and the two types are likely confused using current classification methods due in part to data quality issues in the 25-30 kHz band. Further classifier refinement is needed to reliably distinguish the two.

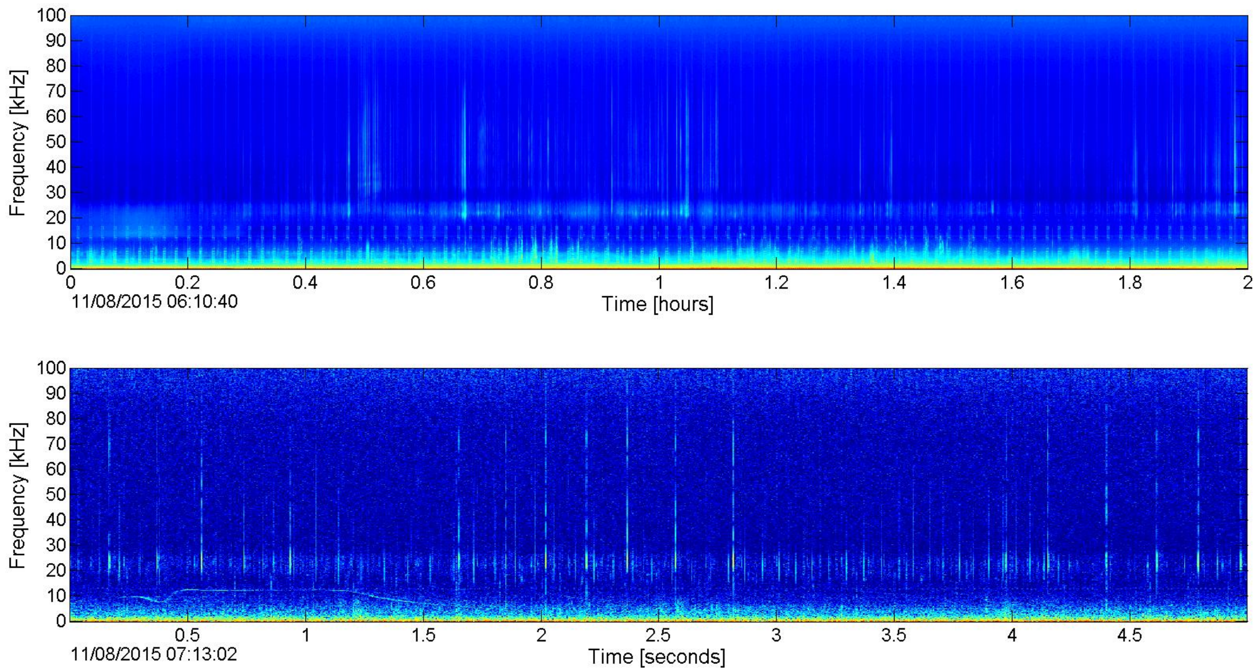

Figure 13. Click type 1 in LTSA (top) and spectrogram (bottom) recorded at site HZ.

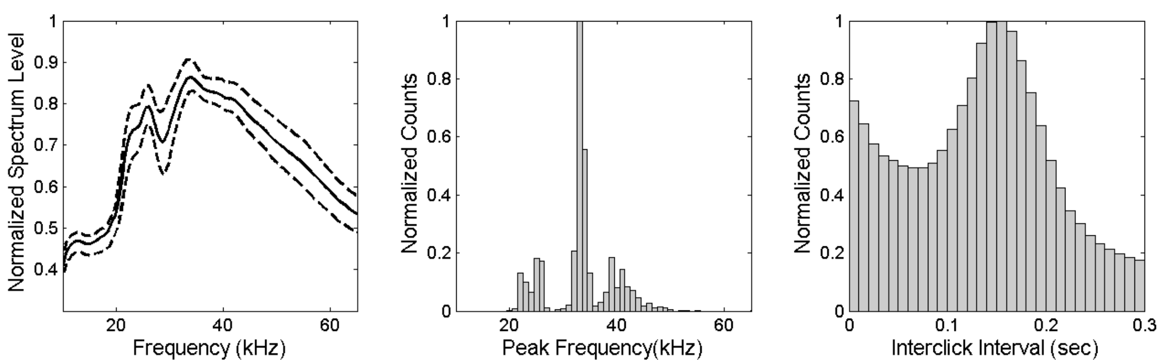

Figure 14. Left: Mean normalized received sound pressure spectrum level of click type 1 cluster (solid line) and 25th and 75th percentiles (dashed lines); Center: Distribution of click cluster peak frequencies with a peak at 33 kHz; Right: Distribution of inter-click-intervals within cluster with modal peak at 0.15 seconds.

Click Type 2

Click type 2 clicks (Figure 15) have a narrow spectral peak at 22 kHz and a broad peak from 32 to 43 kHz. These clicks have a modal ICI of approximately 0.07 seconds (Figure 16).

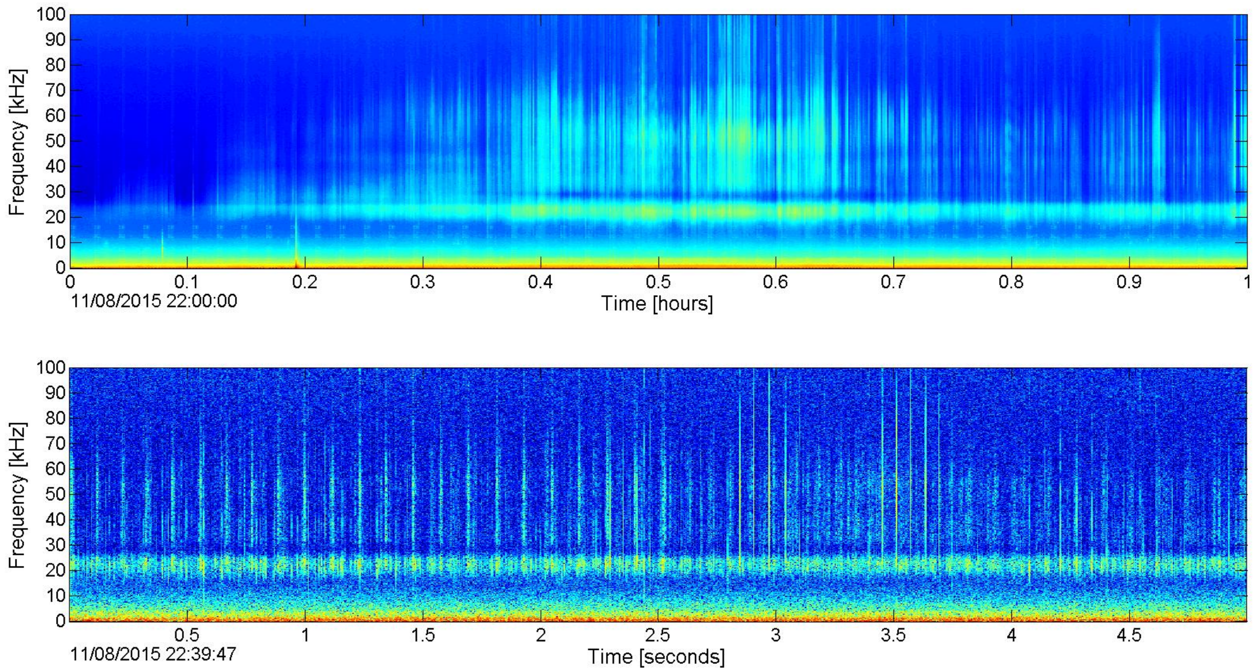

Figure 15. Click type 2 clicks in LTSA (top) and spectrogram (bottom) recorded at site HZ.

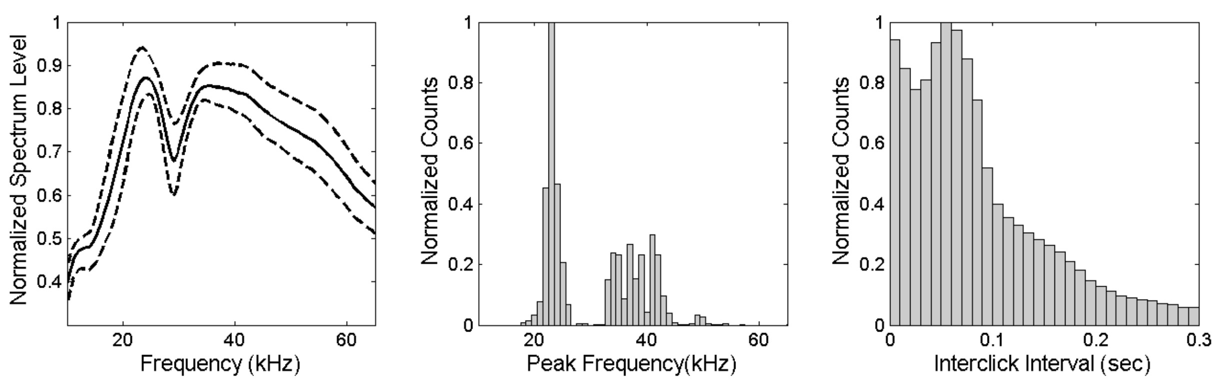

Figure 16. Left: Mean normalized received sound pressure spectrum level of click type 2 cluster (solid line) with 25th and 75th percentiles (dashed lines); Center: Distribution of click cluster peak frequencies with a peak at 22 kHz; Right: Distribution of inter-click-intervals within cluster with modal peak at 0.07 seconds.

Click Type 3

Click type 3 clicks (Figure 17) have a peak frequency of approximately 33 kHz, and a modal ICI of 0.06 seconds (Figure 18).

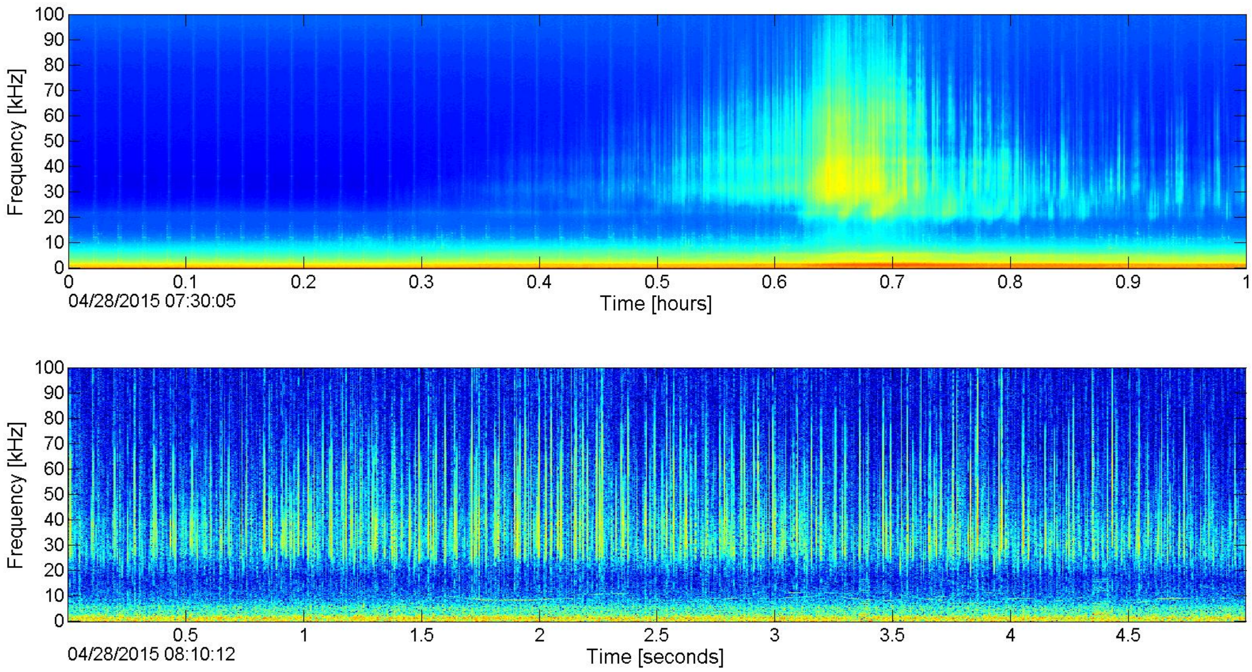

Figure 17. Click type 3 in LTSA (top) and spectrogram (bottom) recorded at site NC.

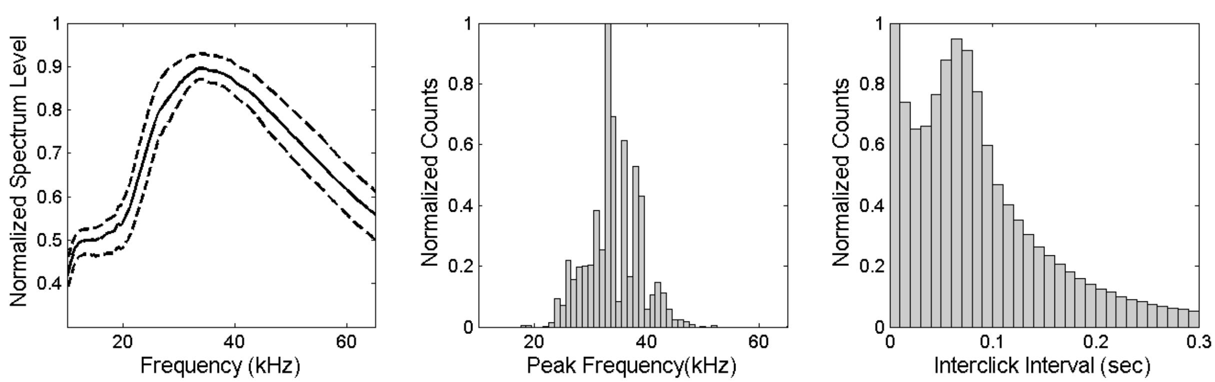

Figure 18. Left: Mean normalized received sound pressure spectrum level of click type 3 cluster (solid line) with 25th and 75th percentiles (dashed lines); Center: Distribution of click cluster peak frequencies with a peak at 33 kHz; Right: Distribution of inter-click-intervals within cluster with modal peak at 0.06 seconds.

Click Type 4

Click type 4 clicks (Figure 19) have a peak frequency of approximately 22 kHz, and a modal ICI of 0.14 seconds (Figure 20).

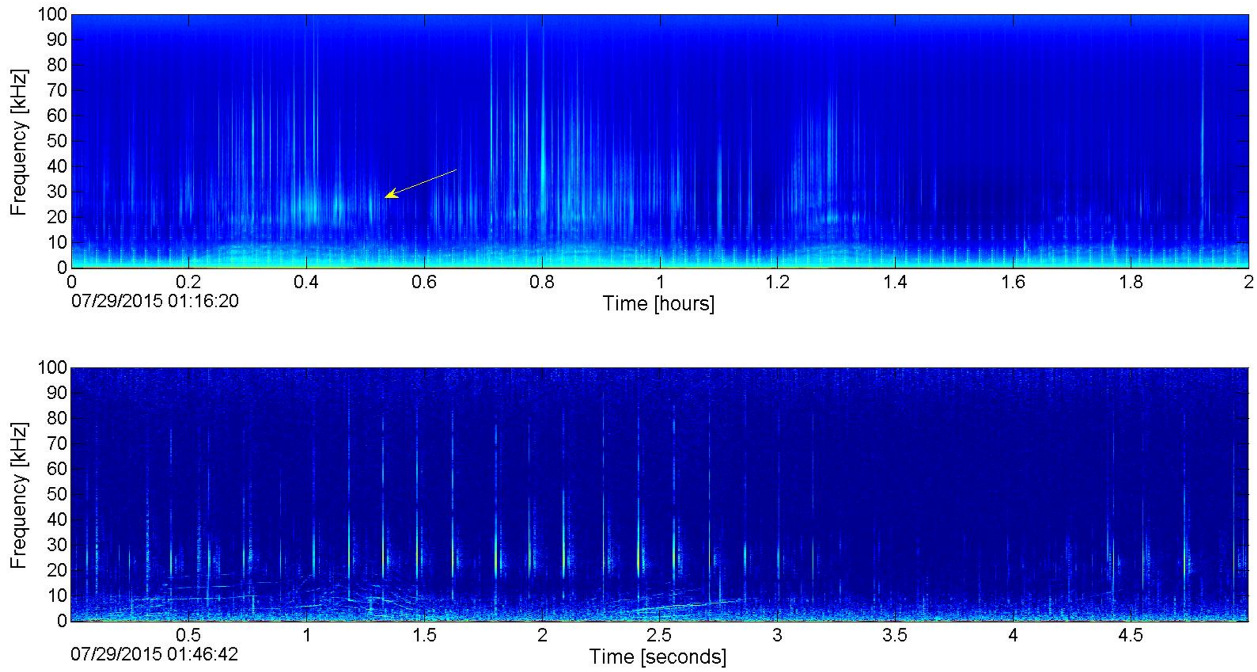

Figure 19. Click type 4 in LTSA (top) and spectrogram (bottom) recorded at site NC. Arrow indicates location of LTSA expanded in the spectrogram.

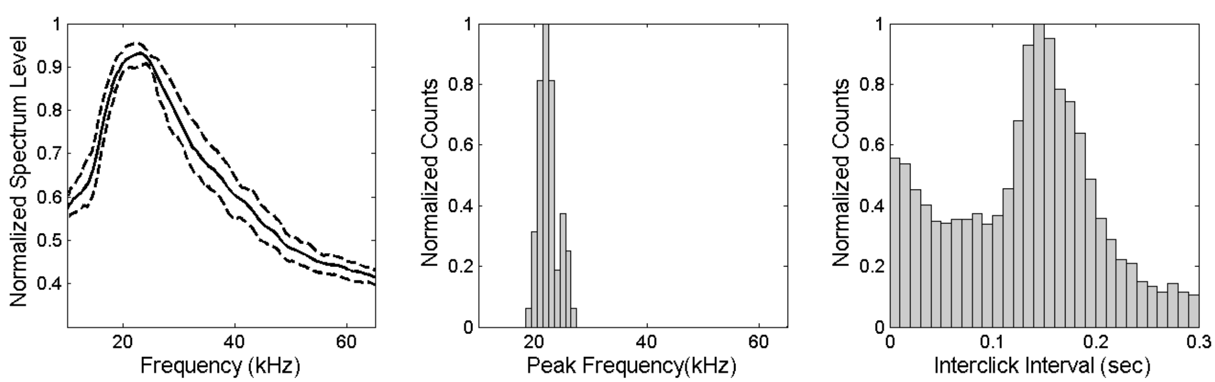

Figure 20. Left: Mean normalized received sound pressure spectrum level of click type 4 cluster (solid line) with 25th and 75th percentiles (dashed lines); Center: Distribution of click cluster peak frequencies with a peak at 22 kHz; Right: Distribution of inter-click-intervals within cluster with modal peak at 0.14 seconds.

Click Type 5

Click type 5 clicks (Figure 21) have a main peak frequency of approximately 46 kHz, and two minor spectral peaks at 20 and 26 kHz. This click type has a bimodal ICI distribution with peaks at 0.04 and 0.10 seconds (Figure 22). These may represent separate subtypes.

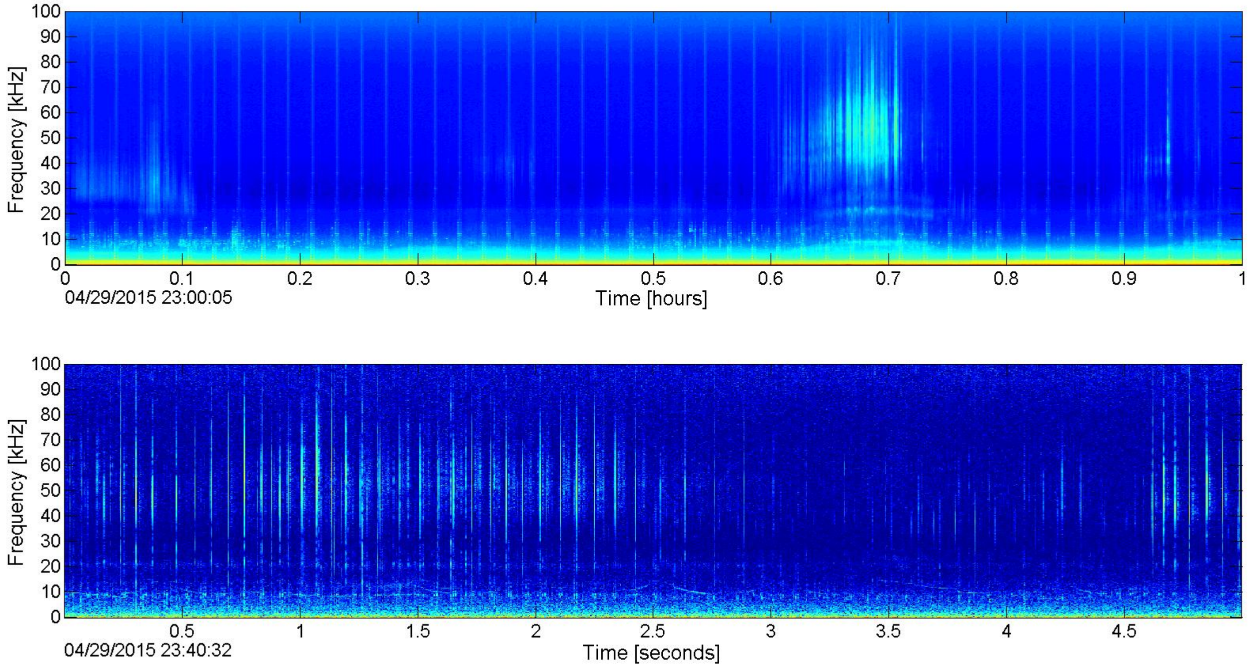

Figure 21. Click type 5 in LTSA (top) and spectrogram (bottom) recorded at site NC.

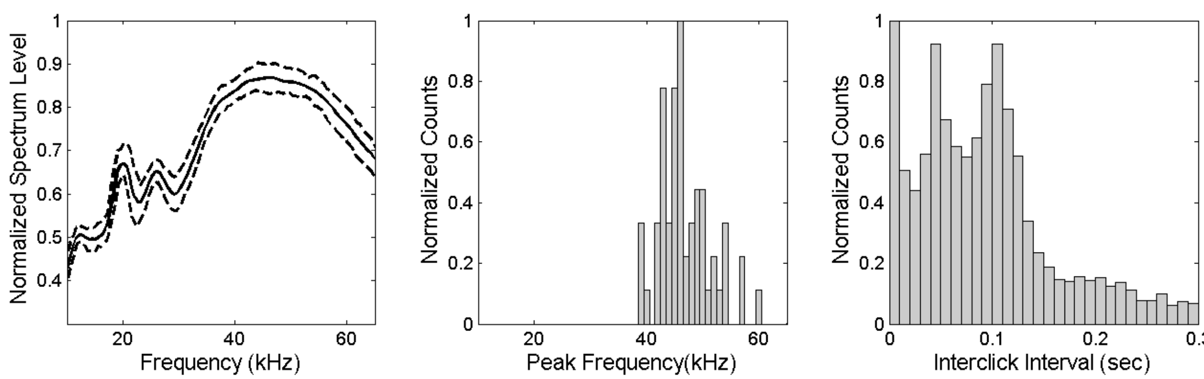

Figure 22. Left: Mean normalized received sound pressure spectrum level of click type 5 cluster (solid line) with 25th and 75th percentiles (dashed lines); Center: Distribution of click cluster peak frequencies with primary peak at 46 kHz; Right: Distribution of inter-click-intervals within cluster with bimodal peaks at 0.04 and 0.10 seconds.

Click Type 6

Click type 6 clicks (Figure 23) have a peak frequency of approximately 19 kHz and a modal ICI of 0.15 seconds (Figure 24).

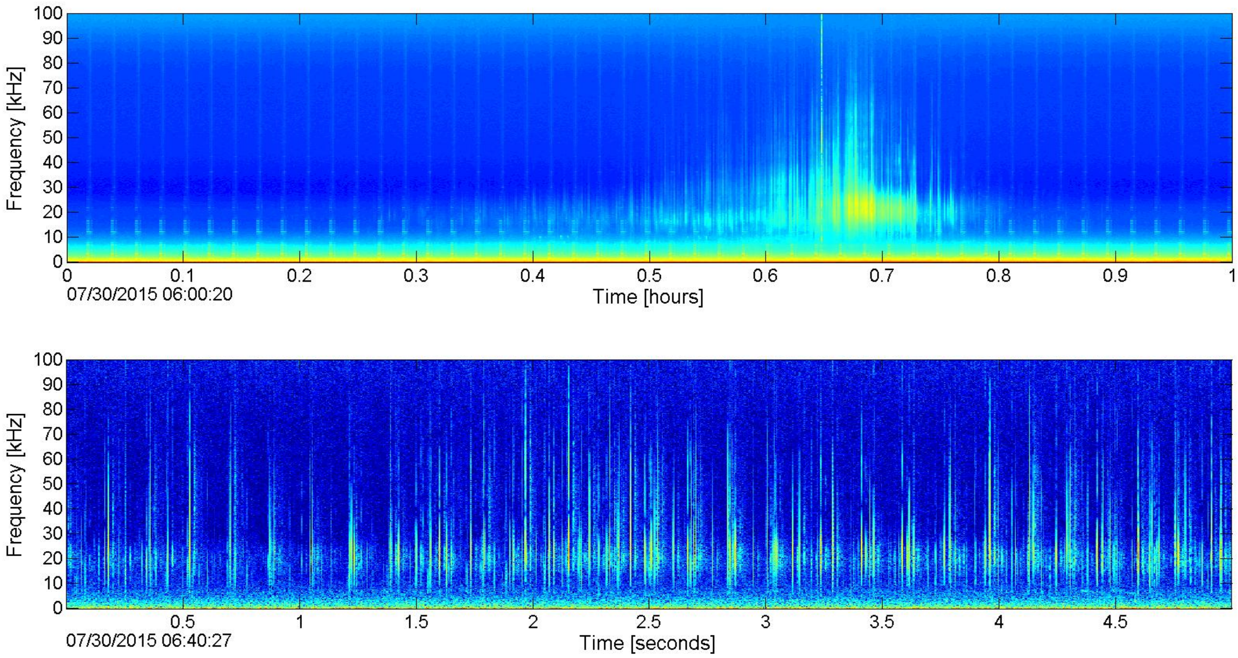

Figure 23. Click type 6 in LTSA (top) and spectrogram (bottom) recorded at site NC.

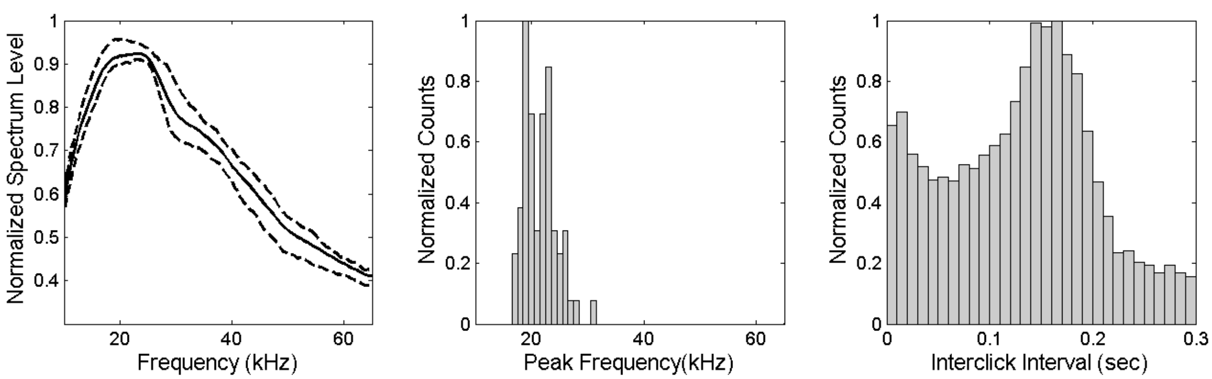

Figure 24. Left: Mean normalized received sound pressure spectrum level of click type 6 cluster (solid line) with 25th and 75th percentiles (dashed lines); Center: Distribution of click cluster peak frequencies with a peak at 19 kHz; Right: Distribution of inter-click-intervals within cluster with modal peak at 0.15 seconds.

Click Type 7

Click type 7 clicks (Figure 25) have a peak frequency of approximately 24 kHz and a modal ICI of 0.07 seconds (Figure 26).

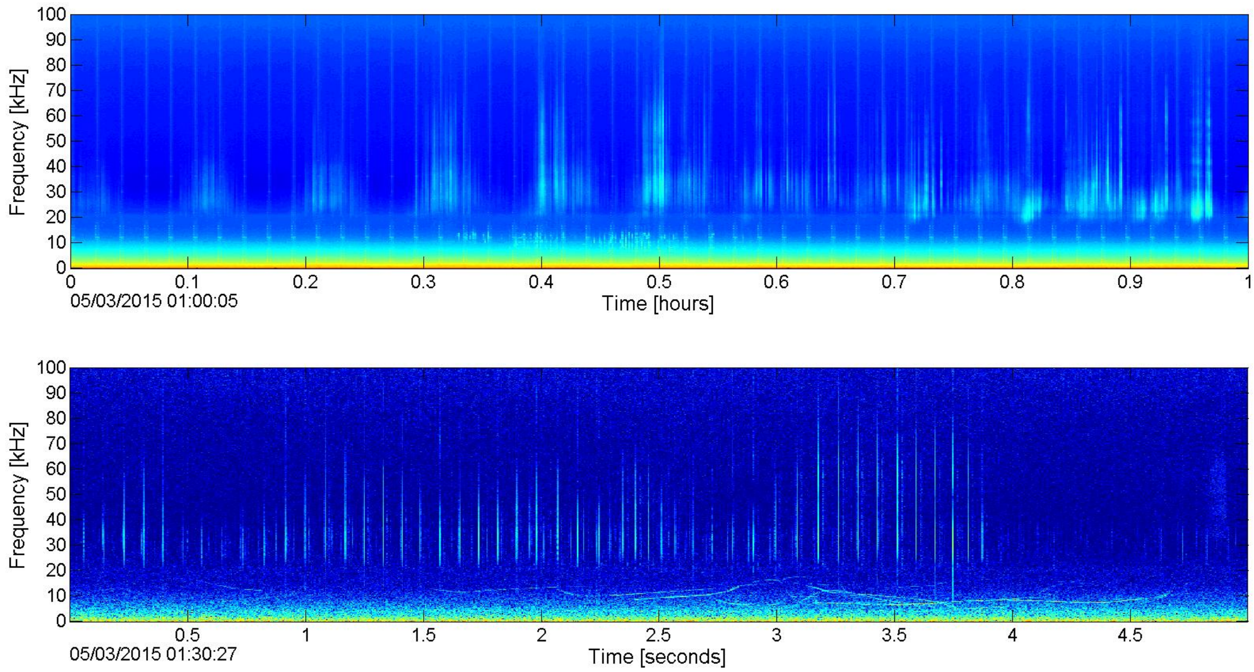

Figure 25. Click type 7 in LTSA (top) and spectrogram (bottom) recorded at site NC.

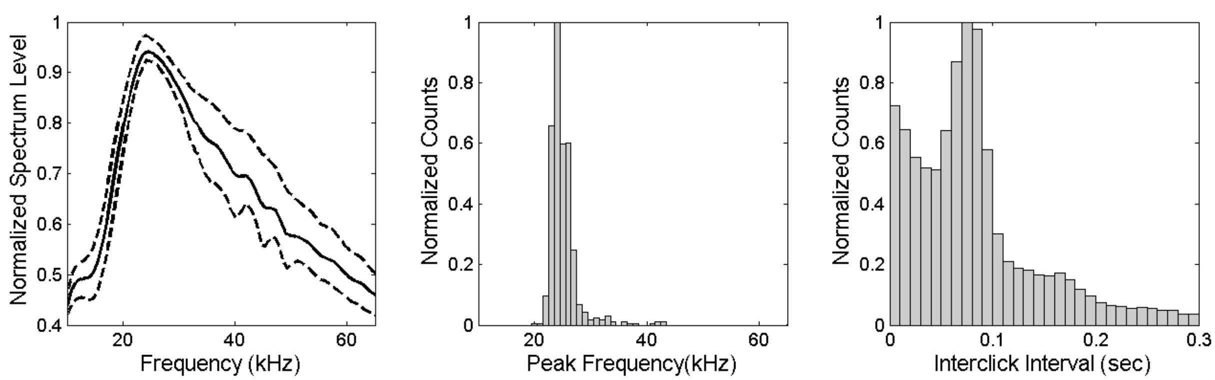

Figure 26. Left: Mean normalized received sound pressure spectrum level of click type 7 cluster (solid line) with 25th and 75th percentiles (dashed lines); Center: Distribution of click cluster peak frequencies with a peak at 24 kHz; Right: Distribution of inter-click-intervals within cluster with modal peak at 0.07 seconds.

Click Type 8

Click type 8 clicks (Figure 27) have a main peak frequency at approximately 41 kHz, and two minor spectral peaks at 15 and 18 kHz (Figure 28). This click type has a modal ICI of 0.11 seconds (Figure 28).

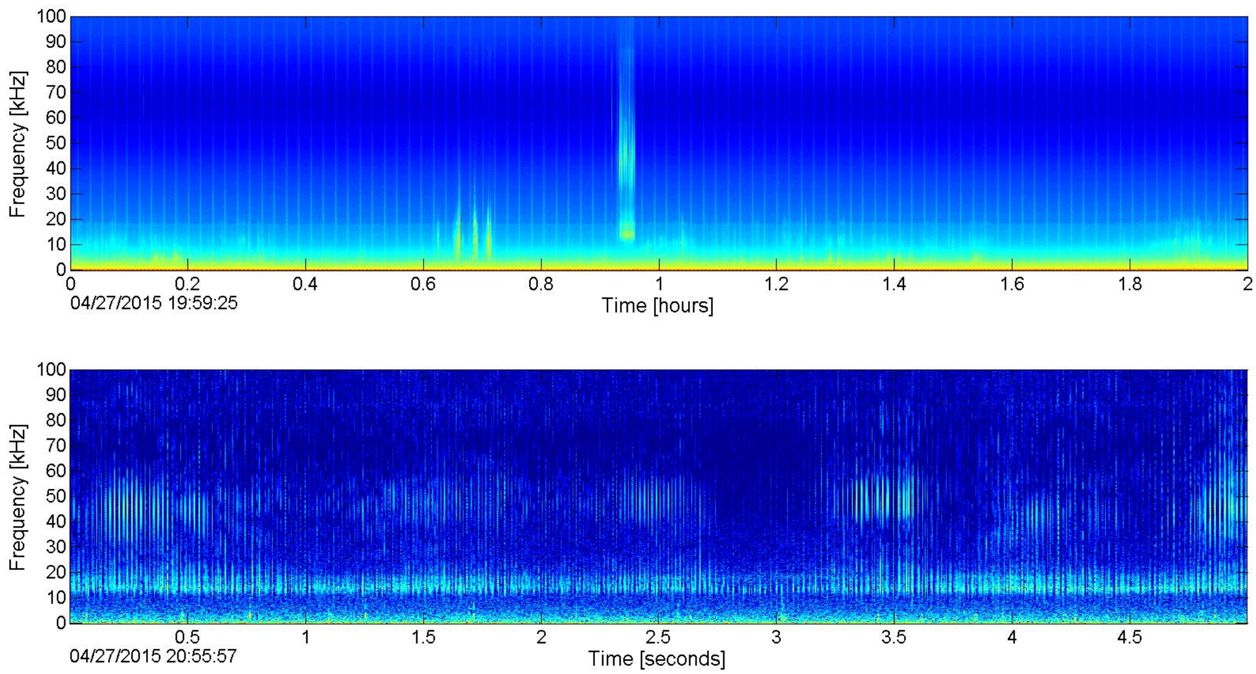

Figure 27. Click type 8 in LTSA (top) and spectrogram (bottom) recorded at site OC.

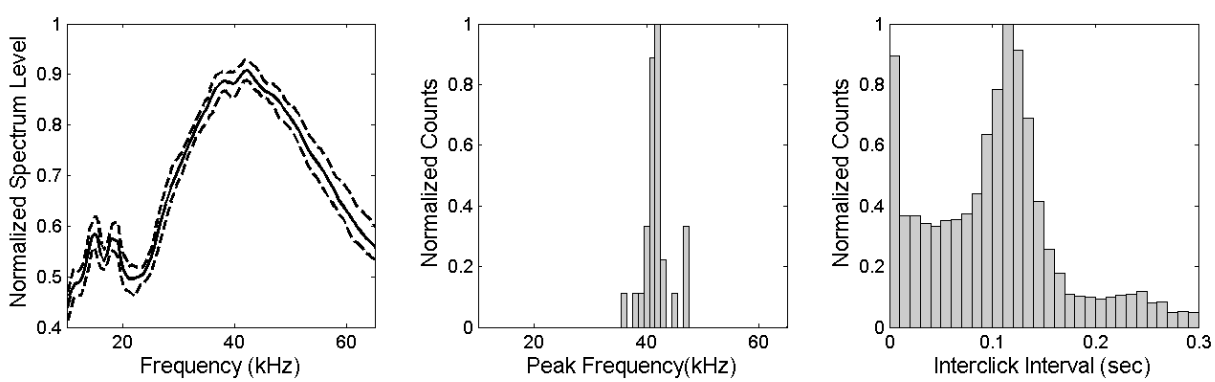

Figure 28. Left: Mean normalized received sound pressure spectrum level of click type 8 cluster (solid line) with 25th and 75th percentiles (dashed lines); Center: Distribution of click cluster peak frequencies with primary peak 41 kHz; Right: Distribution of inter-click-intervals within cluster with modal ICI of 0.11 seconds.

Anthropogenic Sounds

Several anthropogenic sounds were monitored for this report: broadband ship sounds, explosions, airguns, and echosounders. The start and end of each individual sound or overall session was logged and their durations were added to estimate cumulative hourly presence. Manual effort was expended for broadband ship sounds and echosounders (**Table 2**). A detector was used for the airgun and explosion analyses, both described below.

Table 2. Anthropogenic sound data analysis parameters.

Sound Type	LTSA Search Parameters	
	Plot Length (hr)	Frequency Range (Hz)
Broadband Ship Sound	3	10 – 5,000
Explosions	0.75	10 – 1,000
Airguns	0.75	10 – 2,000
Echosounders	1	5,000 – 100,000

Broadband Ship Sound

Broadband ship sound occurs when a ship passes within a few kilometers of the hydrophone. Ship sound can occur for many hours at a time, but broadband ship sound typically lasts from 10 minutes up to 3 hours. Ship sound has a characteristic frequency-range dependent interference pattern in the LTSA (McKenna *et al.*, 2012). Combination of sound wave direct paths and surface reflected paths produce constructive and destructive interference (bright and dark bands) in the spectrogram that varies by frequency and distance between the ship and the receiver (Figure 29). Noise can extend above 10 kHz, though it typically falls off above a few kHz. Broadband ship analysis effort consisted of manual scans of the LTSA set at 3 hours with a frequency range of 10 – 5,000 Hz.

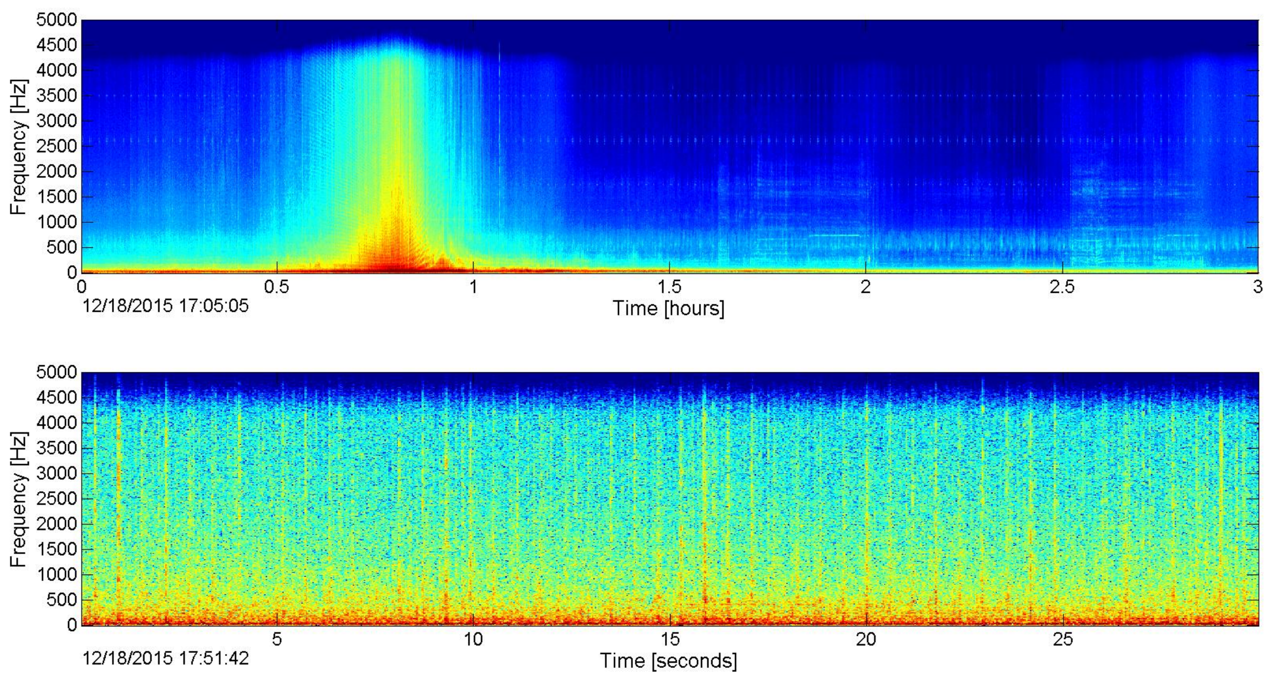

Figure 29. Broadband ship sound in the LTSA (top) and spectrogram (bottom) recorded at site HZ.

Explosions

Effort was directed toward detecting explosive sounds in the recordings including military explosions, shots from sub-seafloor exploration, and seal bombs used by the fishing industry. An explosion appears as a vertical spike in the LTSA that, when expanded in the spectrogram, has a sharp onset with a reverberant decay (Figure 30). Explosions were detected automatically using a matched filter detector on data decimated to 10 kHz sampling rate. The timeseries was filtered with a 10^{th} order Butterworth bandpass filter between 200 and 2,000 Hz. Cross-correlation was computed between 75 seconds of the envelope of the filtered timeseries and the envelope of a filtered example explosion (0.7 s, Hann windowed) as the match filter signal. The cross-correlation was squared to 'sharpen' peaks of explosion detections. A floating threshold was calculated by taking the median cross-correlation value over the current 75 seconds of data to account for detecting explosions within noise, such as shipping. A cross-correlation threshold of $3*10^{-6}$ above the median was set. When the correlation coefficient reached above threshold, the timeseries was inspected more closely. Consecutive explosions were required to have a minimum time distance of 0.5 second to be detected. A 300-point (0.03 s) floating average energy across the detection was computed. The start and end times above the threshold were determined when the energy rose by more than 2 dB above the median energy across the detection. Peak-to-peak (pp) and root-mean-square (rms) received sound pressure levels (RL) were computed over the potential explosion period as well as a timeseries of the length of the explosion template before and after the explosion. The potential explosion was classified as a false detection and deleted if 1) the dB difference of pp and rms levels between signal and time AFTER the detection was less than 4 dB or 1.5 dB respectively; 2) the dB difference of pp and rms levels between signal and time BEFORE the signal was less than 3 dB or 1 dB, respectively; and 3) the detection was shorter than 0.03 or longer than 0.55 seconds of duration. The thresholds were evaluated based on the distribution of histograms of manually verified true and false detections. A trained analyst subsequently verified the remaining potential explosions for accuracy. Explosions have energy as low as 10 Hz and often extend up to 2,000 Hz or higher, lasting for a few seconds including the reverbation.

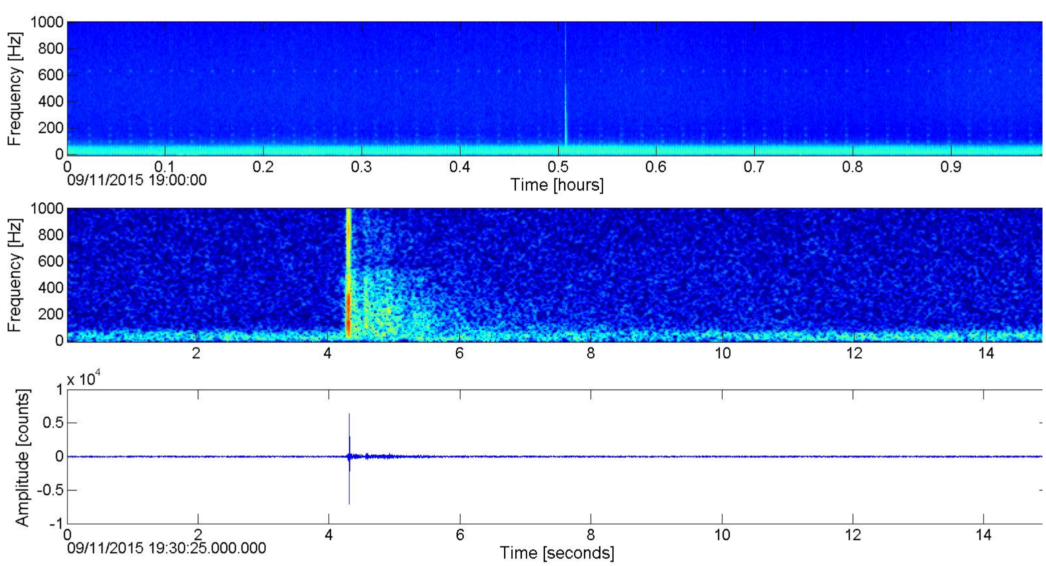

Figure 30. Explosion example in the LTSA (top), spectrogram (middle) and timeseries (bottom) recorded at site OC.

Airguns

Airguns are regularly used in seismic exploration to investigate the ocean floor and what lies beneath it. A container of high-pressure air is momentarily vented to the surrounding water, producing an air-filled cavity which expands and contracts violently several times (Barger and Hamblen, 1980). While most of the energy produced by an airgun array falls below 250 Hz, airguns can produce significant energy at frequencies up to at least 1 kHz (Blackman *et al.*, 2004). Source levels tend to be over 200 dB re 1 μPa-m (Amundsen and Landro, 2010), and have been measured up to 260 dB rms re 1 μPa-m (Hildebrand, 2009). These blasts typically have an inter-pulse interval of approximately 10 seconds and can last from several hours to days (Figure 31). Airguns were detected automatically using a matched filter detector on data decimated to 10 kHz sampling rate. The timeseries was filtered with a 10^{th} order Butterworth bandpass filter between 25 and 200 Hz. Cross correlation was computed between 75 seconds of the envelope of the filtered timeseries and the envelope of a filtered example explosion (0.7 s, Hann windowed) as the matched filter signal. The cross correlation was squared to 'sharpen' peaks of airgun blast detections. A floating threshold was calculated by taking the median cross correlation value over the current 75 seconds of data to account for detecting airguns within noise, such as shipping. A cross correlation threshold of $2*10^{-6}$ above the median was set. When the correlation coefficient reached above this threshold, the timeseries was inspected more closely. Consecutive airgun blasts were required to have a minimum time distance of 2 seconds to be detected. A 300-point (0.03 s) floating average energy across the detection was computed. The start and end times above the threshold were marked when the energy rose by more than 2 dB above the median energy across the detection. Peak-to-peak (pp) and root-mean-square (rms) received sound pressure levels (RL) were computed over the potential blast period as well as a timeseries of the length of the airgun blast template before and after the explosion. The potential airgun blast was classified as a false detection and deleted if 1) the dB difference of pp and rms between signal and time AFTER the detection was less than 4 dB or 0.5 dB respectively; 2) the dB difference of pp and rms between signal and time BEFORE the signal was less than 3 dB or 0.5 dB, respectively; and 3) the detection was shorter than 0.03 or longer than 10 s. The thresholds were evaluated based on the distribution of histograms of manually verified true and false detections. Airgun blast interpulse intervals were used to discard potential airgun detections that were not part of a sequence. A trained analyst subsequently verified the remaining potential airgun detections for accuracy. Airgun blasts have energy as low as 10 Hz and can extend up to 250 Hz or higher, lasting for a few seconds including the reverberation.

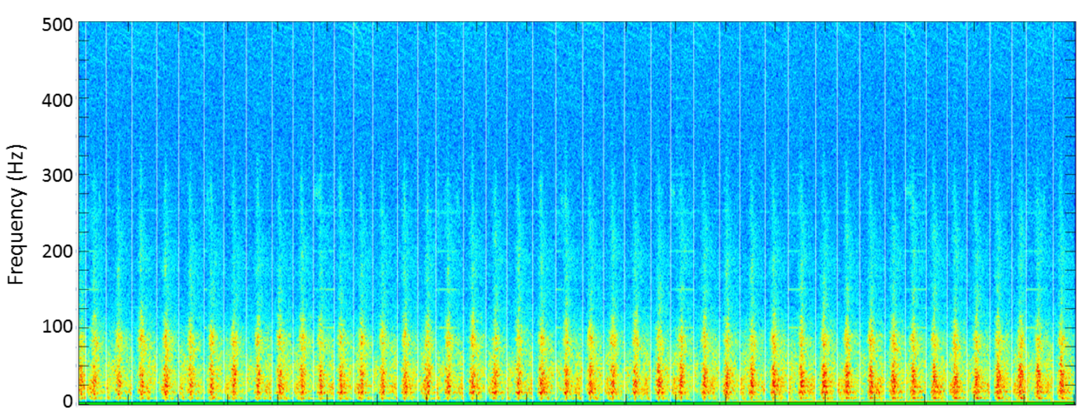

Figure 31. Airgun pulses at site HZ in the analyst verification stage of the detector.

Echosounders
Echosounding sonars transmit short pulses or frequency sweeps, typically in the high-frequency (above 5 kHz) band (Figure 32), though echosounders are occasionally found in the mid-frequency range (2-5 kHz). Many large and small vessels are equipped with echosounding sonar for water depth determination; typically these echosounders are operated much of the time a ship is at sea, as an aid for navigation. In addition, sonars may be used for sea bottom mapping, fish detection, or other ocean sensing. Presence of high-frequency echosounders was manually detected by analysts reviewing LTSA plots.

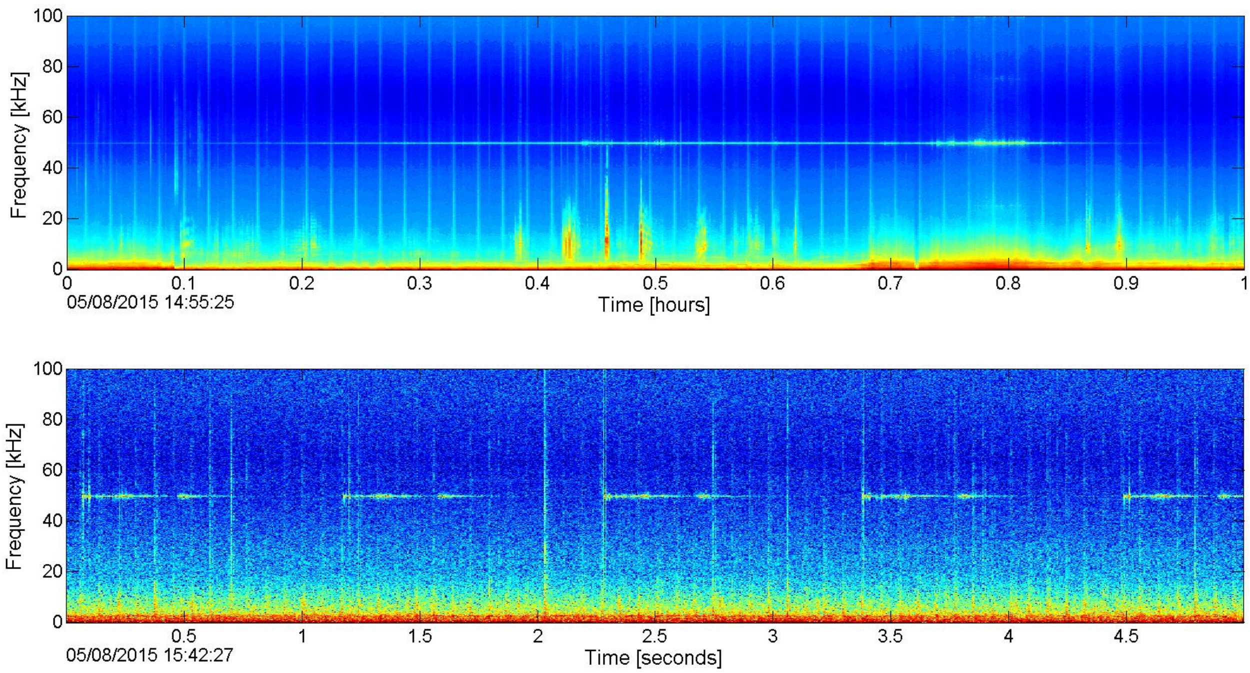

Figure 32. Echosounders in the LTSA (top) and spectrogram (bottom) recorded at site OC.

Results
The results of acoustic data analysis at sites NC (April – September 2015), OC (April 2015 – February 2016), and HZ (June 2015 – March 2016) are summarized below. We describe the low-frequency ambient soundscape and the seasonal occurrence and relative abundance of several marine mammal acoustic signals and detected anthropogenic sounds of interest.

Low-Frequency Ambient Soundscape

Daily-averaged ambient soundscape spectra were processed into monthly-averages and plotted using the same monthly color scheme for each of the deployments so that months from different sites and years can be compared. Partial months, those with less than 90% of total days recorded, include an asterisk (*) in the color legend.

- For all sites, levels between 10-100 Hz were dominated by anthropogenic sounds, primarily ship traffic and seismic exploration (Hildebrand, 2009). In this band, levels across all sites are within 10 dB of one another, with the highest levels at site OC and lowest at site NC (**Figure 33**, **Figure 34**, **Figure 35**, **Figure 36**).
- Between 100-1000 Hz sound pressure spectrum levels are largely a function of wind and sea state. The highest levels are found at site HZ in November 2015, and the lowest at sites HZ and NC in July 2015 (**Figure 33**, **Figure 34**, **Figure 35**, **Figure 36**).
- There is a year-round presence of an unidentified down sweeping signal between ~400-800 Hz at site HZ that can be clearly seen in the summer and fall monthly sound pressure spectrum level averages (**Figure 36**). In July 2015, the signal has its highest signal-to-noise ratio (SNR) due to otherwise particularly low ambient sound levels, with signal levels in that band reaching ~6 dB above ambient levels (**Figure 37**).
- A seasonal 20 Hz fin whale signal is present at all three sites. Highest levels were measured at site HZ in November 2015 (**Figure 33**, **Figure 34**, **Figure 35**, **Figure 36**).

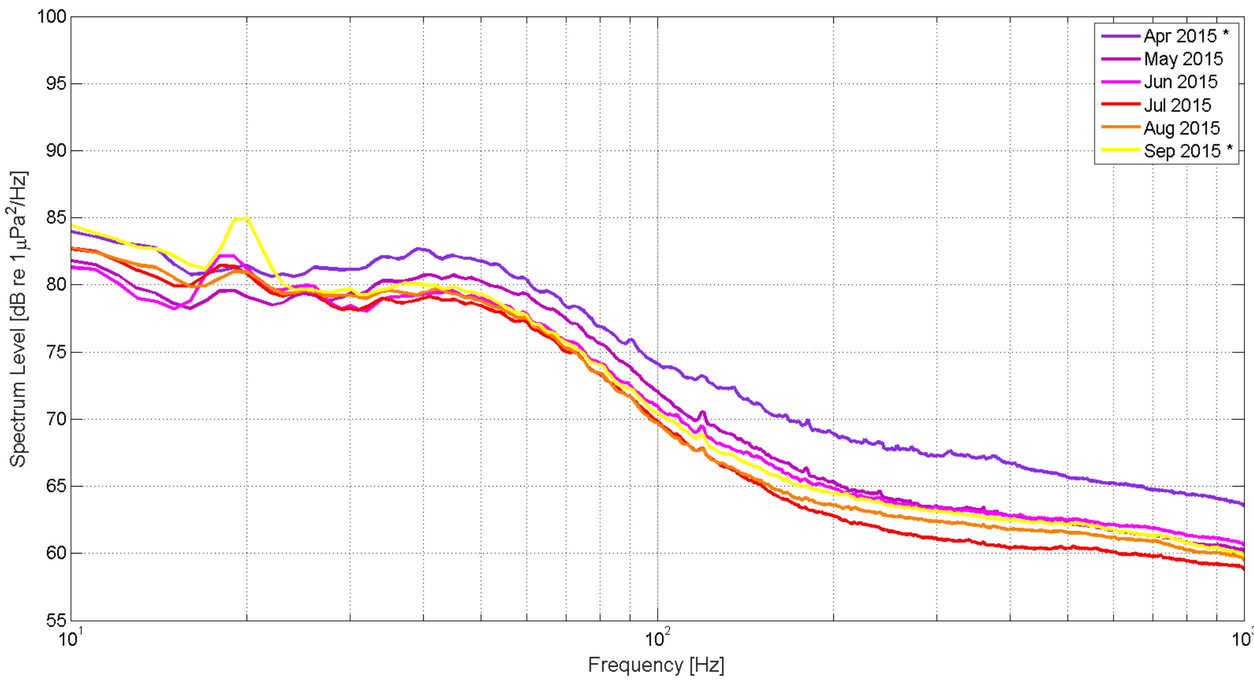

Figure 33. Low-frequency ambient soundscape at site NC from April to September 2015. Legend gives color-coding by month. Months with an asterisk (*) have partial recording effort.

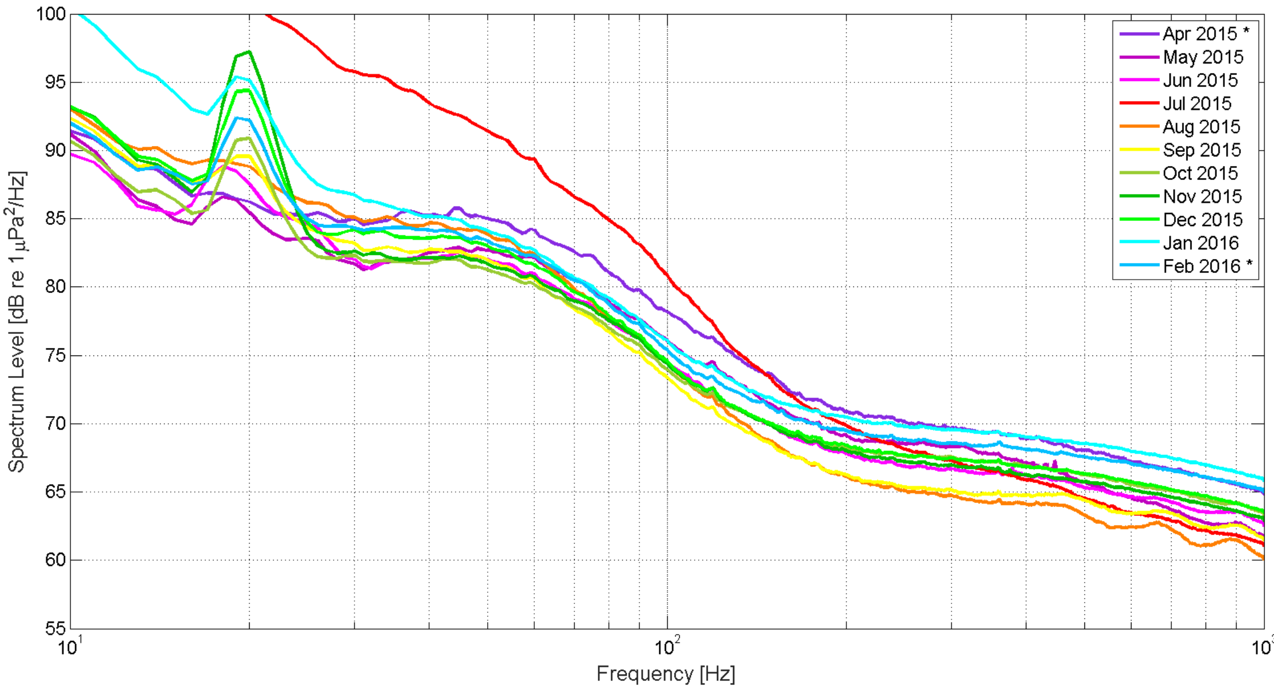

Figure 34. Strumming included low-frequency ambient soundscape at site OC from April 2015 to February 2016 showing monthly sound pressure spectrum level averages. Legend gives color-coding by month. Months with an asterisk (*) have partial recording effort.

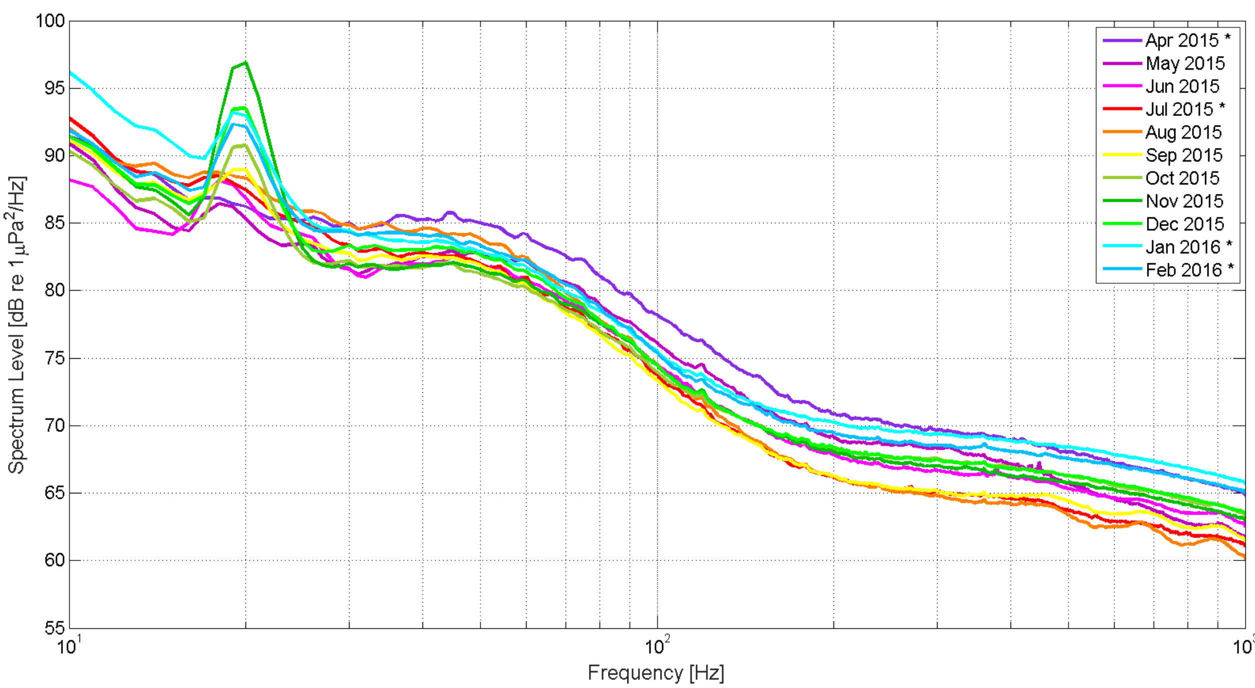

Figure 35. Strumming excluded low-frequency ambient soundscape at site OC from April 2015 to February 2016 showing monthly sound pressure spectrum level averages. Legend gives color-coding by month. April 2015 and February 2016, with an asterisk (*) in the legend, have partial recording effort.

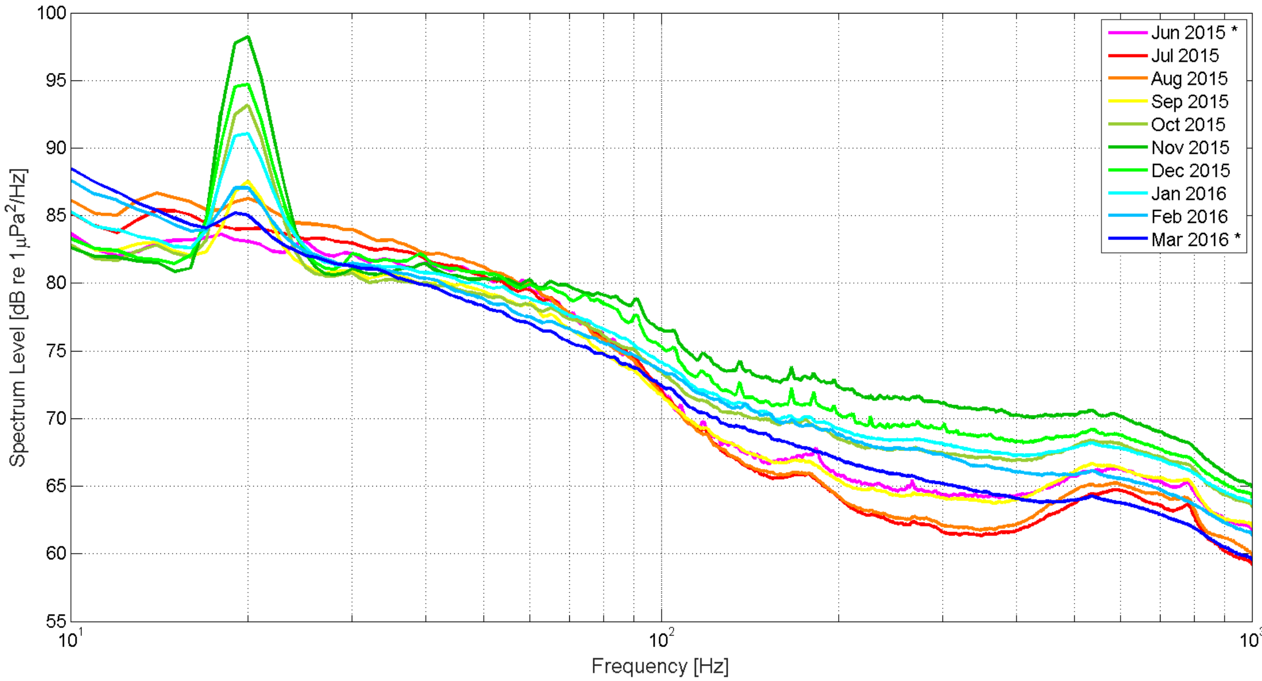

Figure 36. Low-frequency ambient soundscape at site HZ from June 2015 to March 2016. Legend gives color-coding by month. Months with an asterisk (*) have partial recording effort.

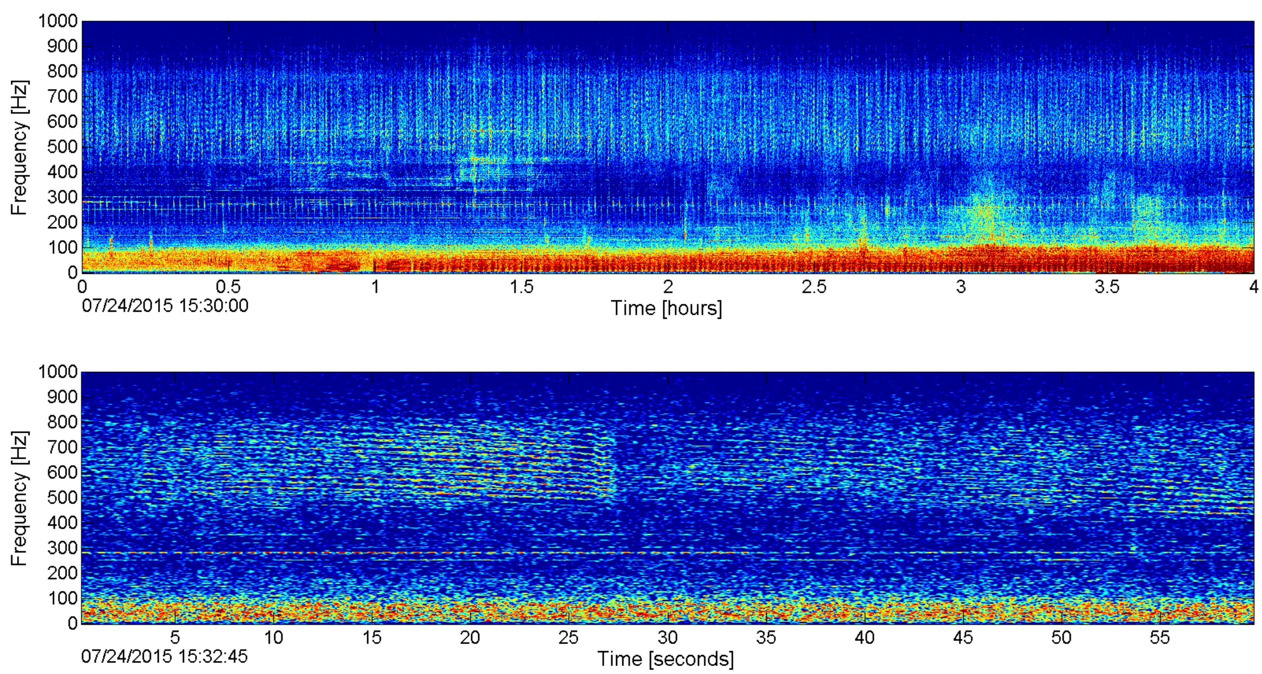

Figure 37. Example of the ~400-800 Hz down swept signal present at site HZ.

Odontocetes

Beaked Whales

Detections of Cuvier's, Gervais', and Sowerby's beaked whale echolocation clicks were detected at all three sites. Northern bottlenose whales and Blainville's beaked whales were not detected at any of the three sites over the recording periods. More details of each species' presence at the three sites are given below.

Cuvier's Beaked Whales

- Cuvier's beaked whale echolocation clicks were detected at all three sites; however there were more detections at site HZ than at sites OC and NC (Figure 38).
- Click detections peaked at site HZ in October 2015 and January 2016 (Figure 38).
- There was no discernible diel pattern for Cuvier's beaked whale echolocation clicks (Figure 39).

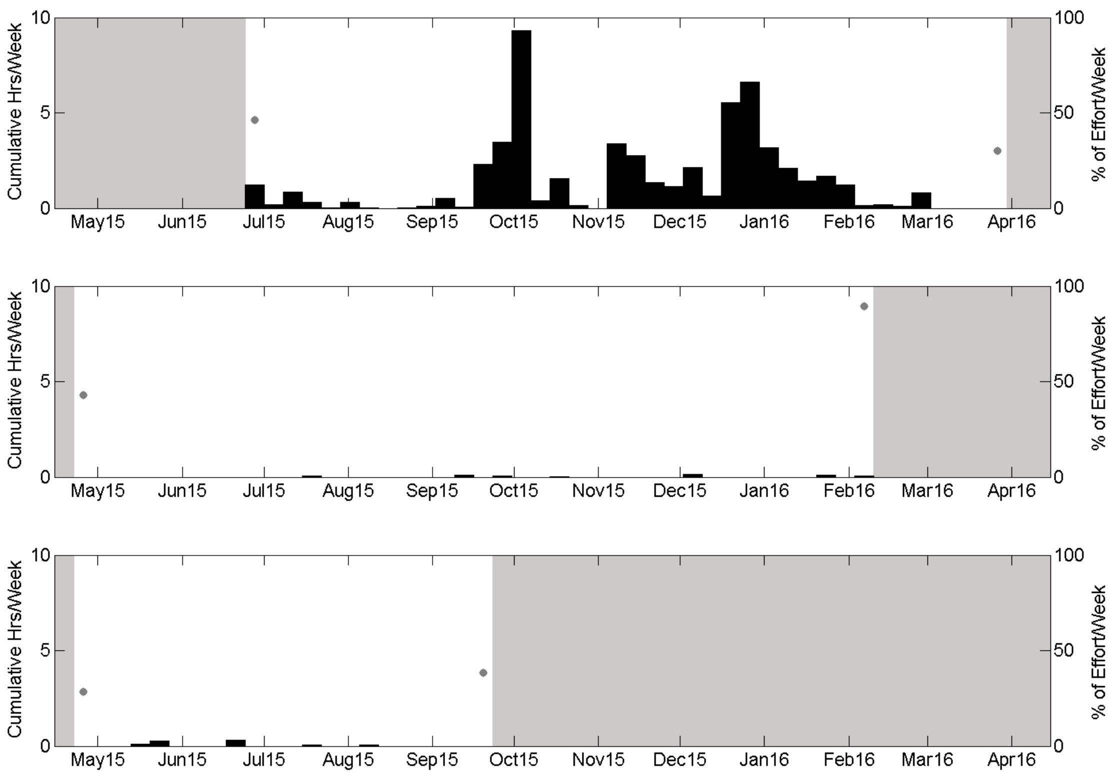

Figure 38. Weekly presence (black bars) of Cuvier's beaked whale echolocation clicks between April 2015 and April 2016 at site HZ (top), OC (middle), and NC (bottom). Gray dots represent percent of effort per week in weeks with less than 100% recording effort, and gray shading represents periods with no recording effort. Where gray dots or shading are absent, full recording effort occurred for the entire week.

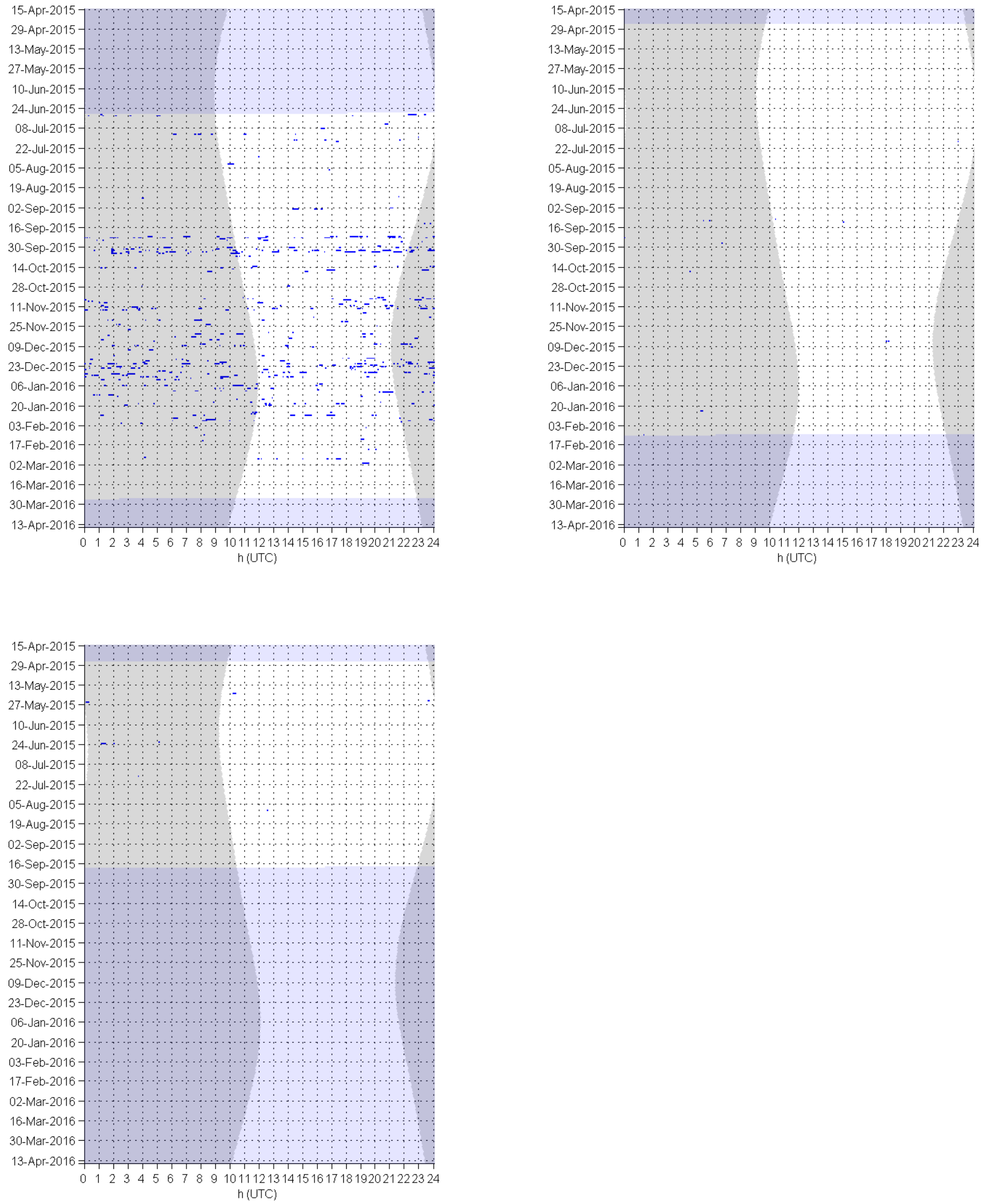

Figure 39. Cuvier's beaked whale echolocation clicks in five-minute bins (blue bars) at sites HZ (top left), OC (top right), and NC (bottom). Gray vertical shading denotes nighttime, and light purple horizontal shading denotes absence of acoustic data.

Gervais' Beaked Whales

- Gervais's beaked whale echolocation clicks were detected at all three sites, with most detections at site NC, and the fewest (just one) at site OC (Figure 40).
- Detections peaked in May 2015 at site NC and in January 2016 at site HZ (Figure 40).
- There was no diel pattern for Gervais' beaked whale echolocation clicks (Figure 41).

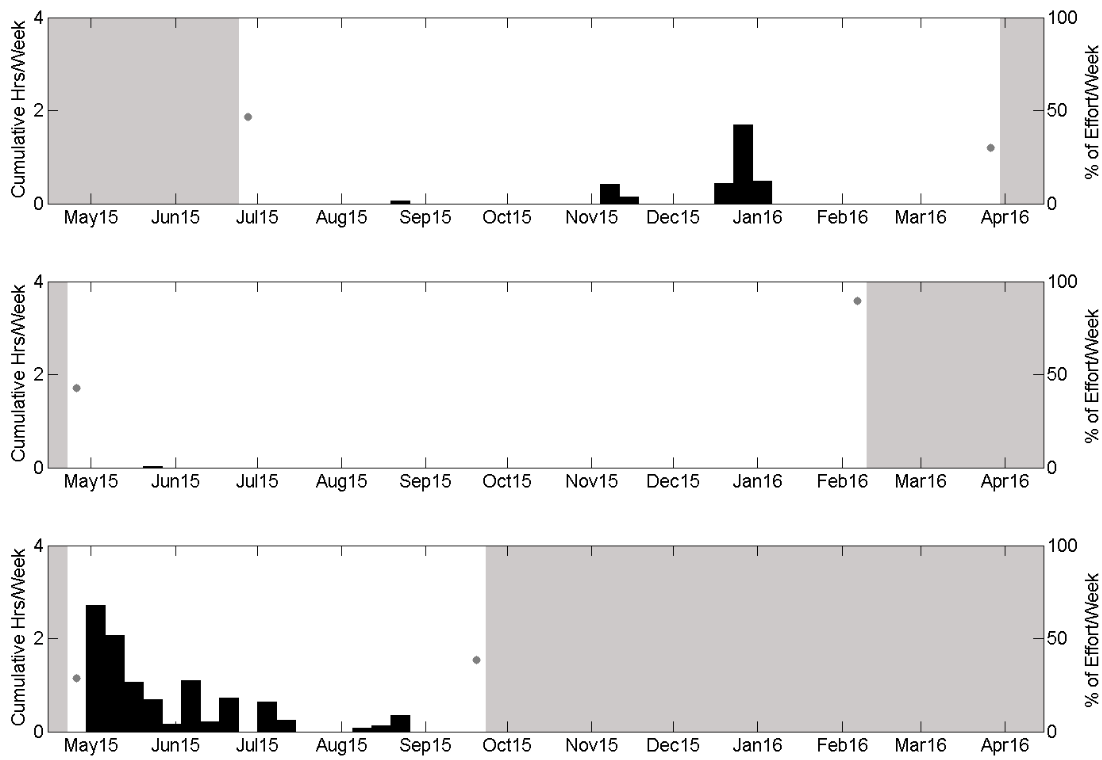

Figure 40. Weekly presence (black bars) of Gervais' beaked whale echolocation clicks between April 2015 and April 2016 at site HZ (top), OC (middle), and NC (bottom). Effort markings are described in Figure 38.

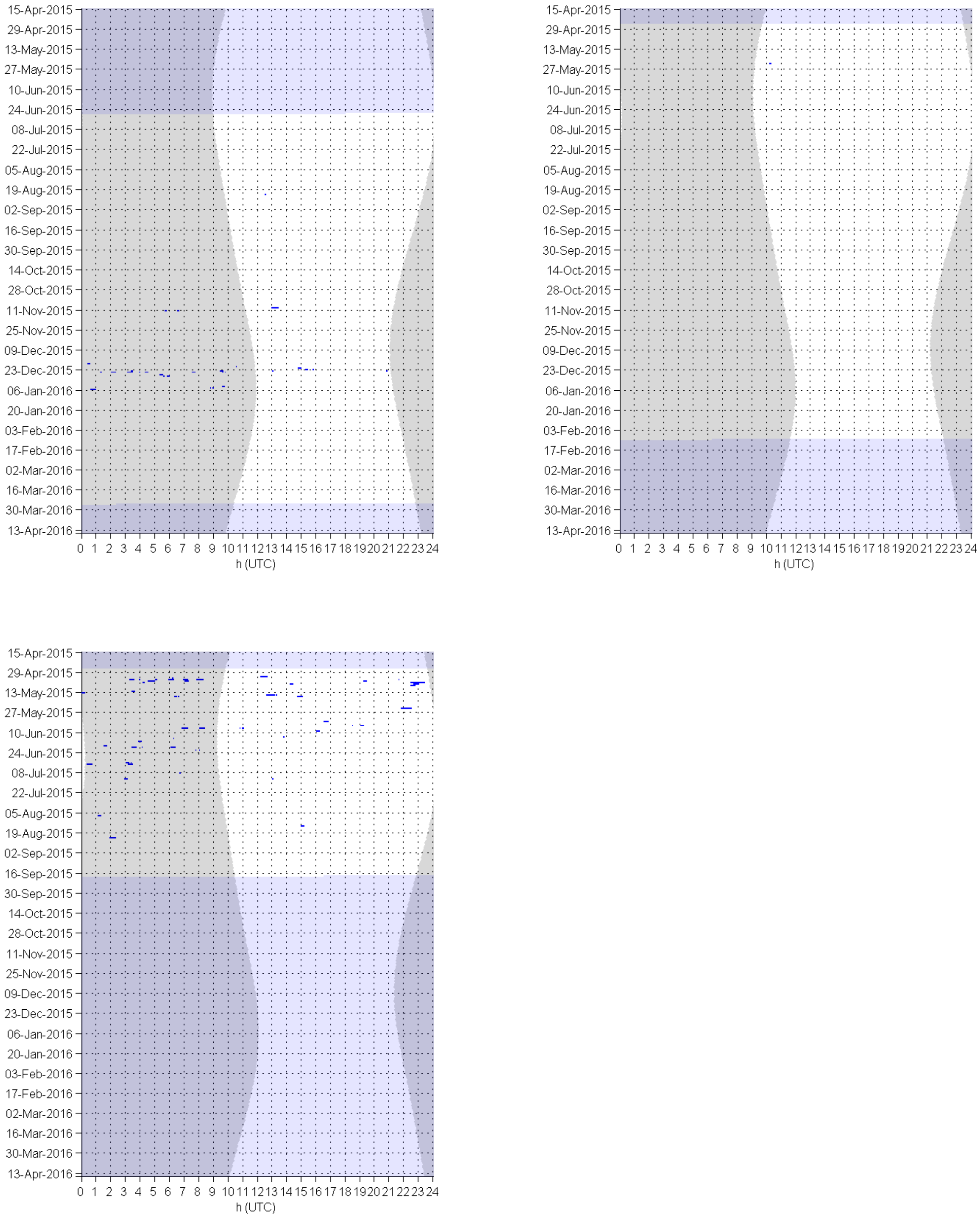

Figure 41. Gervais' beaked whale echolocation clicks in five-minute bins (blue bars) at sites HZ (top left), OC (top right), and NC (bottom). Effort markings are described in Figure 39.

Sowerby's Beaked Whales

- Sowerby's beaked whale echolocation clicks were detected in low numbers at sites NC and OC, and in higher numbers at site HZ (Figure 42).
- There was no discernible diel pattern for Sowerby's beaked whale echolocation clicks (Figure 43).

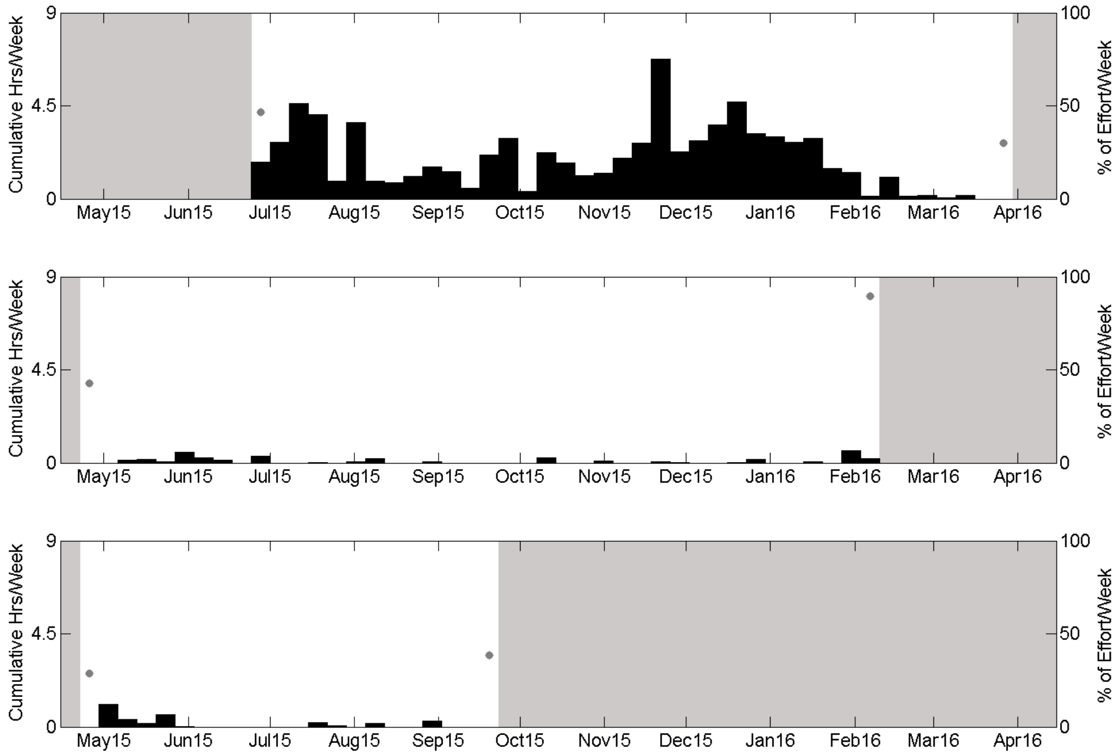

Figure 42. Weekly presence (black bars) of Sowerby's beaked whale echolocation clicks between April 2015 and April 2016 at site HZ (top), OC (middle), and NC (bottom). Effort markings are described in Figure 38.

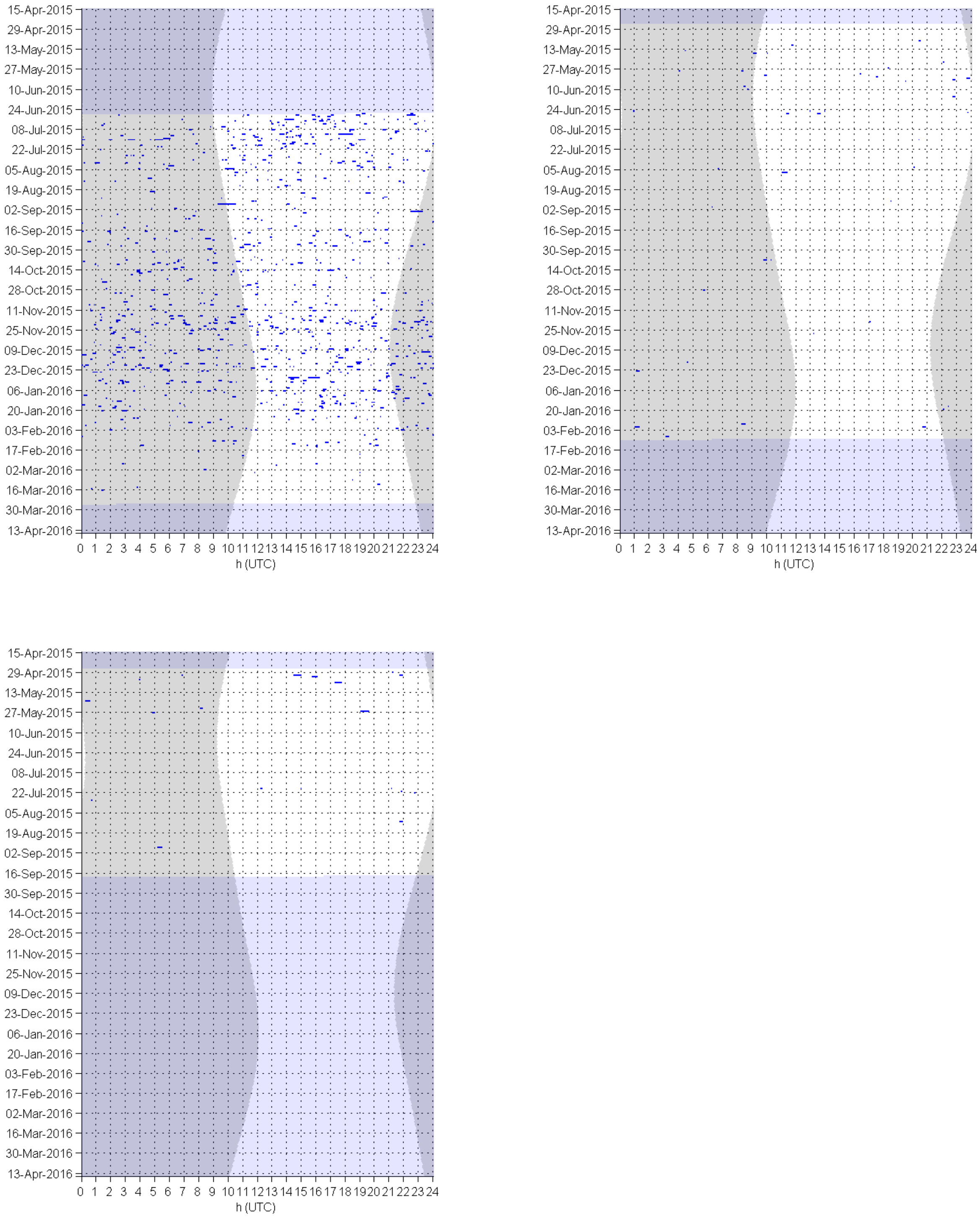

Figure 43. Sowerby's beaked whale echolocation clicks in five-minute bins (blue bars) at sites NC (top left), OC (top right), and HZ (bottom). Effort markings are described in Figure 39.

Sperm Whales

- Sperm whale clicks were detected at all three sites (Figure 44).
- There was no diel pattern for Sperm whale clicks at any of the sites (Figure 45).

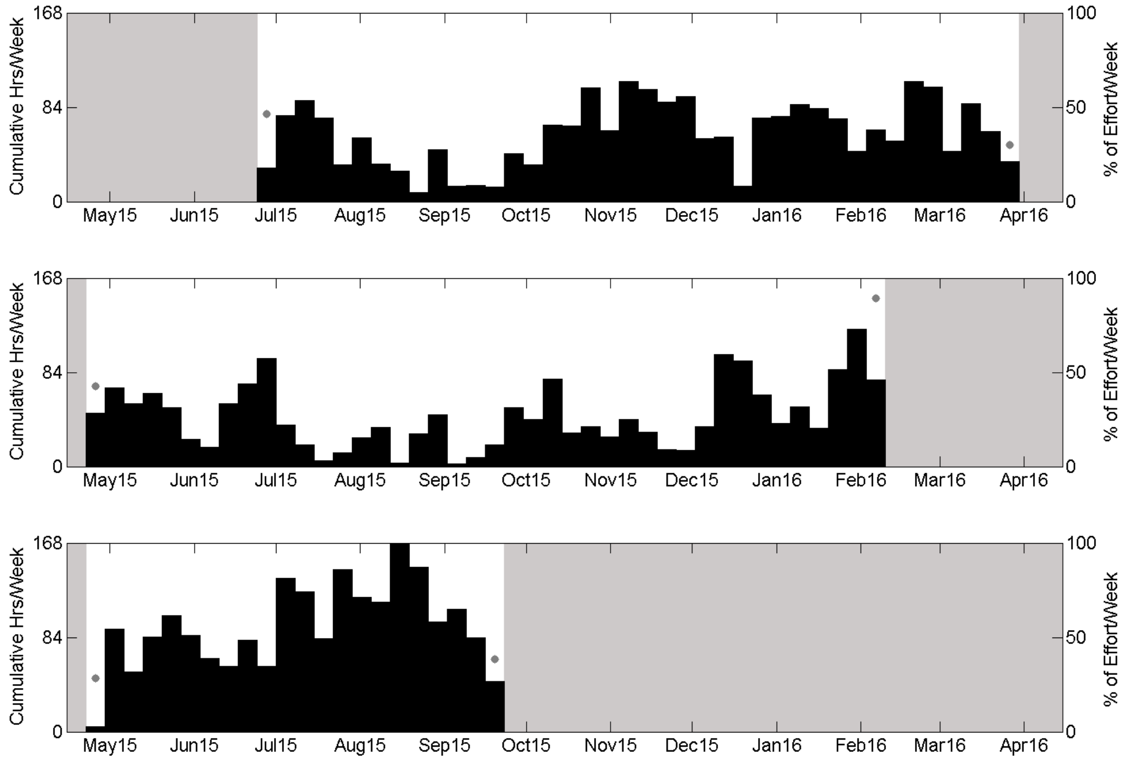

Figure 44. Weekly presence (black bars) of sperm whale echolocation clicks between April 2015 and April 2016 at site HZ (top), OC (middle), and NC (bottom). Effort markings are described in Figure 38.

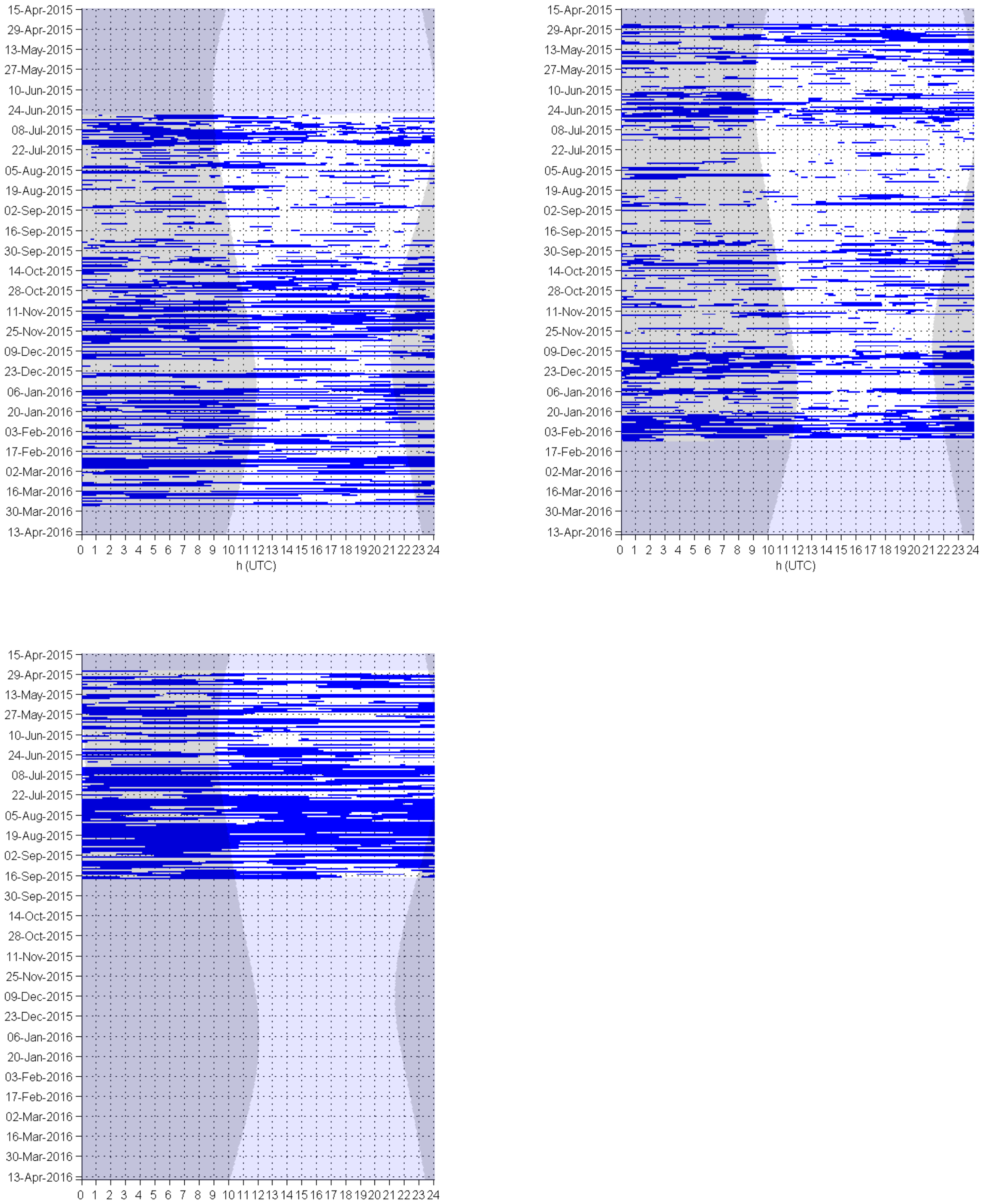

Figure 45. Sperm whale echolocation clicks in five-minute bins (blue bars) at sites HZ (top left), OC (top right), and NC (bottom). Effort markings are described in Figure 39.

***Kogia* spp.**

- *Kogia* spp. click were detected at all three sites, with the fewer detections at site OC than at sites NC and HZ (Figure 46).
- Detections at site NC peaked in May, late July, and September 2015 (Figure 46).
- Detections at site HZ peaked in August and early December 2015 (Figure 46).
- There was no diel pattern for *Kogia* spp. clicks (Figure 47).

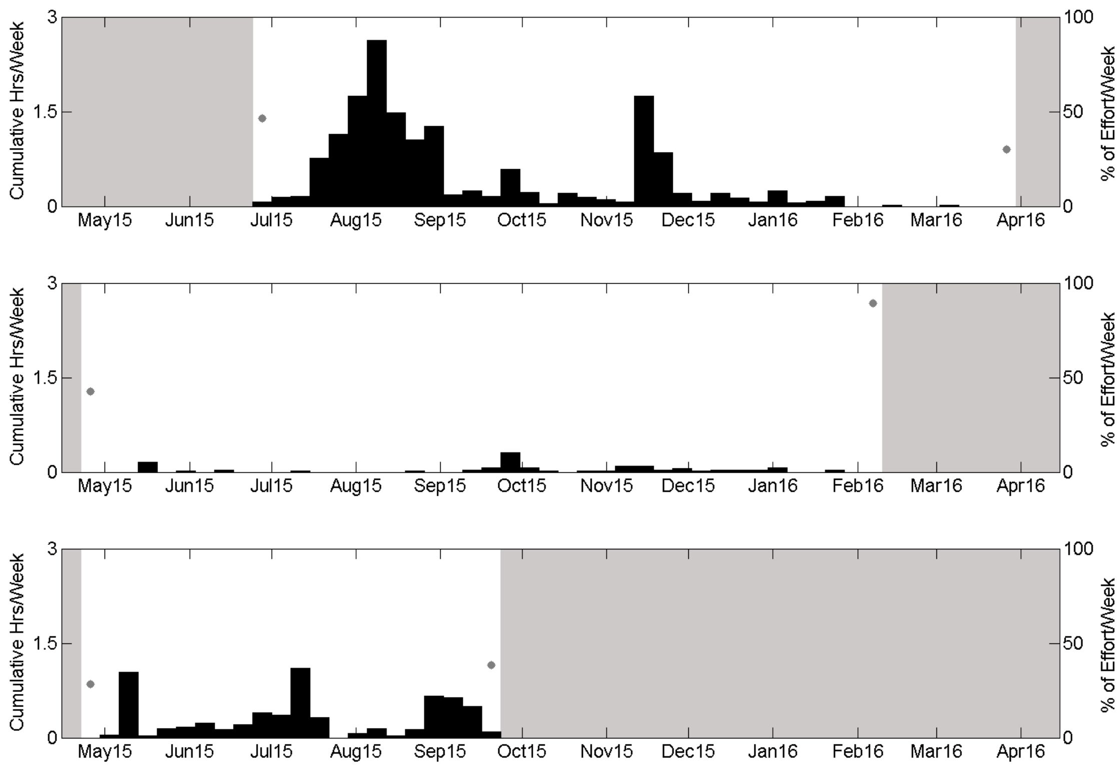

Figure 46. Weekly presence (black bars) of *Kogia* spp. echolocation clicks between April 2015 and April 2016 at site HZ (top), OC (middle), and NC (bottom). Effort markings are described in Figure 38.

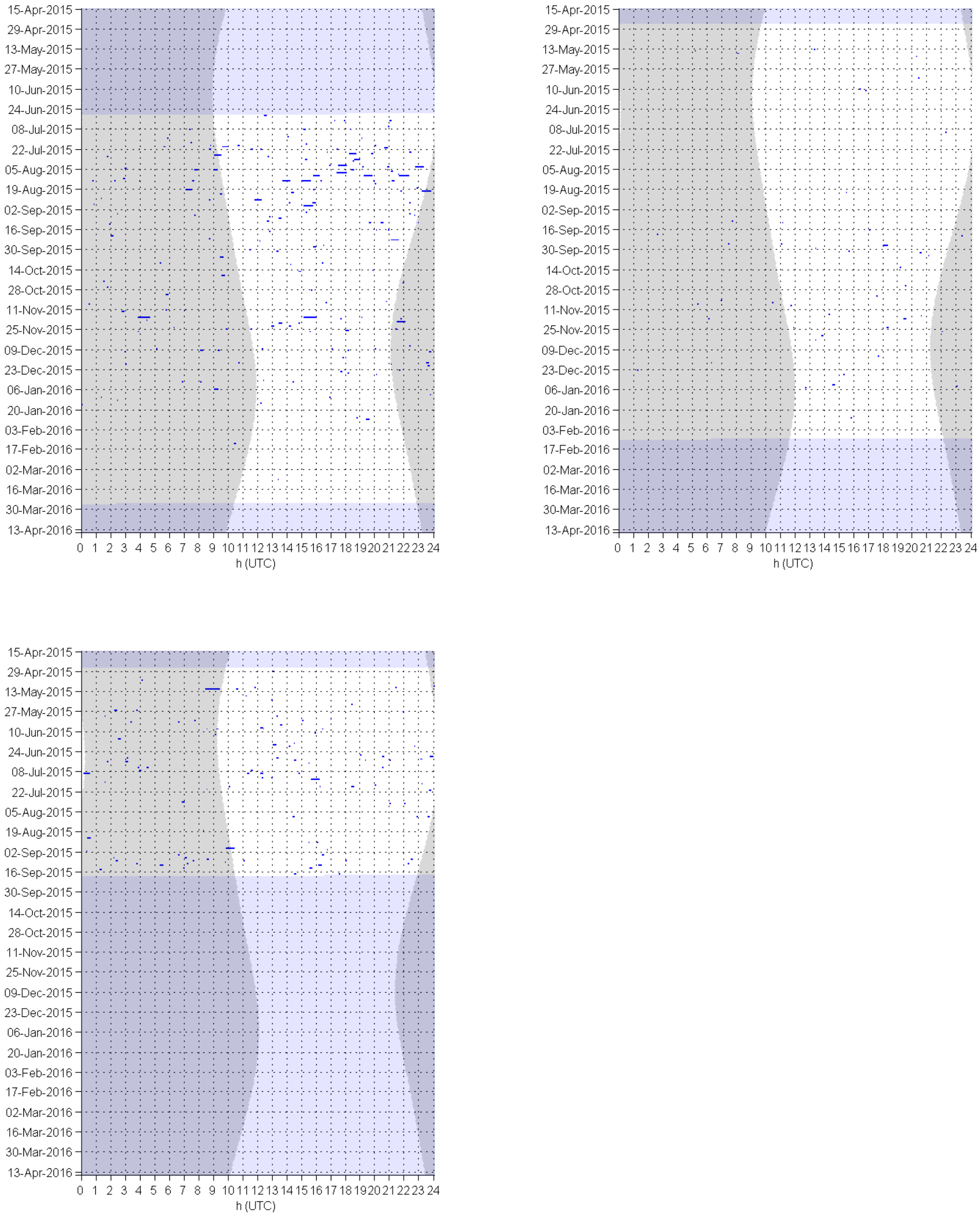

Figure 47. ***Kogia*** **spp. echolocation clicks in five-minute bins (blue bars) at sites HZ (top left), OC (top right), and NC (bottom). Effort markings are described in Figure 39.**

Delphinid Click Types

Risso's Dolphins

- Risso's dolphins were detected at all three sites, with a peak in May 2015 at site NC and July and September 2015 at site OC (Figure 48).
- Detections were fewest at site HZ (Figure 48).
- There were three distinctly different diel patterns for Risso's dolphins. At site HZ the clicks were crepuscular (near sunrise and sunset); at OC they were primarily at nighttime; and at NC they were primarily during daytime – at least in the springtime (Figure 49). These site-specific patterns should be a topic for further investigation.

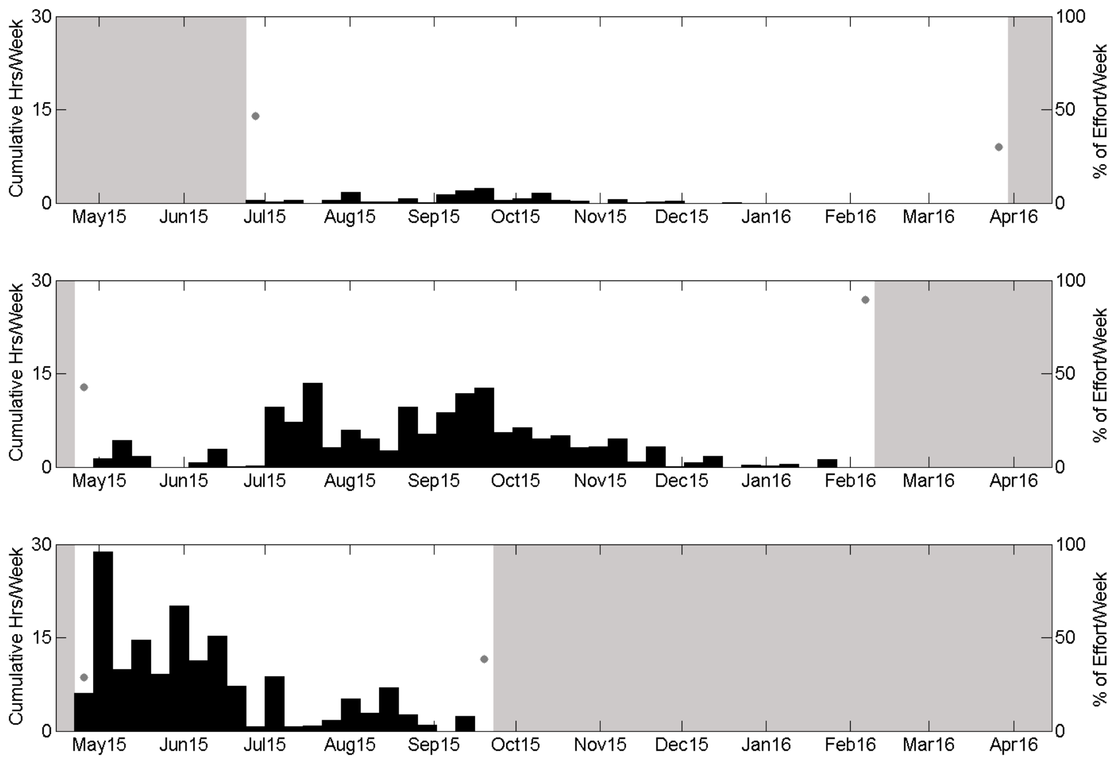

Figure 48. Weekly presence (black bars) of Risso's dolphin clicks between April 2015 and April 2016 at site HZ (top), OC (middle), and NC (bottom). Effort markings are described in Figure 38.

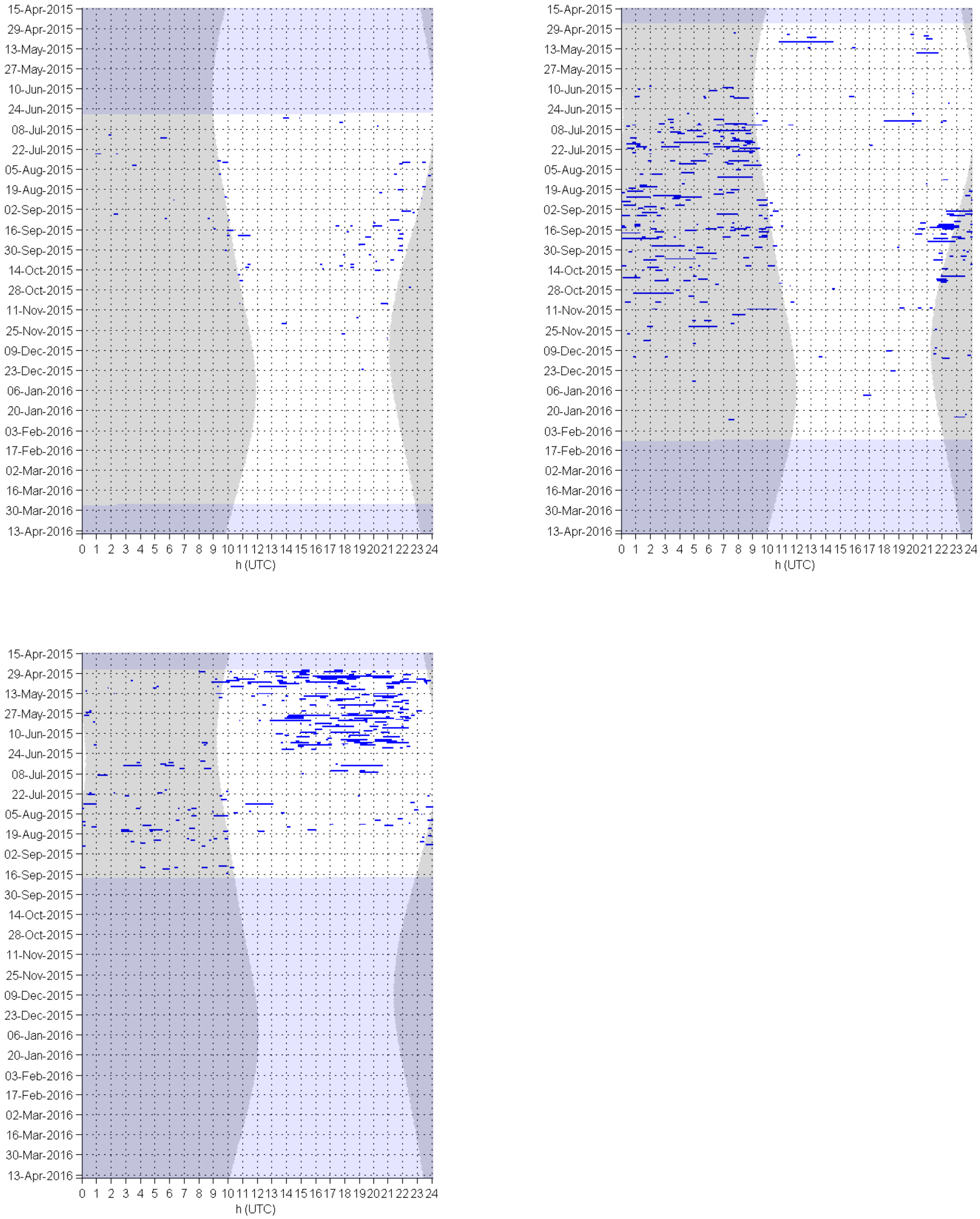

Figure 49. Risso's dolphin clicks in five-minute bins (blue bars) at sites HZ (top left), OC (top right), and NC (bottom). Effort markings are described in Figure 39.

Click Type 1

- Click type 1 was detected at all three sites, with the highest number detected at site HZ (Figure 50).
- Detections peaked in late September 2015 at site OC, and in September and late October 2015 at site HZ (Figure 50).
- The majority of type 1 clicks were detected during nighttime hours (Figure 51).

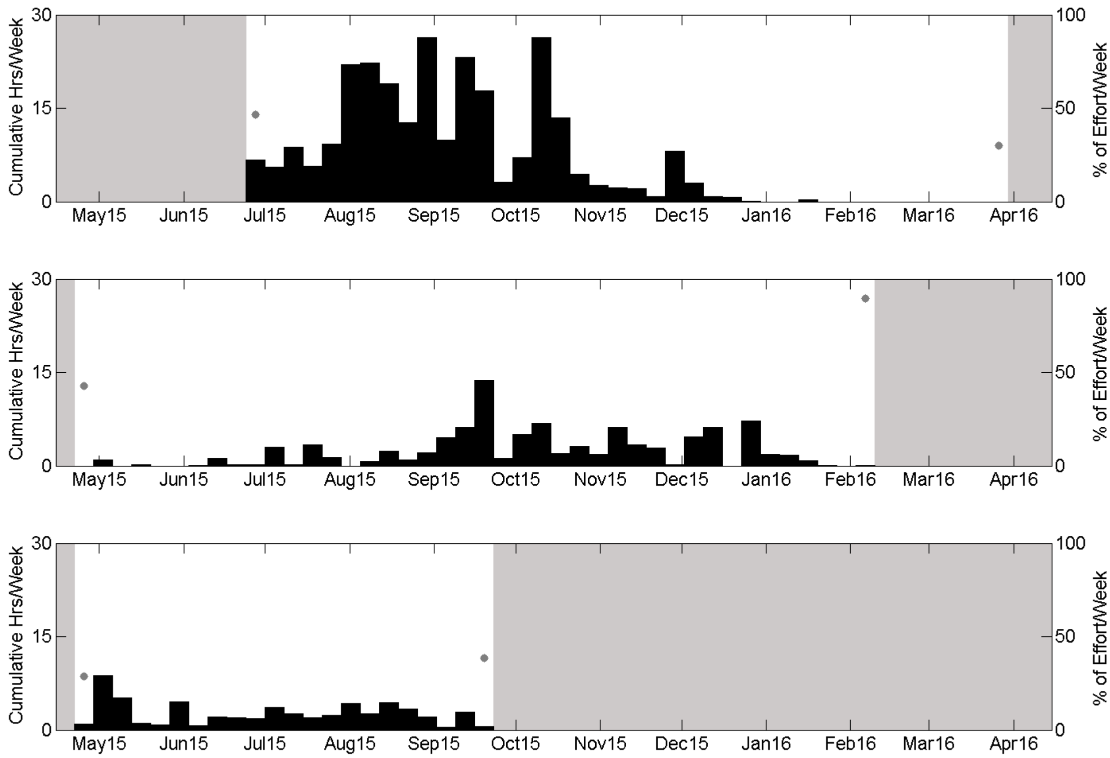

Figure 50. Weekly presence (black bars) of click type 1 detections between April 2015 and April 2016 at site HZ (top), OC (middle), and NC (bottom). Effort markings are described in Figure 38.

Figure 51. Click type 1 detections in five-minute bins (blue bars) at sites HZ (top left), OC (top right), and NC (bottom). Effort markings are described in Figure 39.

Click Type 2

- Click type 2 was not detected at site NC and was detected in low numbers at site OC (Figure 52).
- Detections were highest at site HZ, and peaked in July 2015 and late January 2016 (Figure 52).
- Type 2 clicks occurred predominantly during nighttime hours (Figure 53).

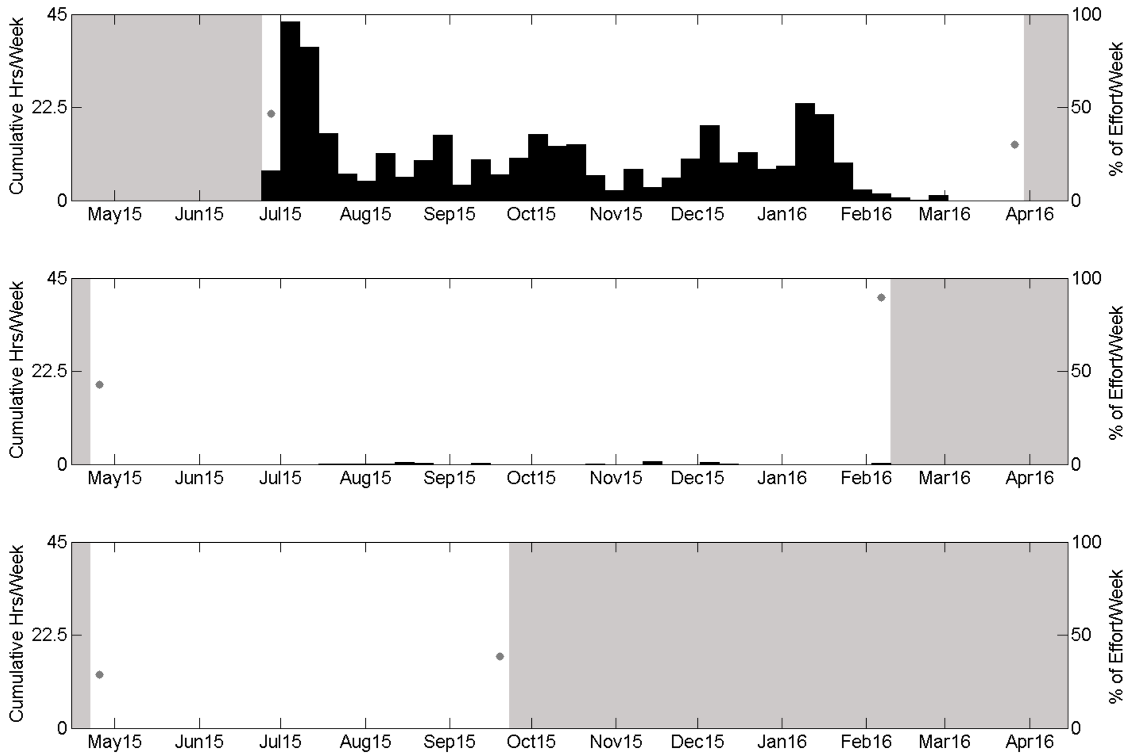

Figure 52. Weekly presence (black bars) of click type 2 detections between April 2015 and April 2016 at site HZ (top), OC (middle), and NC (bottom). Effort markings are described in Figure 38.

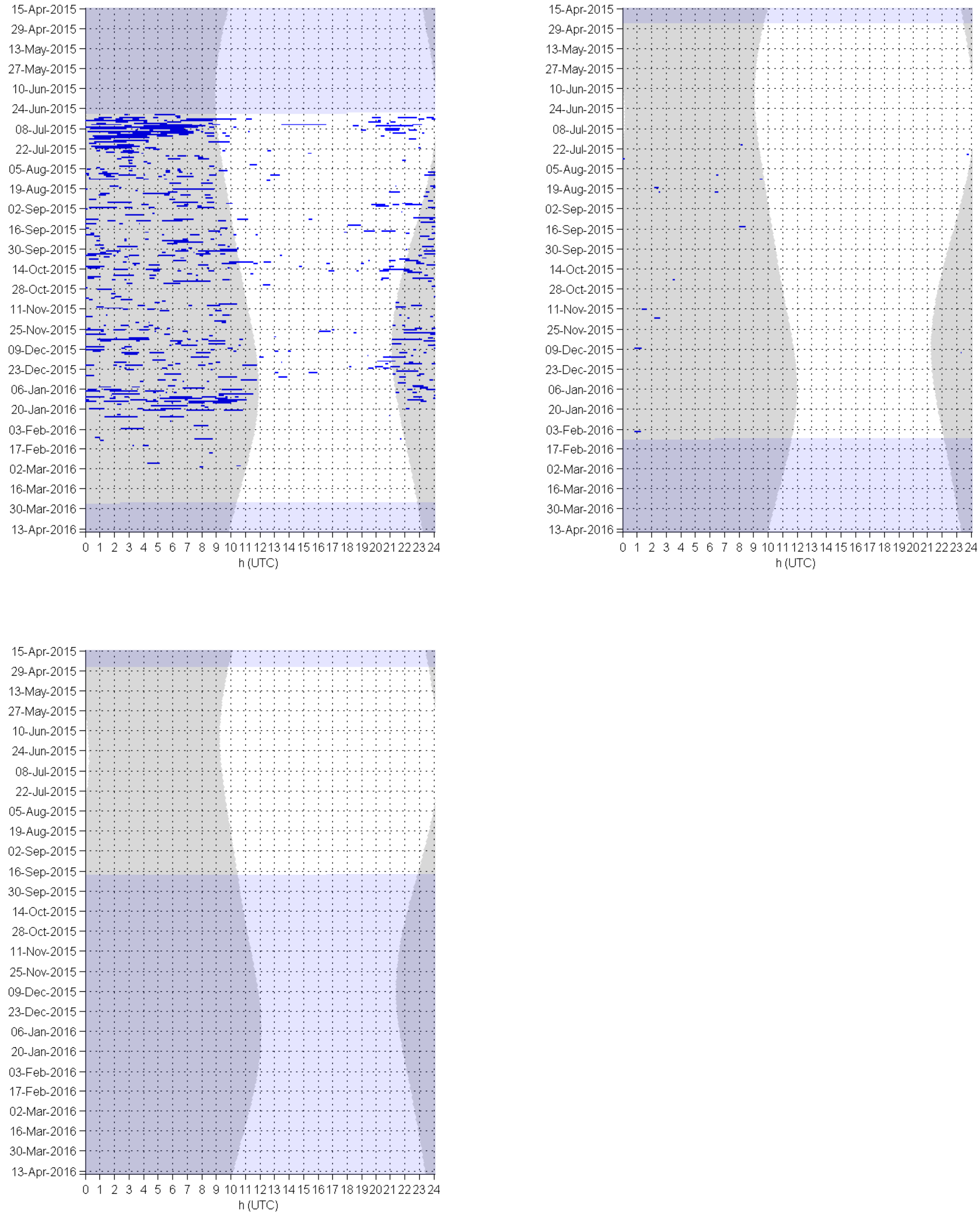

Figure 53. Click type 2 detections in five-minute bins (blue bars) at sites HZ (top left), OC (top right), and NC (bottom). Effort markings are described in Figure 39.

Click Type 3

- Click type 3 was detected at all three sites (Figure 54).
- Detections were highest at site OC, and peaked in May and November 2015, and February 2016 (Figure 54).
- The majority of click type 3 detections occurred during nighttime hours (Figure 55).

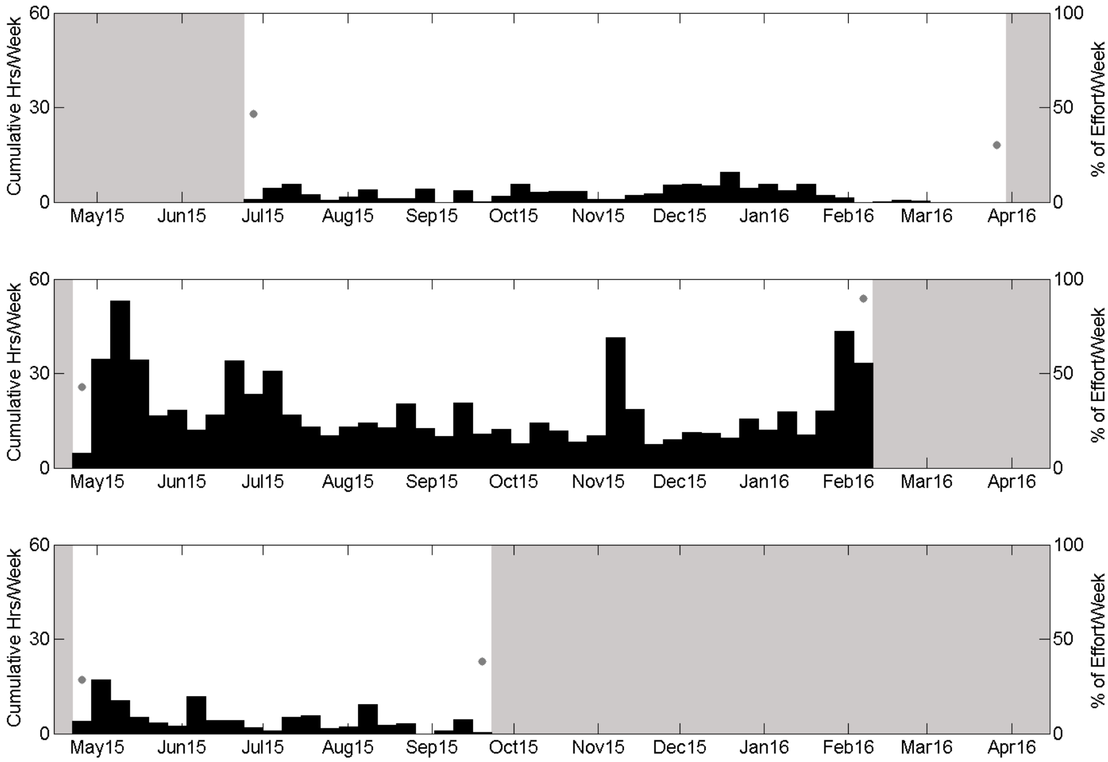

Figure 54. Weekly presence (black bars) of click type 3 detections between April 2015 and April 2016 at site HZ (top), OC (middle), and NC (bottom). Effort markings are described in Figure 38.

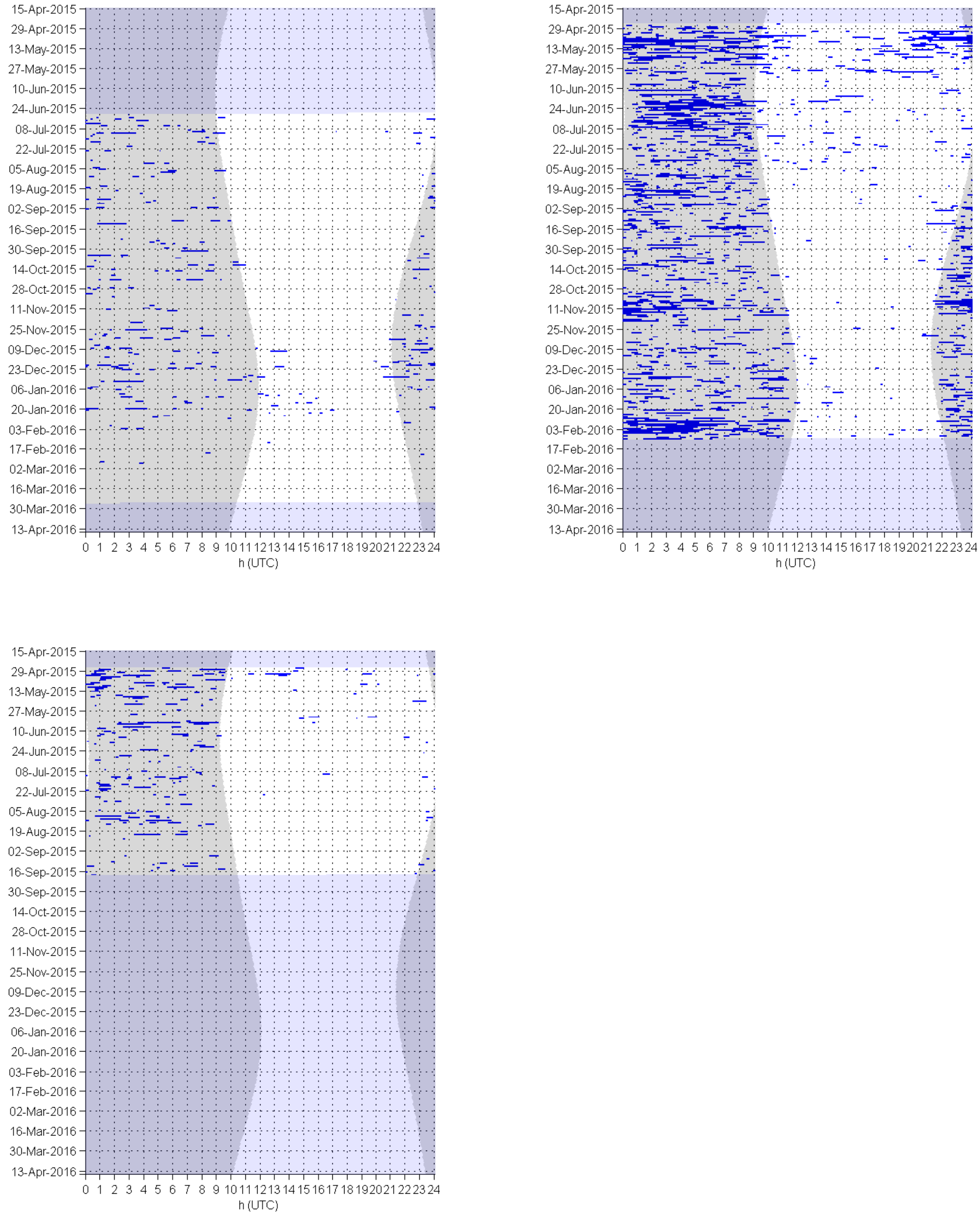

Figure 55. Click type 3 detections in five-minute bins (blue bars) at sites HZ (top left), OC (top right), and NC (bottom). Effort markings are described in Figure 39.

Click Type 4

- Click type 4 was detected intermittently at the three sites (Figure 56).
- Detections peaked in August 2015 at site NC, in November 2015 at site OC, and in late December 2015 at site HZ (Figure 56).
- Detections occurred mostly during nighttime hours (Figure 57).

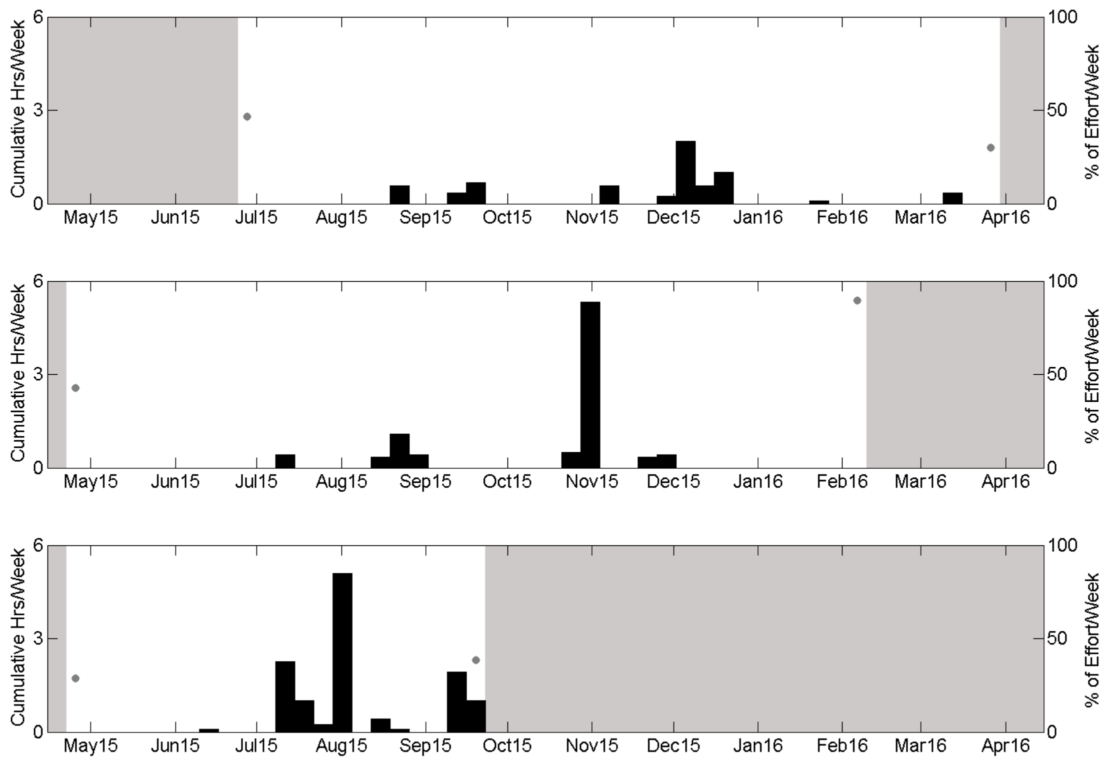

Figure 56. Weekly presence (black bars) of click type 4 detections between April 2015 and April 2016 at site HZ (top), OC (middle), and NC (bottom). Effort markings are described in Figure 38.

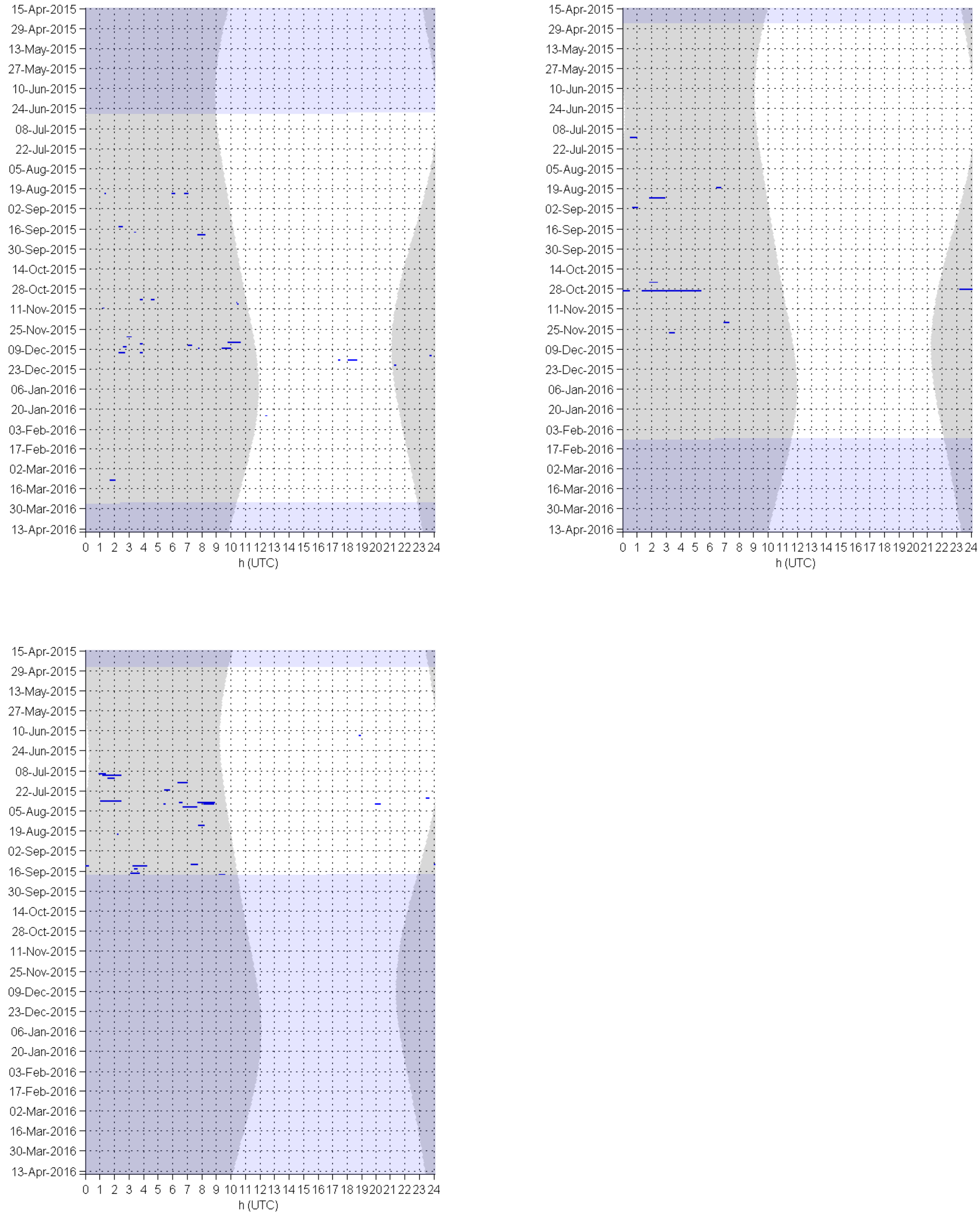

Figure 57. Click type 4 detections in five-minute bins (blue bars) at sites HZ (top left), OC (top right), and NC (bottom). Effort markings are described in Figure 39.

Click Type 5

- Click type 5 was detected at all three sites, with the fewest detections at site NC (Figure 58).
- Detections peaked at site HZ in October 2015 (Figure 58).
- Click type 5 occurred primarily during nighttime hours (Figure 59).

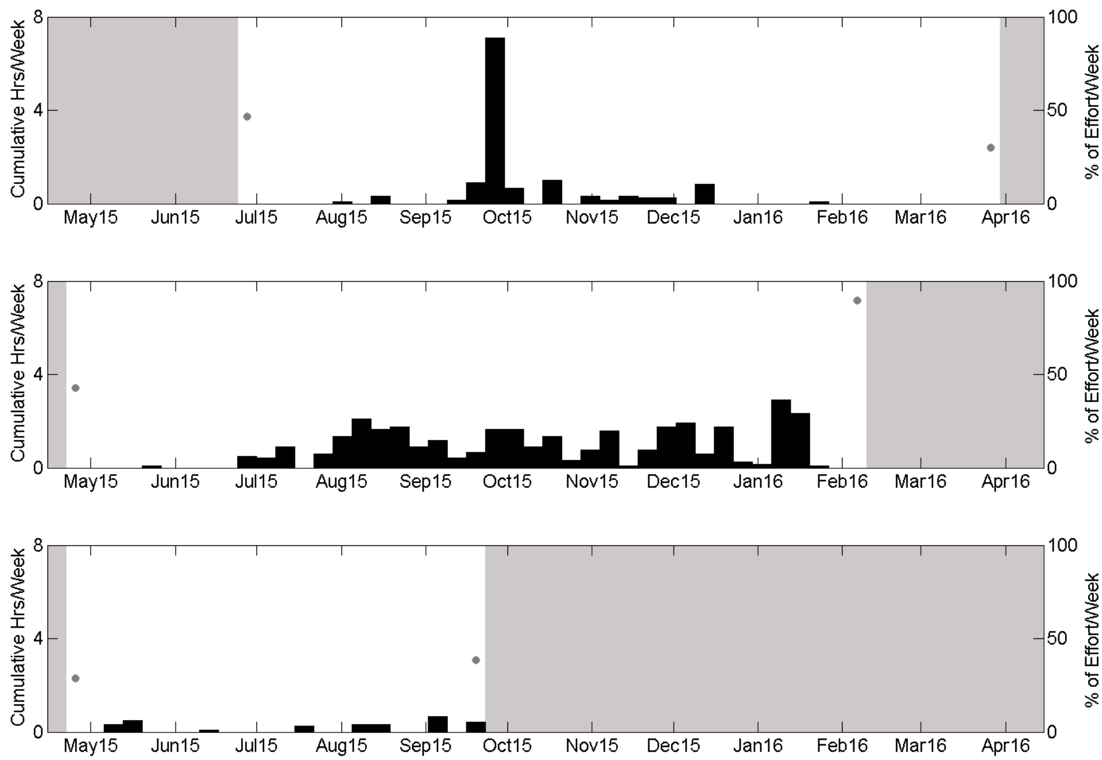

Figure 58. Weekly presence (black bars) of click type 5 detections between April 2015 and April 2016 at site HZ (top), OC (middle), and NC (bottom). Effort markings are described in Figure 38.

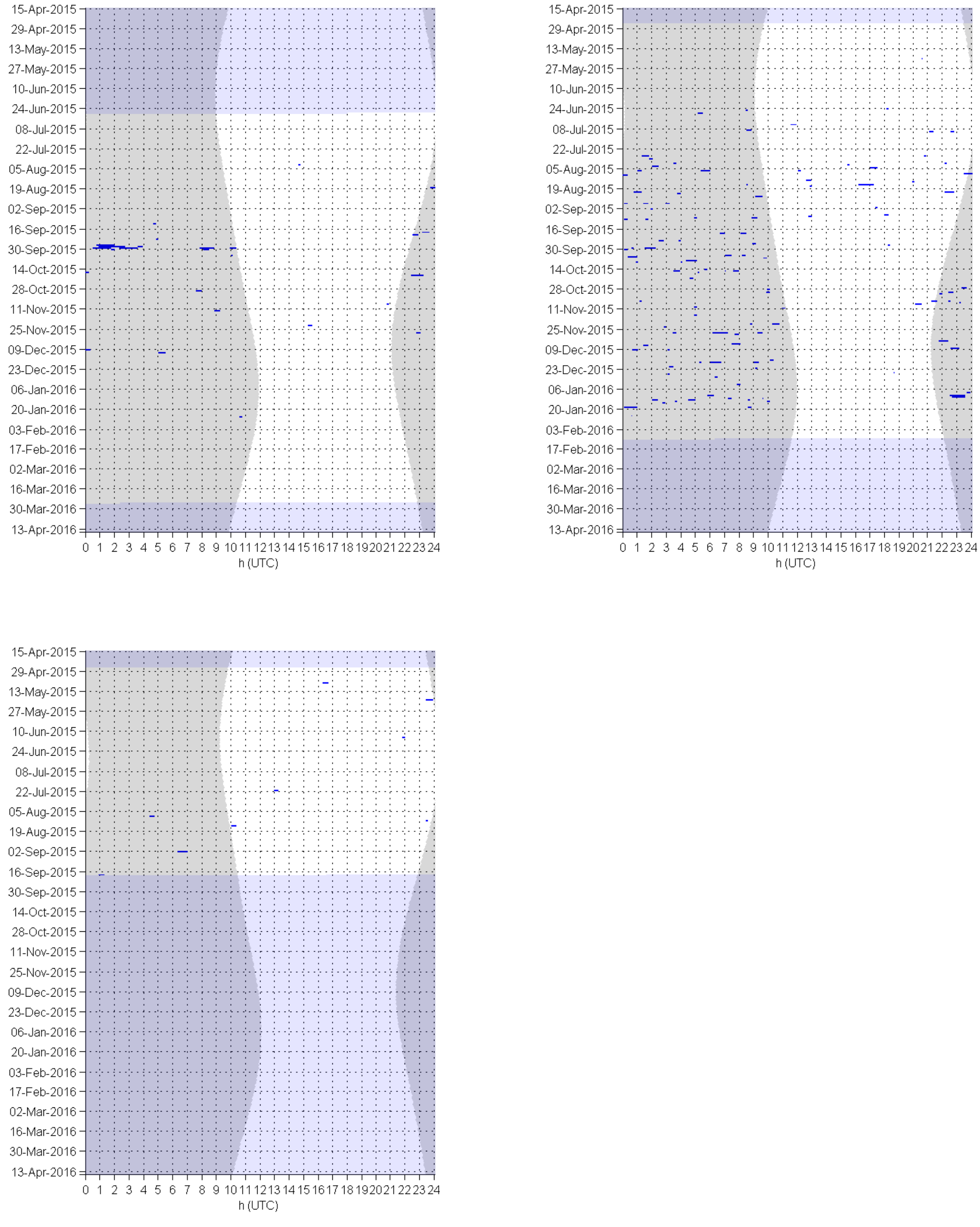

Figure 59. Click type 5 detections in five-minute bins (blue bars) at sites HZ (top left), OC (top right), and NC (bottom). Effort markings are described in Figure 39.

Click Type 6

- Click type 6 was detected at all three sites (Figure 60).
- Site HZ had the highest number of detections, with peaks in late September 2015 and late December 2015 (Figure 60).
- There was no discernible diel pattern for click type 6 (Figure 61).

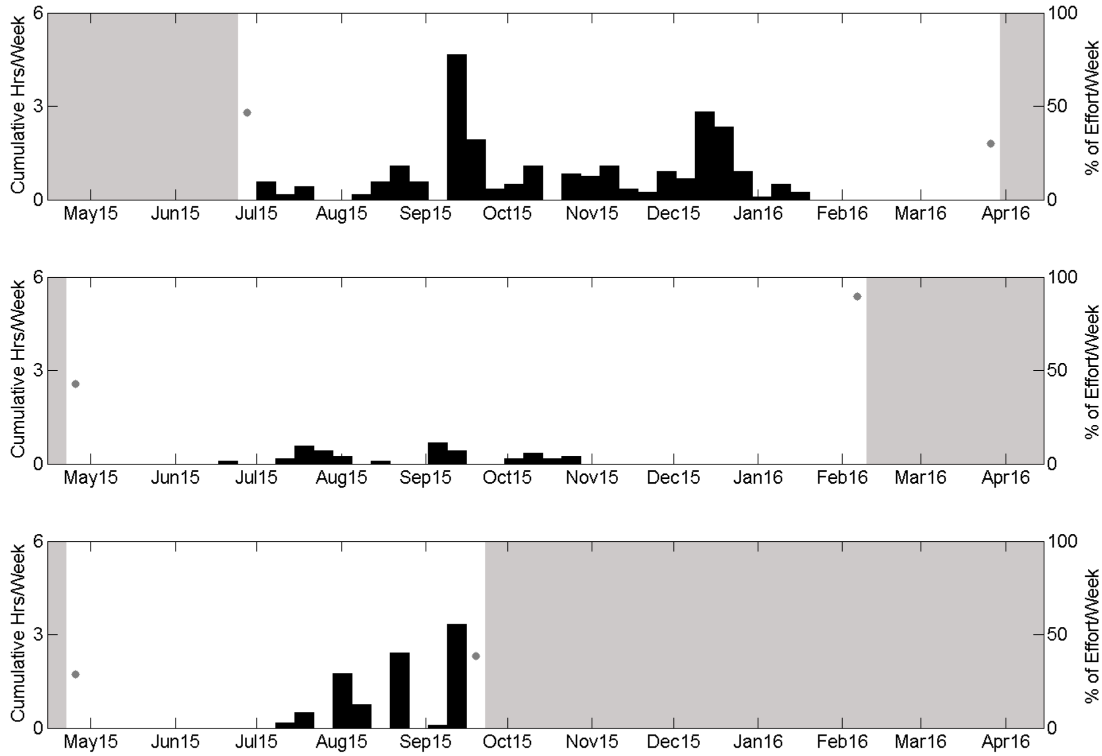

Figure 60. Weekly presence (black bars) of click type 6 detections between April 2015 and April 2016 at site HZ (top), OC (middle), and NC (bottom). Effort markings are described in Figure 38.

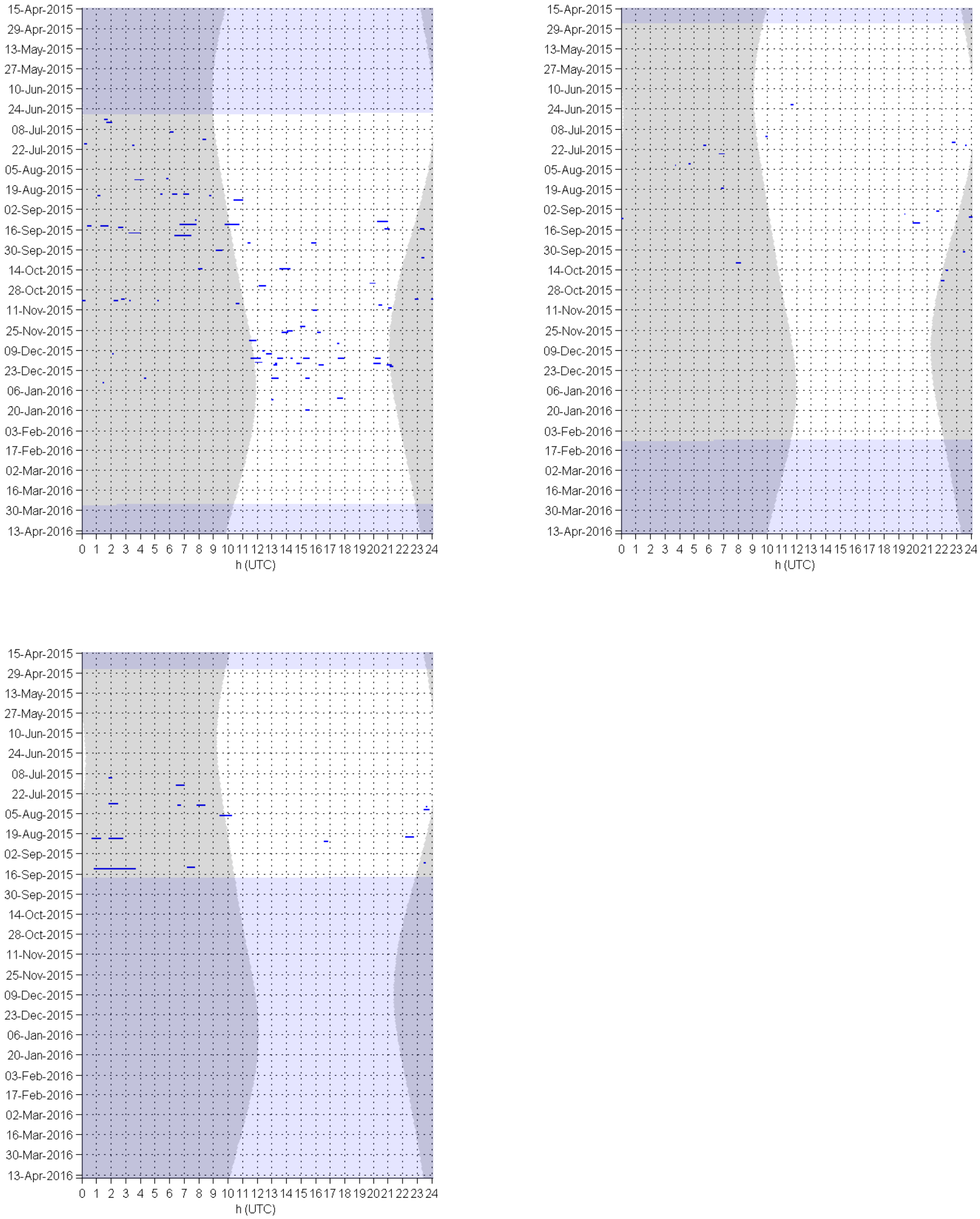

Figure 61. Click type 6 detections in five-minute bins (blue bars) at sites HZ (top left), OC (top right), and NC (bottom). Effort markings are described in Figure 39.

Click Type 7

- Click type 7 was detected at all three sites, with the most detections at site HZ and the fewest detections at site OC (Figure 62).
- Detections peaked at site HZ in the winter months (Figure 62).
- Click type 7 occurred almost exclusively during nighttime hours (Figure 63).

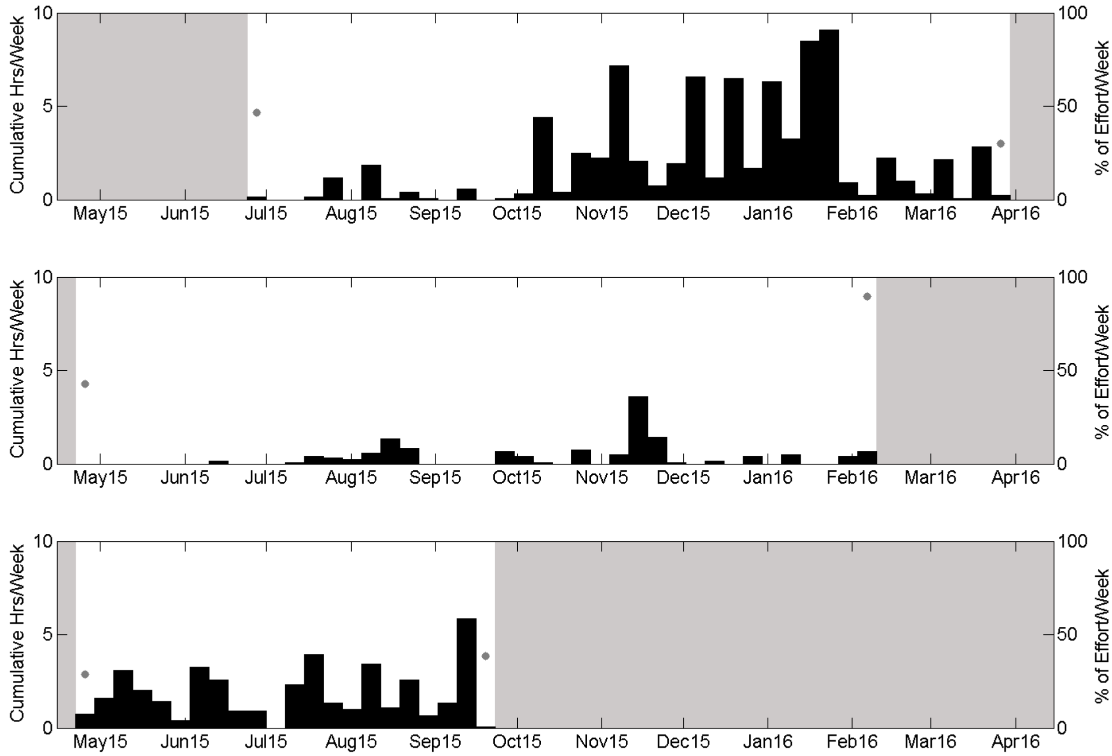

Figure 62. Weekly presence (black bars) of click type 7 detections between April 2015 and April 2016 at site HZ (top), OC (middle), and NC (bottom). Effort markings are described in Figure 38.

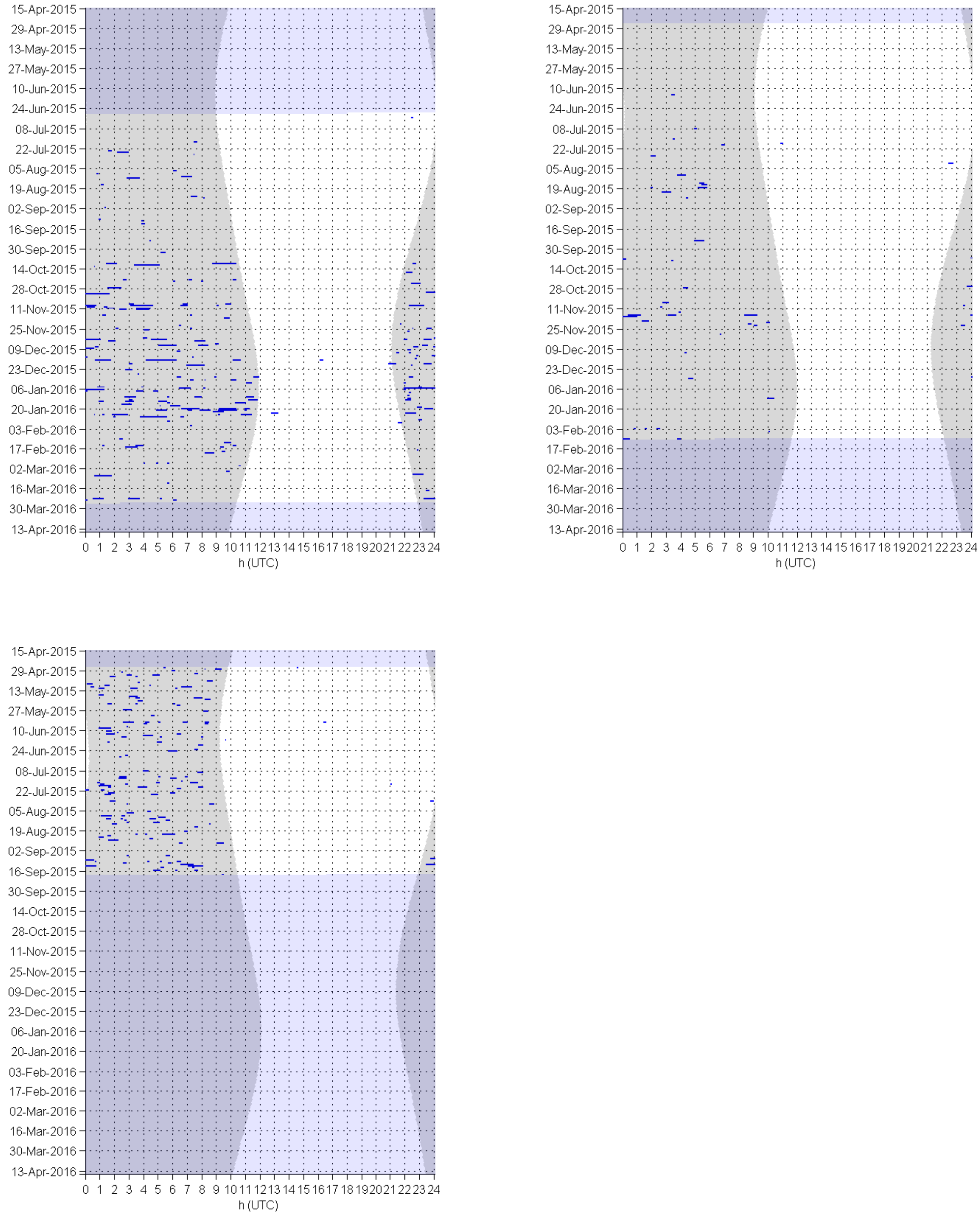

Figure 63. Click type 7 detections in five-minute bins (blue bars) at sites HZ (top left), OC (top right), and NC (bottom). Effort markings are described in Figure 39.

Click Type 8

- Click type 8 was detected sporadically at all three sites (Figure 64).
- Sites NC and HZ had few detections, while site OC had peaks in September and November of 2015, and January of 2016 (Figure 64).
- Type 8 clicks occurred primarily during nighttime hours (Figure 65).

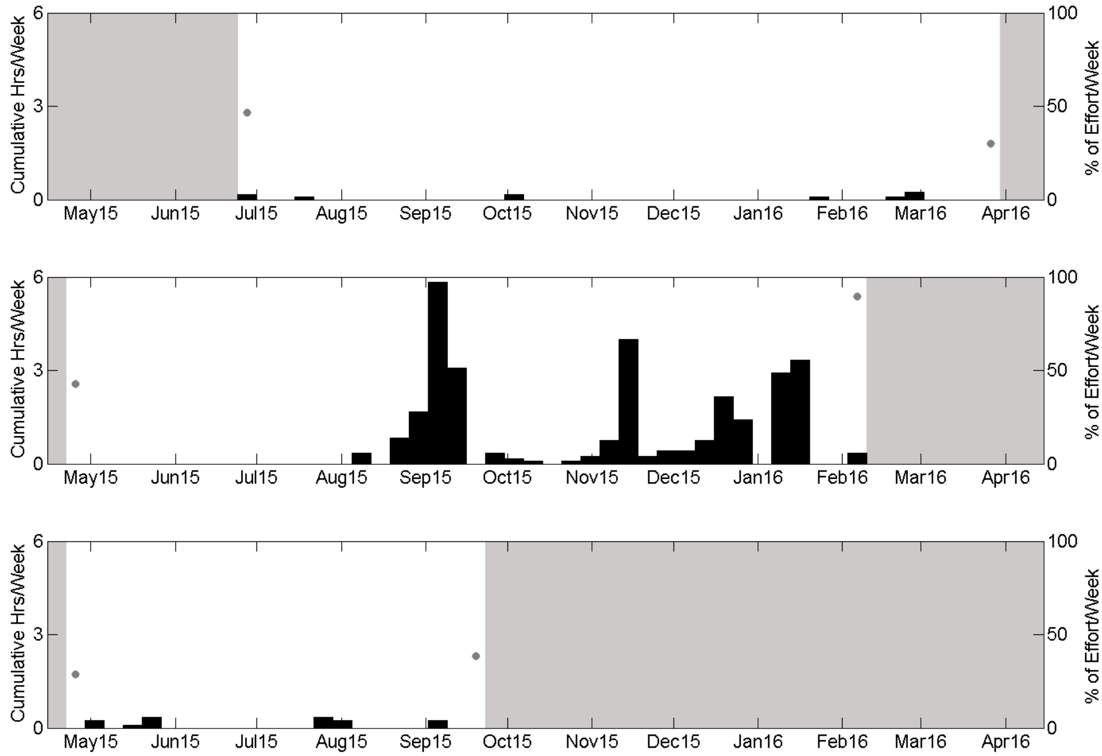

Figure 64. Weekly presence (black bars) of click type 8 detections between April 2015 and April 2016 at site HZ (top), OC (middle), and NC (bottom). Effort markings are described in Figure 38.

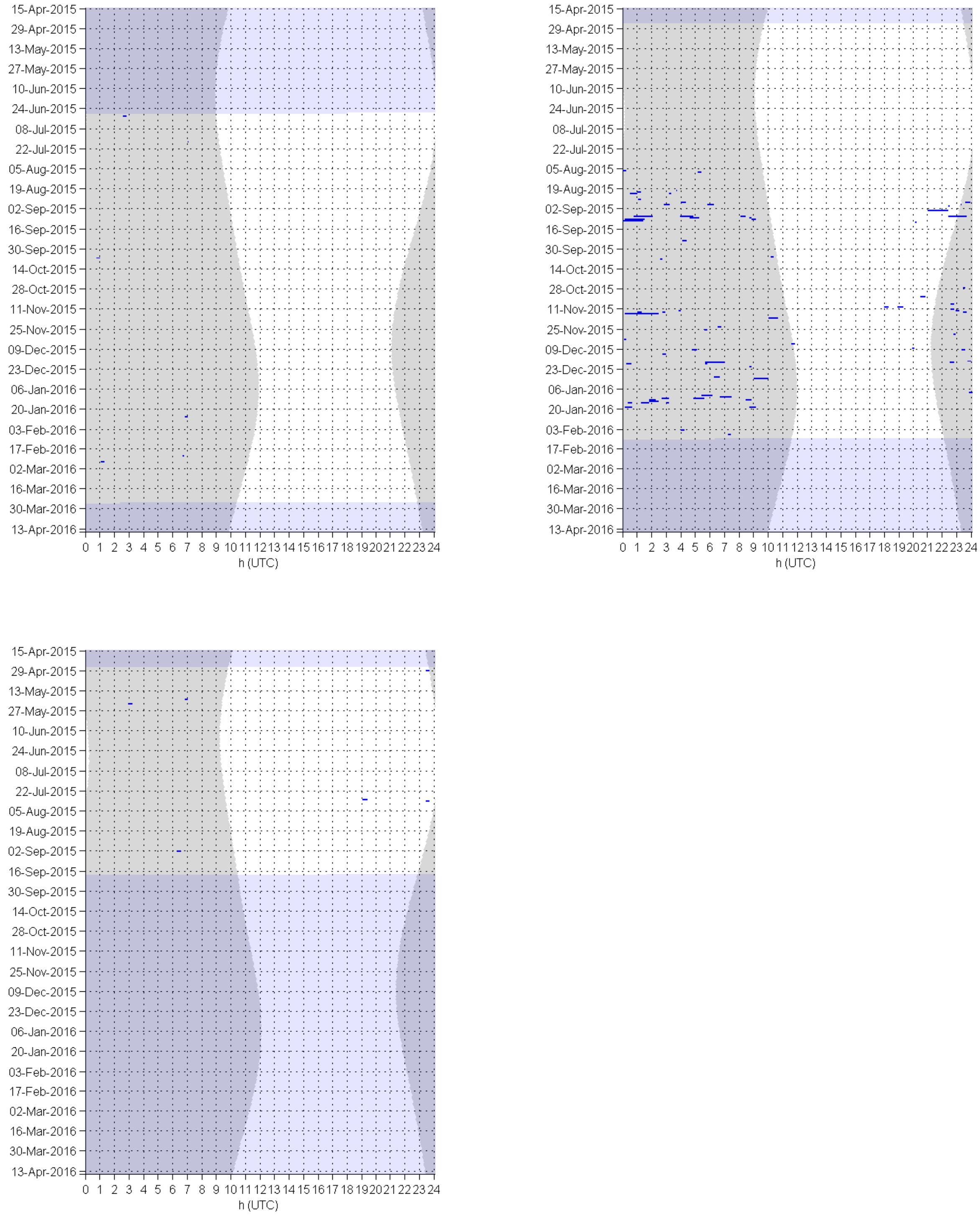

Figure 65. Click type 8 detections in five-minute bins (blue bars) at sites HZ (top left), OC (top right), and NC (bottom). Effort markings are described in Figure 39.

Unclassified Odontocete Clicks

Signals that had characteristics of odontocete clicks, but could not be classified to species were labeled as unclassified odontocetes.

- Clicks were left unclassified if too few clicks were detected in a time bin (<20 clicks/min), if they did not match documented click type, or if detected clicks were of poor quality (e.g. low amplitude or masked).
- Unclassified clicks were detected throughout the recording period at all three sites (Figure 66).
- Unclassified odontocete clicks were predominantly detected during nighttime hours (Figure 67).

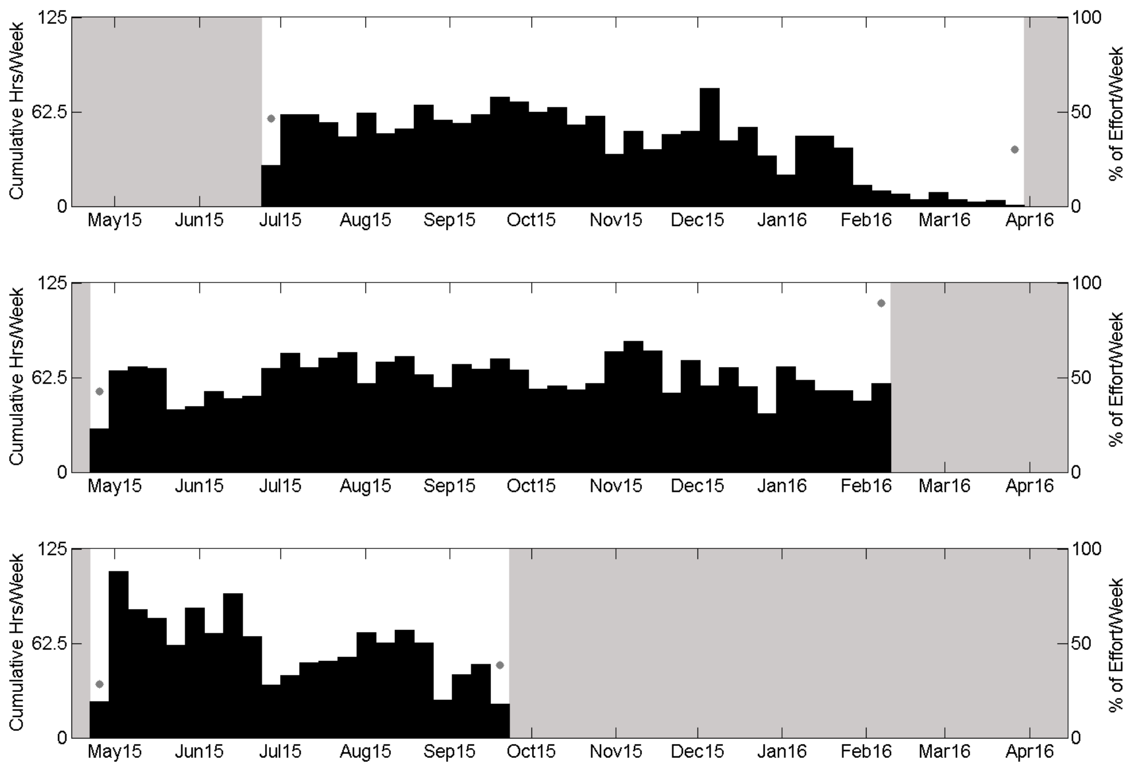

Figure 66. Weekly presence (black bars) of unclassified click detections between April 2015 and April 2016 at site HZ (top), OC (middle), and NC (bottom). Effort markings are described in Figure 38.

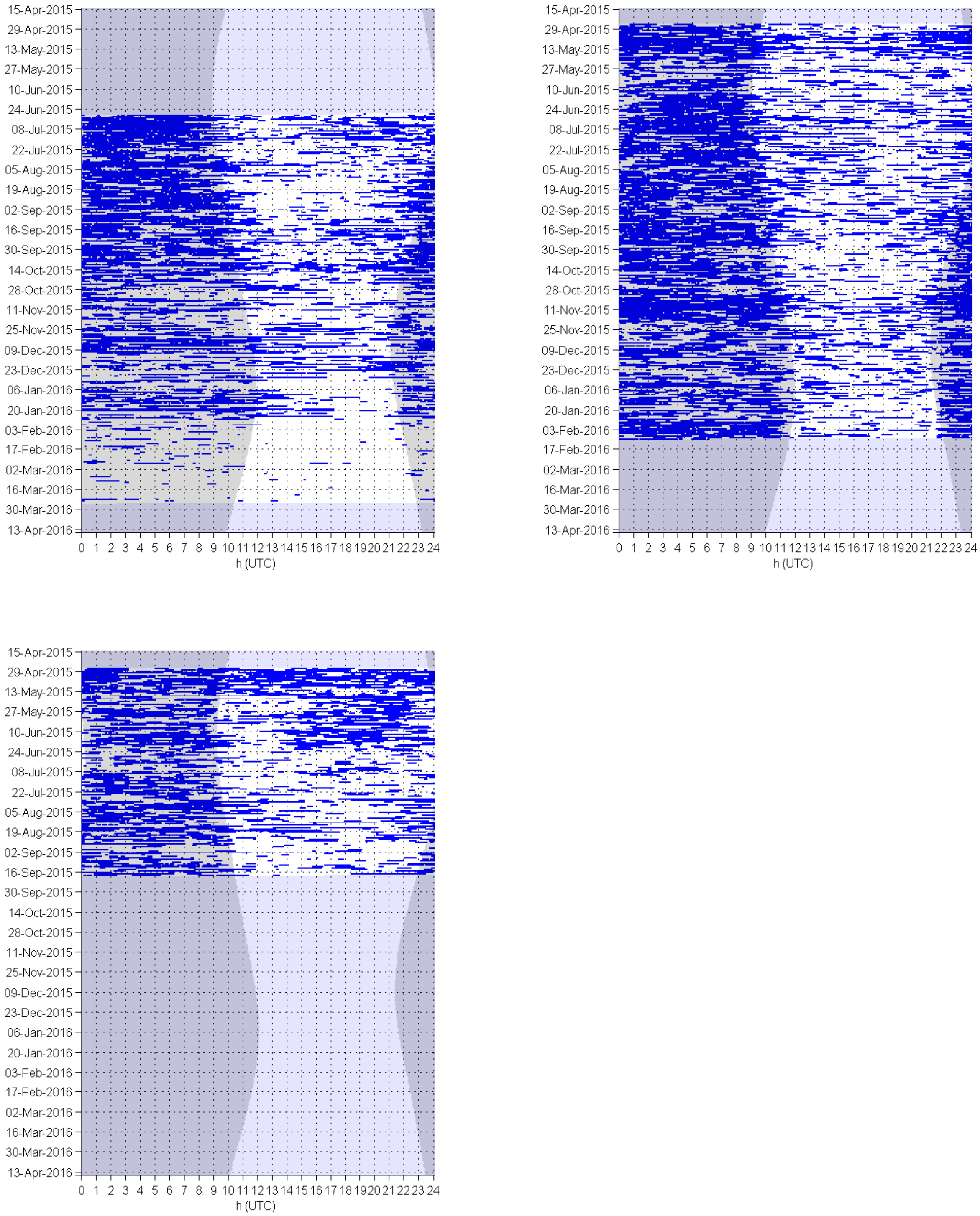

Figure 67. Unclassified click detections in five-minute bins (blue bars) at sites HZ (top left), OC (top right), and NC (bottom). Effort markings are described in Figure 39.

Anthropogenic Sounds

Four types of anthropogenic sounds were detected: broadband ship sounds, explosions, airguns, and echosounders.

Broadband Ship Sounds

- Broadband ship sounds were detected at all three sites during the recording period (Figure 68).
- Site HZ had the fewest broadband ship sound detections, and site OC had a peak in detections in late June 2015 (Figure 68).
- There was no diel pattern for broadband ship sounds at the three sites (Figure 69).

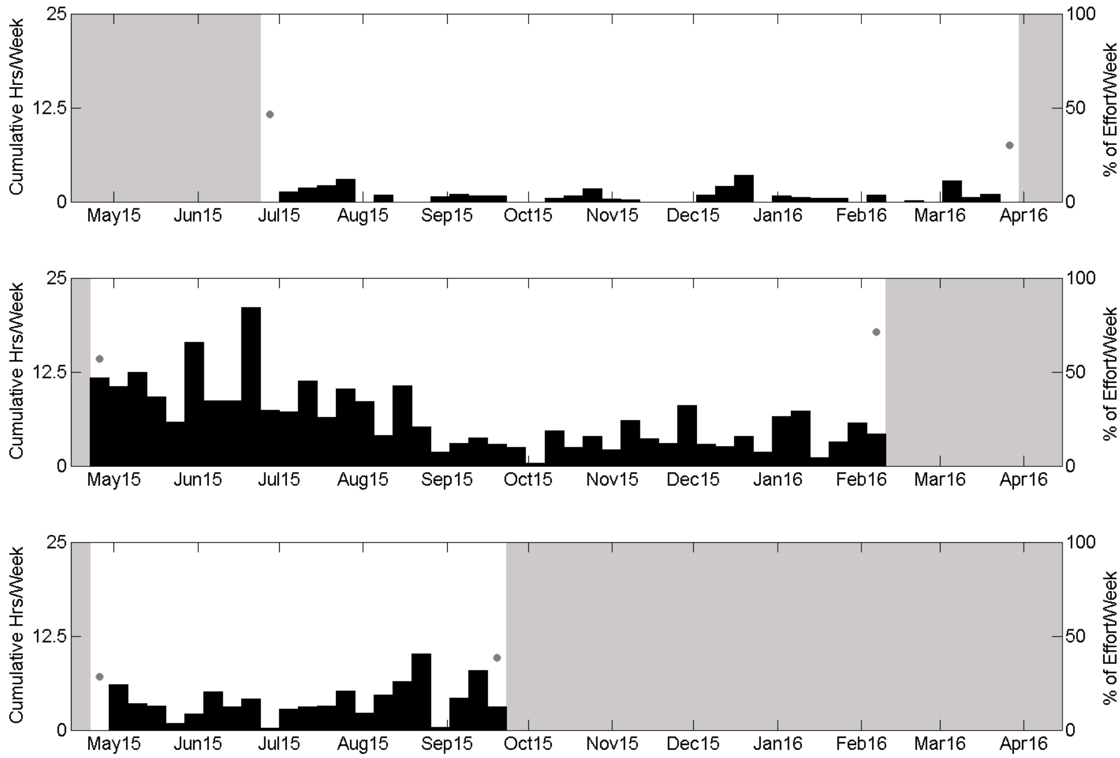

Figure 68. Weekly presence (black bars) of broadband ship sounds between April 2015 and April 2016 at site HZ (top), OC (middle), and NC (bottom). Effort markings are described in Figure 38.

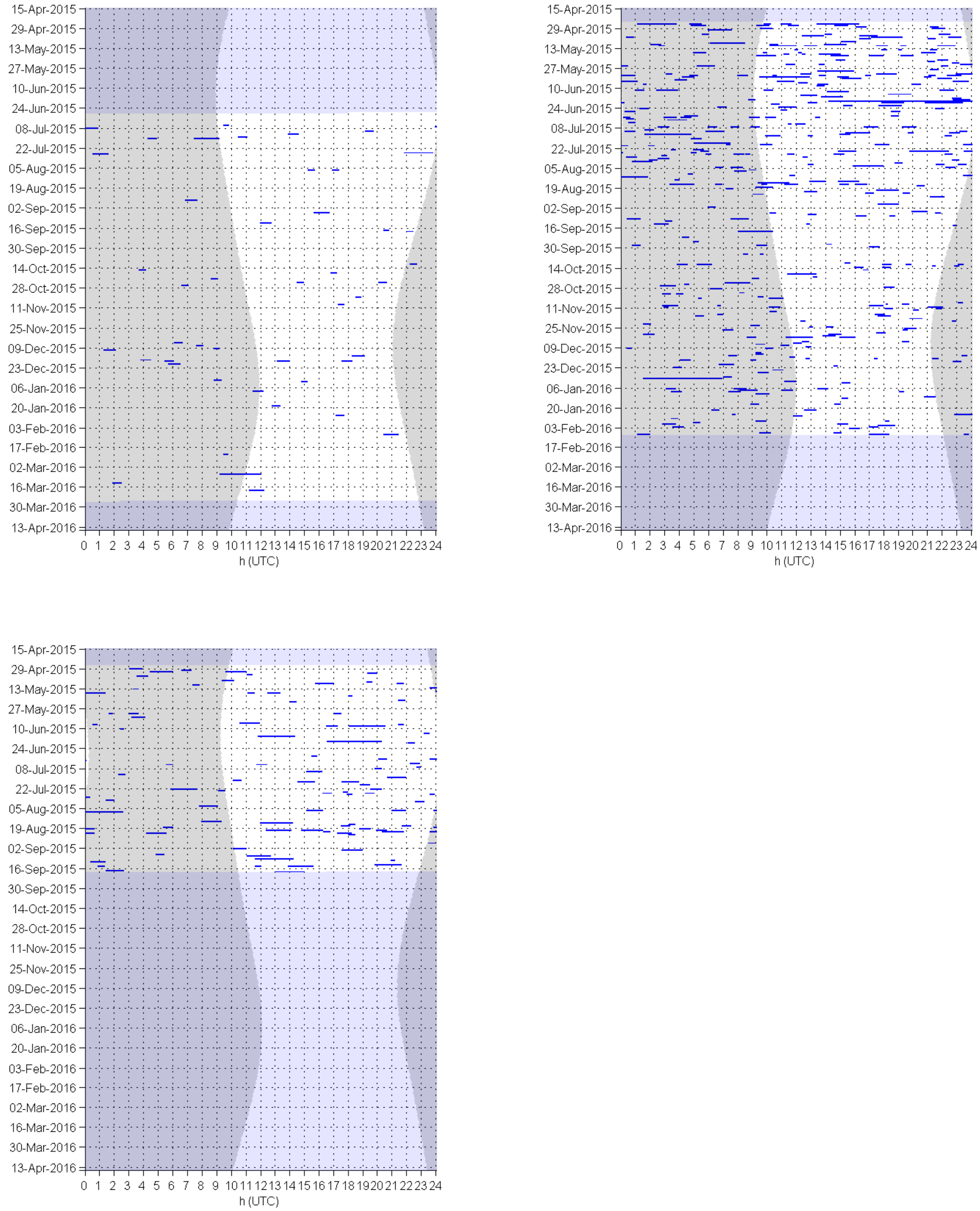

Figure 69. Broadband ship sounds in five-minute bins (blue bars) at sites HZ (top left), OC (top right), and NC (bottom). Effort markings are described in Figure 39.

Explosions

- There was one explosion detected at site OC, in September 2015 (Figure 70, Figure 71).
- There were no detections at sites NC or HZ.

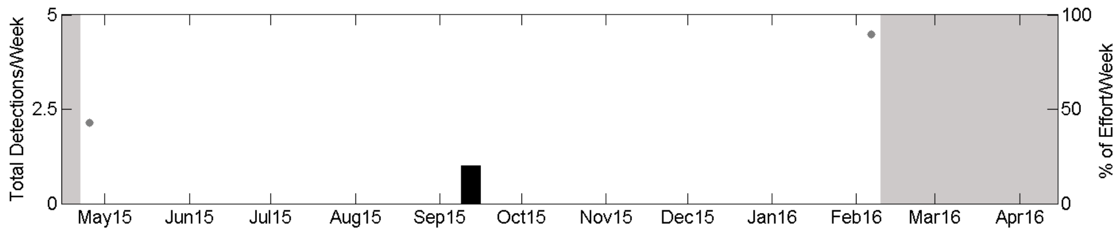

Figure 70. Weekly presence (black bars) of explosions between April 2015 and April 2016 at site OC. Effort markings are described in Figure 38.

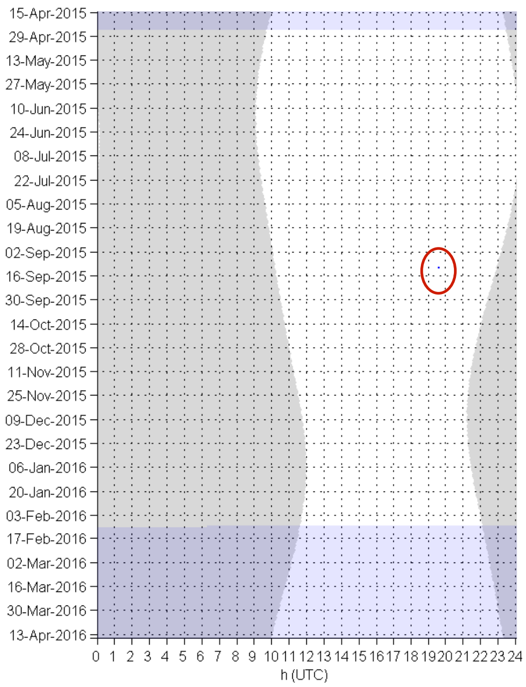

Figure 71. Explosion detections in five-minute bins (blue bars) at site OC. Effort markings are described in Figure 39. Red circle indicates single detection.

Airguns

- Airguns were detected at all three sites over the recording period (Figure 72).
- Detections at site NC peaked in August and September 2015 (Figure 72).
- At sites OC and HZ, detections peaked in the summer months of 2015 and January 2016 (Figure 72).
- There was no diel pattern for airgun detections at any of the three sites (Figure 73).

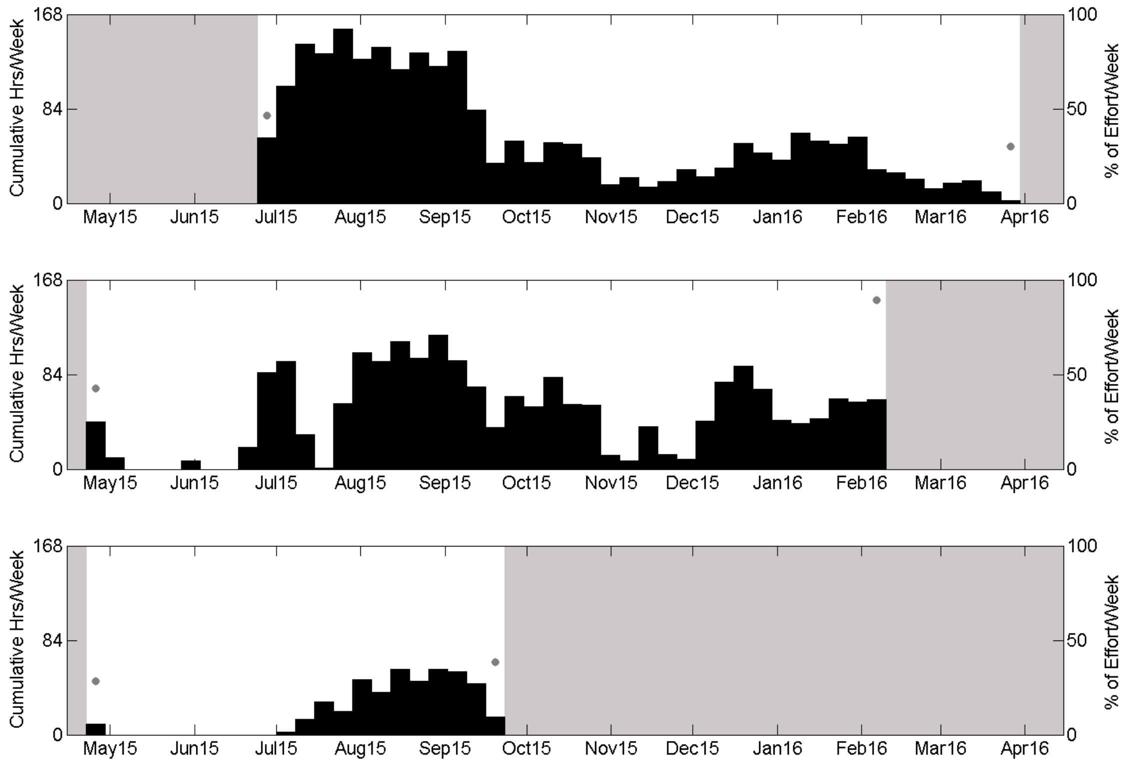

Figure 72. Weekly presence (black bars) of airguns between April 2015 and April 2016 at site HZ (top), OC (middle), and NC (bottom). Effort markings are described in Figure 38.

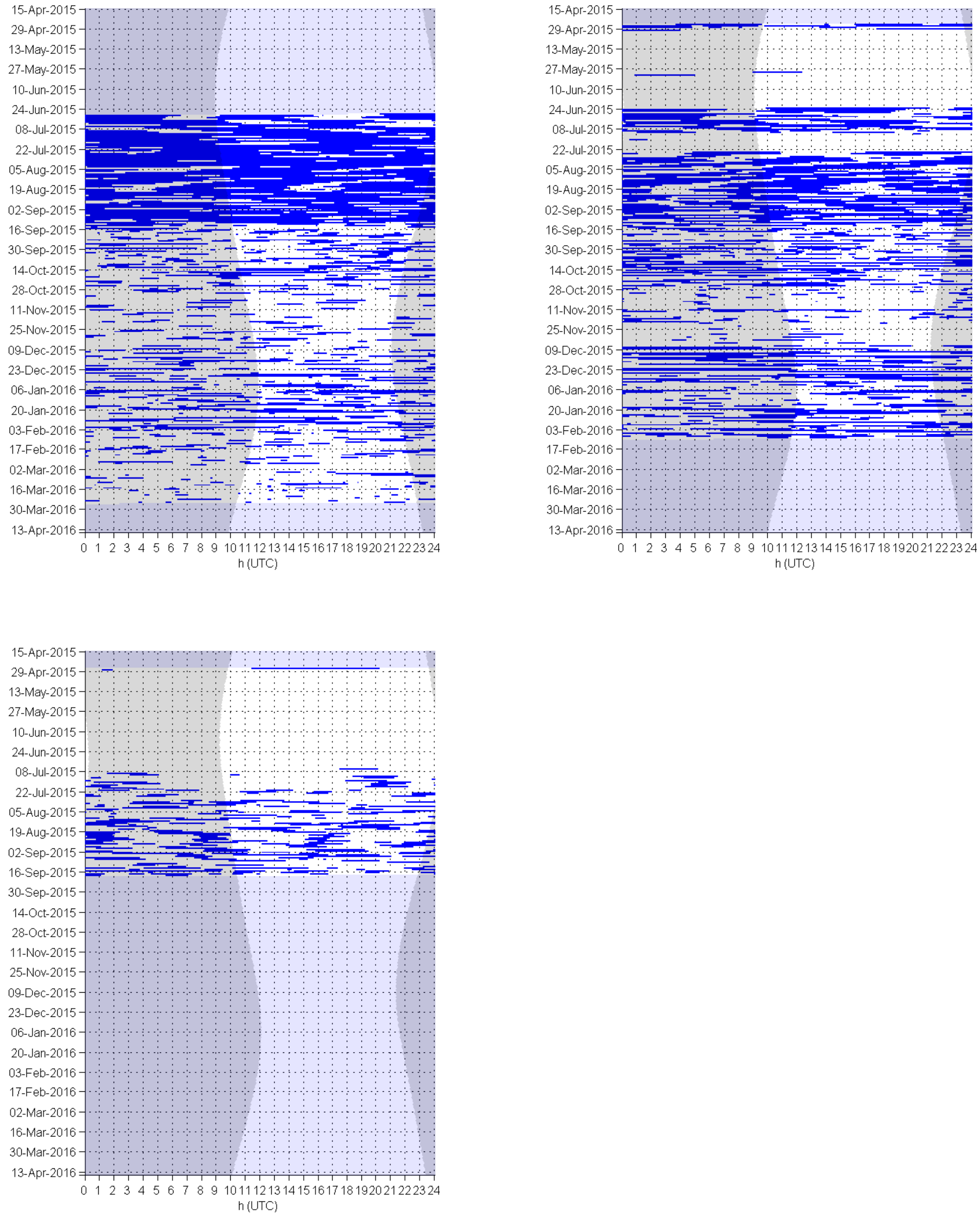

Figure 73. Airgun detections in five-minute bins (blue bars) at sites HZ (top left), OC (top right), and NC (bottom). Effort markings are described in Figure 39.

Echosounders

- Echosounders were detected intermittently at all three sites (Figure 74).
- Detections at site HZ peaked in October 2015 (Figure 74).
- There was no diel pattern for echosounder detections (Figure 75).

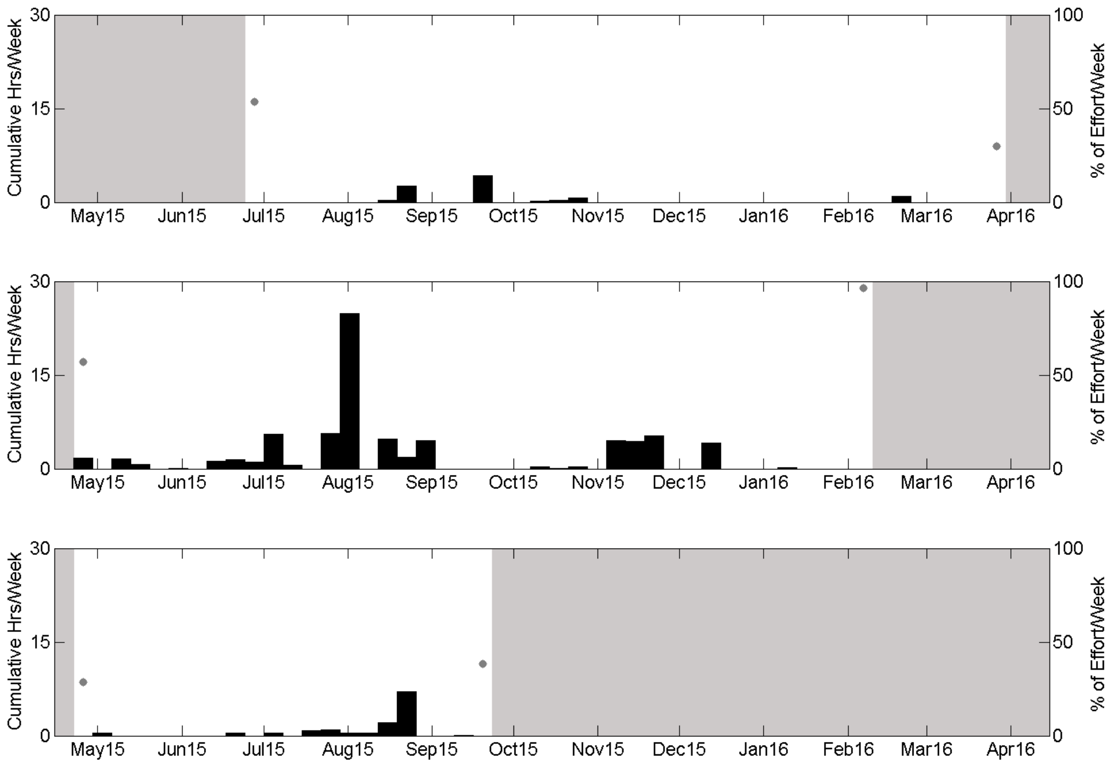

Figure 74. Weekly presence (black bars) of echosounders between April 2015 and April 2016 at site HZ (top), OC (middle), and NC (bottom). Effort markings are described in Figure 38.

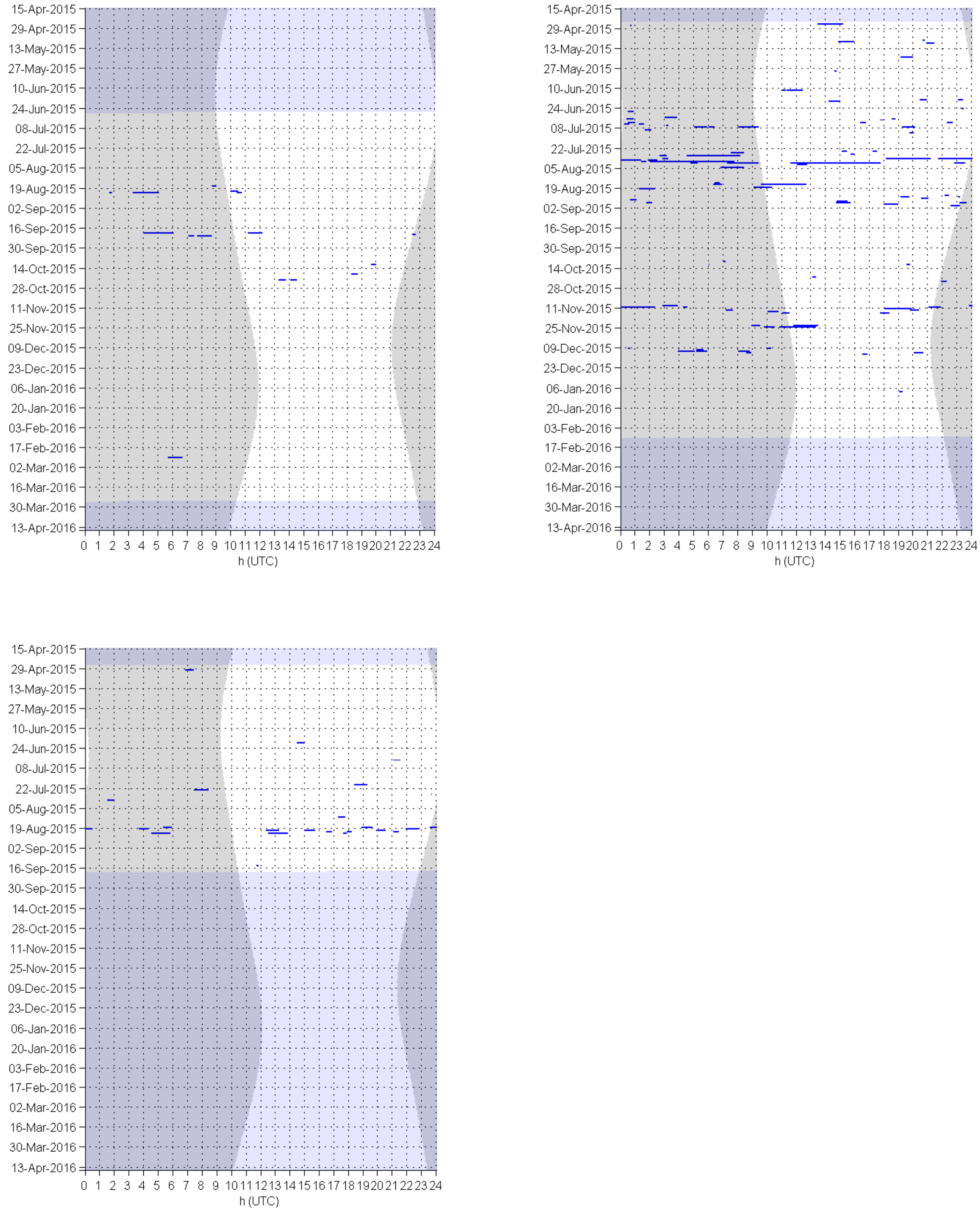

Figure 75. Echosounder detections in five-minute bins (blue bars) at sites HZ (top left), OC (top right), and NC (bottom). Effort markings are described in Figure 39.

References

Amundsen, L., and Landro, M. (**2010**). "Marine Seismic Sources, Part 1 - Air-guns for no experts," (Geo ExPro), pp. 32-34.

Au, W. W. L. (**1993**). *The Sonar of Dolphins* (Springer).

Barger, J. E., and Hamblen, W. R. (**1980**). "The air gun impulsive underwater transducer," The Journal of the Acoustical Society of America **68**, 1038-1045.

Baumann-Pickering, S., McDonald, M. A., Simonis, A. E., Berga, A. S., Merkens, K. P. B., Oleson, E. M., Roch, M. A., Wiggins, S. M., Rankin, S., Yack, T. M., and Hildebrand, J. A. (**2013**). "Species-specific beaked whale echolocation signals," The Journal of the Acoustical Society of America **134**, 2293-2301.

Baumann-Pickering, S., Roch, M. A., Brownell Jr, R. L., Simonis, A. E., McDonald, M. A., Solsona-Berga, A., Oleson, E. M., Wiggins, S. M., and Hildebrand, J. A. (**2014**). "Spatio-Temporal Patterns of Beaked Whale Echolocation Signals in the North Pacific," PLOS ONE **9**, e86072.

Blackman, D. K., Groot-Hedlin, C. d., Harben, P., Sauter, A., and Orcutt, J. A. (**2004**). "Testing low/very low frequency acoustic sources for basin-wide propagation in the Indian Ocean," The Journal of the Acoustical Society of America **116**, 2057-2066.

Cholewiak, D., Baumann-Pickering, S., and Parijs, S. V. (**2013**). "Description of sounds associated with Sowerby's beaked whales (Mesoplodon bidens) in the western North Atlantic Ocean," The Journal of the Acoustical Society of America **134**, 3905-3912.

Frasier, K. E. (**2015**). "Density estimation of delphinids using passive acoustics: A case study in the Gulf of Mexico," (University of California San Diego, Scripps Institution of Oceanography, La Jolla, CA, USA), p. 321.

Gillespie, D., Dunn, C., Gordon, J., Claridge, D., Embling, C., and Boyd, I. (**2009**). "Field recordings of Gervais' beaked whales Mesoplodon europaeus from the Bahamas," The Journal of the Acoustical Society of America **125**, 3428-3433.

Goold, J. C., and Jones, S. E. (**1995**). "Time and frequency domain characteristics of sperm whale clicks," The Journal of the Acoustical Society of America **98**, 1279-1291.

Hildebrand, J. A. (**2009**). "Anthropogenic and natural sources of ambient noise in the ocean," Marine Ecology Progress Series **395**, 5-20.

Johnson, M., Madsen, P. T., Zimmer, W. M. X., de Soto, N. A., and Tyack, P. L. (**2004**). "Beaked whales echolocate on prey," Proceedings of the Royal Society B: Biological Sciences **271**, S383-S386.

Johnson, M., Madsen, P. T., Zimmer, W. M. X., de Soto, N. A., and Tyack, P. L. (**2006**). "Foraging Blainville's beaked whales (Mesoplodon densirostris) produce distinct click types matched to different phases of echolocation," Journal of Experimental Biology **209**, 5038.

Madsen, P. T., Payne, R., Kristiansen, N. U., Wahlberg, M., Kerr, I., and Møhl, B. (**2002a**). "Sperm whale sound production studied with ultrasound time/depth-recording tags," Journal of Experimental Biology **205**, 1899.

Madsen, P. T., Wahlberg, M., and Møhl, B. (**2002b**). "Male sperm whale (Physeter macrocephalus) acoustics in a high-latitude habitat: implications for echolocation and communication," Behavioral Ecology and Sociobiology **53**, 31-41.

McKenna, M. F., Ross, D., Wiggins, S. M., and Hildebrand, J. A. (**2012**). "Underwater radiated noise from modern commercial ships," The Journal of the Acoustical Society of America **131**, 92-103.

Møhl, B., Wahlberg, M., Madsen, P. T., Heerfordt, A., and Lund, A. (**2003**). "The monopulsed nature of sperm whale clicks," The Journal of the Acoustical Society of America **114**, 1143-1154.

Roch, M. A., Klinck, H., Baumann-Pickering, S., Mellinger, D. K., Qui, S., Soldevilla, M. S., and Hildebrand, J. A. (**2011**). "Classification of echolocation clicks from odontocetes in the Southern California Bight," The Journal of the Acoustical Society of America **129**, 467-475.
Soldevilla, M. S., Henderson, E. E., Campbell, G. S., Wiggins, S. M., Hildebrand, J. A., and Roch, M. A. (**2008**). "Classification of Risso's and Pacific white-sided dolphins using spectral properties of echolocation clicks," The Journal of the Acoustical Society of America **124**, 609-624.
Watkins, W. A., and Schevill, W. E. (**1977**). "Sperm whale codas," The Journal of the Acoustical Society of America **62**, 1485-1490.
Watwood, S. L., Miller, P. J. O., Johnson, M., Madsen, P. T., and Tyack, P. L. (**2006**). "Deep-diving foraging behaviour of sperm whales (Physeter macrocephalus)," Journal of Animal Ecology **75**, 814-825.
Wiggins, S. M., and Hildebrand, J. A. (**2007**). "High-frequency Acoustic Recording Package (HARP) for broad-band, long-term marine mammal monitoring.," (IEEE, Tokyo, Japan, International Symposium on Underwater Technology and Workshop on Scientific Use of Submarine Cables and Related Technologies), pp. 551-557.
Zimmer, W. M. X., Johnson, M. P., Madsen, P. T., and Tyack, P. L. (**2005**). "Echolocation clicks of free-ranging Cuvier's beaked whales (Ziphius cavirostris)," The Journal of the Acoustical Society of America **117**, 3919-3927.